Jason-2 validation and cross calibration activities (Annual report 2012)

Contract No 104685/00 - lot 1.2A

Reference : CLS.DOS/NT/12-223

Nomenclature : SALP-RP-MA-EA-22141-CLS

Issue : 1rev 1

Date : March 26, 2013

CLS - 8-10 Rue Hermès - Parc Technologique du Canal - 31520 Ramonville St-Agne - FRANCE
Telephone 33 5 61 39 47 00 / Fax 33 5 61 75 10 14

List of tables and figures

List of Tables

List of Figures

List of items to be defined or to be confirmed

Applicable documents / reference documents

Contents

1. Introduction

This document presents the synthesis report concerning validation activities of Jason-2 GDRs under SALP contract (N° 104685/00 Lot 1.2A) supported by CNES at the CLS Space Oceanography Division. It covers several points: CAL/VAL Jason-2 activities, Jason-2 / Jason-1 cross-calibration, reprocessing of Jason-2 GDR data in version D, particular studies and investigations.
The OSTM/Jason-2 satellite was successfully launched on June, 20th 2008. Since July, 4th, Jason-2 is on its operational orbit. Until January 2009, it was flying in tandem with Jason-1, only 55s apart. From May 2012 onwards, Jason-1 is on a geodetic orbit (see note on Jason-1 geodetic mision [7]). Since the beginning of the mission, Jason-2 data have been analyzed and monitored in order to assess the quality of Jason-2 products. Cycle per cycle reports are available on AVISO webpage (http://www.aviso.oceanobs.com/en/calval/systematic-calval/validation-reports.html).
This present report assesses the Jason-2 data quality. Missing and edited measurements are monitored. Furthermore relevant parameters derived from instrumental measurements and geophysical corrections are analyzed.
During 2012, the whole Jason-2 mission was reprocessed in GDR-D standard. The present report contains some results from comparisons between Jason-2 GDR-T and GDR-D. Nevertheless for more details, please refer to the reprocessing report ([10]), spanning the reprocessing period (cycles 001 to 145), which contains comparisons between previous GDR-T and current GDR-D standard, as well as comparison between Jason-2 GDR-D and Jason-1 and Envisat data. Another report ([11]) focuses on the comparison of Jason-2 GDR-T and GDR-D with Jason-1 data during the first 20 Jason-2 cycles (the formation flight phase, when both satellites were on the same ground-track only 55s apart).

Hereafter, analyzes focuse on Jason-1/Jason-2 cross-calibration. During the formation flight configuration (4th July 2008 to 26th January 2009) both satellites were on the same orbit. This allowed to precisely assess parameter discrepancies between both missions in order to detect geographically correlated biases, jumps or drifts. The SLA performances and consistency with Jason-1 are also described. But even after the end of the flight formation phase, comparison are still possible. Even if only low order statistics are mainly presented here, other analyzes including histograms, plots and maps are continuously produced and used in the quality assessment process.
Indeed, it is now well recognized that the usefulness of any altimeter data only makes sense in a multi-mission context, given the growing importance of scientific needs and applications, in particular for operational oceanography. One major objective of the Jason-2 mission is to continue the Jason-1 and T/P high precision altimetry and to allow combination with other missions (ENVISAT, Jason-1). This kind of comparisons between different altimeter missions flying together provides a large number of estimations and consequently efficient long term monitoring of instrument measurements.

2. Processing status

2.1. Processing

End of 2008 Jason-2 data were already available to end users in OGDR (3h data latency) and IGDR (1-2 days data latency). They were first released in version T and switched at cycle 015 to version C. They stayed in this version till cycle 149 (till 2012/07/31 12:01:59 for OGDR), this is the same version (concerning the geophysical standards) as Jason-1 data (for better compatibility). GDR data were released in version T during August 2009. During 2012 the whole GDR dataset was reprocessed in GDR-D version. **In this report, GDR-D from cycle 1 to 157 are used (until 15/10/2012)**. A description of the different Jason-2 products is available in the OSTM/Jason-2 Products handbook ([35]).

The purpose of this document is to report the major features of the data quality from the Jason-2 mission. As Jason-2 was in formation flight with Jason-1 (only 55 s apart) until January 2009, this report also uses results from intercalibration with Jason-1.

2.2. CAL/VAL status

2.2.1. List of events

The following table shows the major plannified events during the beginning of Jason-2 mission.

Dates	Events	Impacts
4 July 2008 5h57	Start of Jason-2 Cycle 0	
4 July 2008 12h15	Start of Poseidon3 altimeter. Tracking mode : autonomous acquisition, median	Start of level2 product generation.
04 July 2008 13:47:52 to 04 July 2008 14:13:36	Poseidon3 altimeter. Tracking mode : Diode acquisition, median	
04 July 2008 14:14:39 to 17 July 2008 15:30:22	Poseidon3 altimeter. Tracking mode : Diode acquisition, SGT	
8 July 2008 4h45 - 5h25	Poseidon3 altimeter. Dedicated period for validation of tracking mode performances	small data gaps on corresponding passes [Cycle 0]
		.../...

Dates	Events	Impacts
11 July 2008 13h00-13h01 and 13h04-13h12	Poseidon3 altimeter. Tracking mode : Diode-DEM (functional)	Functional test of DIODE-DEM tracking mode while onboard DEM was not correct, leading to wrong waveforms and so impacts on altimeter retracking outputs.
12 July 2008 1h20	Start of Jason-2 Cycle 1	
16 July 2008 7h10-17h08	upload POS3 - DEM	Data gap on corresponding passes [Cycle 1, Pass 108-144]
17 July 2008 7h29-11h30	upload POS3 - DEM	Data gap on corresponding passes [Cycle 1, Pass 108-144]
17 July 2008 15:30:22 to 31 July 2008 21:17:08 UTC	Poseidon3 altimeter. Tracking mode : Diode acquisition, median	
21 July 2008 23h18	Start of Jason-2 Cycle 2	
31 July 2008 21:17:09 to 10 August 2008 19:15:39	Jason-2 Cycle 3: Poseidon3 altimeter. Tracking mode : Diode-DEM	
10 August 2008 19:15:40 to 20 August 2008 17:14:10	Jason-2 Cycle 4: Poseidon3 altimeter. Tracking mode : Diode acquisition, median	
20 August 2008 17:14:11 to 30 August 2008 15:12:43	Jason-2 Cycle 5: Poseidon3 altimeter. Tracking mode : Diode-DEM	
30 August 2008 15:12:43 to 9 September 2008 13:11:15	Jason-2 Cycle 6: Poseidon3 altimeter. Tracking mode : Diode acquisition, median	
9 September 2008 13:11:15 to 19 September 2008 11:09:47	Jason-2 Cycle 7: Poseidon3 altimeter. Tracking mode : Diode-DEM	
19 September 2008 11:09:47 to 29 September 2008 09:08:19	Jason-2 Cycle 8: Poseidon3 altimeter. Tracking mode : Diode acquisition, median	
11 Mai 2009 12:09 to 14 Mai 2009 13:09	Upload POS3 (new DEM)	data gaps (northern hemisphere) for passes 154 to 231
		.../...

Dates	Events	Impacts
2 February 2009 06:55:11 to 15:58:05	software upload to Poseidon-3	data gap between passes 204 and 213
4 June 2009 06:31:27 to 14 June 2008 04:29:59	Jason-2 Cycle 34: Poseidon3 altimeter. Tracking mode : Diode-DEM	
12 February 2010	Upload of Doris V8.0 flight software	improved OGDR orbit accuracy
16 September 2010	Jason-2 Cycle 81: Upload of DEM patch for Gavdos transponder calibration	data gap for passes 087 and 237
17 February 2011	GPSP OBS revert upload	
12-14 September 2012	DORIS OBS upload (DORIS restart on 19th September)	OGDR data gap (during the DORIS restart)

Table 1: *P*lannified events

2.2.2. Missing measurements

This section presents a summary of major satellite or ground segment events that occurred from cycle 0 to 157. Table 2 gives a status about the number of missing passes (or partly missing) for GDRs, as well as the associated events for each cycle.
Up to now, Jason-2 has little missing measurements. In the begining, they were mainly caused by station acquisition problems. Now, they are mostly due to scheduled events (like altimeter expert calibrations performed every 6 month or software upload). During 2011, there was a telemetry outage at Usingen station leading to approximatly 2h of missing data on 04/04/2011. During 2012, less than 2h of altimetry data were missing due to technical or operator problems.

Jason-2 Cycles/Pass	Dates	Events
000/222-224	10/07/2008 - 18:28:02 to 20:25:04	Missing telemetry (Usingen station pb)
000/232	11/07/2008 - 03:57:08 to 04:30:30	Partly missing due to altimeter calibration (long LPF)
000/235	11/07/2008 - 07:01:28 to 07:27:41	Partly missing due to altimeter calibration (CNG step)
001/44-46	13/07/2008 - 17:40:00 to 19:37:30	Missing telemetry (Usingen station pb)
		.../...

Jason-2 Cycles/Pass	Dates	Events
001/48-50	13/07/2008 - 21:37:02 to 23:30:00	Missing telemetry (NOAA station pb)
001/108-144		several passes partly missing due to upload of new DEM (plannified unavailability)
003/032-035	02/08/2008 - 02:23:45 to 05:46:30	Passes 32 and 35 are partly missing, passes 33 and 34 are completely missing due to missing telemetry (Usingen)
005/236-241	29/08/2008 - 21:44:56 to 30/08/2008 02:52:07	Missing telemetry (Usingen station pb): passes 237 to 240 completely missing, passes 236 and 241 partly missing
006/232	08/09/2008 - 15:48:00 to 16:21:22	pass 232 partially missing due to altimeter calibration (long LPF)
006/235	08/09/2008 - 18:53:00 to 19:19:10	pass 235 partially missing due to altimeter calibration (CNG step)
016/73	10/12/2008 - 15:11:19 to 15:13:27	pass 73 partially missing due to 1) upload of correction for low signal tracking anomaly and 2) memory dumps (planned unavailability)
026/33	18/03/2009 - 05:09:15 to 05:10:44	pass 33 has approximatly 90 seconds of missing ocean measurements in gulf of guinea (probably due to missing telemetry)
029/209-210	23/04/2009 - 20:18:36 to 20:35:11	data gap over land (on transition between passes 209 and 210) due to missing telemetry
031/154-231	11/05/2009 12:09 to 14/05/2009 13:09	Upload of new DEM leading to missing portions (northern hemisphere) for passes 154 to 231
033/204-213	02/06/2009 - 06:55:11 to 15:58:05	Passes 205 to 212 are completely missing. Passes 204 and 213 are partly missing with respectively 100% and 96% of missing measurements over ocean. This is due to software upload to Poseidon-3.
034/232	13/06/2009 - 07:07:03 to 07:40:23	Due to long calibration, pass 232 is partly missing with 65% of missing measurements over ocean.
034/235	13/06/2009 - 10:11:41 to 10:37:50	Due to calibration CNG step, pass 235 is partly missing with 8% of missing measurements over ocean.
037/54	06/07/2009 - 02:33:12 to 02:34:33	pass 054 has a small data gap due to missing PLTM
		.../...

Jason-2 Cycles/Pass	Dates	Events
053/57	11/12/2009 - 20:38:19 to 21:29:43	passes 57 and 58 have a data gap due to Gyro calibration
053/232	18/12/2009 - 16:39 to 17:12	pass 232 has a data gap due to CAL2 calibration
053/235	18/12/2009 - 19:43	pass 235 has a 26 minutes data gap due to CNG calibration (mostly over land)
072/199	23/06/2010 - 19:15:37 to 19:16:59	pass 199 has small data gap due to missing telemetry
073/232	05/07/2010 - 00:09:33 to 00:42:54	pass 232 has a data gap due to CAL2 calibration
073/235	05/07/2010 - 03:14:11 to 03:40:20	pass 235 has a data gap due to CNG calibration (mostly over land)
081/087	16/09/2010 - 16:40:22 to 16:52:48	pass 087 has a data gap due to upload of DEM update (for GAVDOS transponder calibration)
081/237	22/09/2010 - 13:07:27 to 13:18:12	pass 237 has a data gap due to upload of DEM update (for GAVDOS transponder calibration)
084/031	14/10/2010 - 06:02 to 06:11:15	Calibration (I2 and Q2)
084/031-032	14/10/2010 - 06:12 to 06:21:15	Calibration (I and Q)
084/043	14/10/2010 - 17:00:57 to 17:02:39	pass 043 has a small data gap due to missing PLTM
094/231	29/01/2011 - 04:50 to 04:55	Calibration CAL1 (14% of missing ocean data)
094/232	29/01/2011 - 05:38 to 06:11	Calibration CAL2 (65% of missing ocean data)
094/235	29/01/2011 - 08:37 to 09:03	Calibration CNG (mostly over land, 9% of missing ocean data)
101/133-135	04/04/2011 - 18:49:08 to 21:03:48	Telemery outage at Usingen, passes 133 to 135 have respectively 23%, 100%, and 91% of missing ocean data
110/158-159	04/07/2011 - 00:27:29 to 01:27:29	Gyro calibration. Passes 158 and 159 have respectively 18% and 88% of missing ocean data
115/232	25/08/2011 - 11:07:35 to 11:40:56	Calibration CAL2: 65% of missing ocean data
		.../...

Jason-2 Cycles/Pass	Dates	Events
115/235	25/08/2011 - 14:12 to 14:38	Calibration CNG: mostly over land, 8% of missing ocean data
132/232	10/02/2012 - 00:42:26 to 01:14:03	Calibration CAL2: 65% of missing ocean data
132/235	10/02/2012 - 03:47:11 to 04:13:20	Calibration CNG: mostly over land, 8% of missing ocean data
135/105	05/03/2012 - 19:54:49 to 20:26:14	technical problem and operator error: 25% of missing ocean data
136/191	19/03/2012 - 02:15:18 to 02:50:11	problem of ACK: 56% of missing ocean data
145/143	14/06/2012 - 11:41:15 to 11:42:58	pass 143 has a small data gap due to missing telemetry
145/248	18/06/2012 - 13:20:10 to 13:21:29	pass 248 has a small data gap
147/022	29/06/2012 - 13:45:30 to 13:49:46	pass 022 has a small data gap due to missing telemetry (8% of missing ocean data)
147/134	03/07/2012 - 22:41:25 to 22:43:58	pass 134 has a small data gap due to operator error (5% of missing ocean data)
154/210	14/09/2012 - 07:45:08 to 07:46:07	pass 210 has a small portion of missing data in central Pacific
156/232	05/10/2012 - 00:07:08 to 00:40:30	Calibration CAL2: 66% of missing ocean data
156/235	05/10/2012 - 03:11:47 to 03:37:57	Calibration CNG: mostly over land, 9% of missing ocean data

Table 2: *M*issing pass status

2.2.3. Edited measurements

Table 3 indicates particular high editing periods (see section 3.2.1.). Most of the occurrences correspond to radiometer wet troposphere correction at default value (due to AMR unavailability) or altimeter low signal tracking anomaly (AGC anomaly), though the latter concerns only few measurements and was corrected during cycle 16 (see section 8.1.).

Jason-2 Cycles/Passes	Date	Comments
000/89	05/07/08 - 14:22:07 to 14:23:38	Partly edited by several parameters out of threshold (AGC anomaly)
000/134	07/07/08 - 08:06:37 to 08:28:57	Partly edited by several parameters out of threshold (AGC anomaly)
000/156	08/07/08 - 04:35:12 to 05:31:01	rain flag is set (dotted), probably related to start/stop sequence (from 04:45 to 05:24)
000/234	11/07/08 - 05:45:12 to 05:49:03	Partly edited by several parameters out of threshold (AGC anomaly)
000/241	11/07/08 - 13:04:27 to 13:09:11	Partly edited by ice flag (number of elementary Ku-band measurements at 0, AGC=16.88) due to test of altimeter DEM mode
001/		several passes partly edited by several parameters out of threshold (AGC anomaly)
002/		several passes partly edited by several parameters out of threshold (AGC anomaly)
004/		several passes partly edited by several parameters out of threshold (AGC anomaly)
006/		several passes partly edited by several parameters out of threshold (AGC anomaly)
008/		several passes partly edited by several parameters out of threshold (AGC anomaly)
009/		several passes partly edited by several parameters out of threshold (AGC anomaly)
010/		several passes partly edited by several parameters out of threshold (AGC anomaly)
011/		several passes partly edited by several parameters out of threshold (AGC anomaly)
012/		several passes partly edited by several parameters out of threshold (AGC anomaly)
013/		several passes partly edited by several parameters out of threshold (AGC anomaly)
014/		several passes partly edited by several parameters out of threshold (AGC anomaly)
		.../...

Jason-2 Cycles/Passes	Date	Comments
015/		several passes partly edited by several parameters out of threshold (AGC anomaly)
019/024-042	07/01/ 11:00:35 to 08/01/2009 03:23:34	radiometer wet troposphere correction at default value due to AMR unavailability
019/119-161	11/01/ 03:56:38 to 12/01/2009 19:26:14	radiometer wet troposphere correction at default value due to AMR unavailability
110/047	29/09/2011 16:14 to 16:20	a portion of pass 47 is edited by radiometer wet troposphere correction out of threshold or at default values (radio-frequency interference from a ground based source)

Table 3: *E*dited measurement status

2.3. Models and Standards History

Three versions of the Jason-2 Operational Geophysical Data Records (OGDRs) and Interim Geophysical Data Records (IGDRs) have been generated up to now. These three versions are identified by the version numbers "T" (for test), "c" and "d" in the product filename. For example, version "T" IGDRs are named "JA2_IPN_2PT", version "c" IGDRs are named "JA2_IPN_2Pc", and version "d" IGDRs are named "JA2_IPN_2Pd". All three versions adopt an identical data record format as described in Jason-2 User Handbook ([35]). Versions "T" and "c" differ only sligthly (names of variables are corrected and 3 variables added). Version "T" O/IGDRs were the first version released soon after launch and was disseminated only to OSTST community. Version "c" O/IGDRs were first implemented operationally from data segment 141 of cycle 15 for the OGDRs (3rd December 2008) and cycle 15 for the IGDRs. Version "c" of Jason-2 data is consistent with version "c" of Jason-1 data. Version "d" O/IGDRs were first implemented operationally from data segment 78 of cycle 150 for the OGDRs (31st July 2012) and cycle 150 for the IGDRs. GDR data switched to version "d" from cycle 146 onwards, but previous cycles 1 to 145 were reprocessed in version "d" during 2012. Therefore the whole Jason-2 mission is available in GDR version "d". The tables 4 and 5 below summarize the models and standards that are adopted for versions "T" / "c" and "d" of Jason-2 data. More details on some of these models are provided in Jason-2 User Handbook document ([35]).
Impact of GDR reprocessing can be found in the reprocessing reports [10] and [11].

Model	Product version "T" and "c"
Orbit	Based on Doris onboard navigator solution for OGDRS. DORIS tracking data for IGDRs (DORIS + SLR tracking for cycles 20 to 78) DORIS+SLR+GPS tracking data for GDRs. Using POE-C
Altimeter Retracking	"Ocean" retracking: MLE4 fit from 2nd order Brown model: MLE4 simultaneously retrieves the following 4 parameters from the altimeter waveforms: • Epoch (tracker range offset) → altimeter range • Composite Sigma → SWH • Amplitude → Sigma0 • Trailing Edge slope → Square of mispointing angle "Ice" retracking: Geometrical analysis of the altimeter waveforms, which retrieves the following parameters: • Epoch (tracker range offset) → altimeter range • Amplitude → Sigma0
	.../...

Model	Product version "T" and "c"
Altimeter Instrument Corrections	Consistent with MLE4 retracking algorithm.
Jason-2 Advanced Microwave Radiometer (AMR) Parameters	Using calibration parameters derived from long term calibration tool developed and operated by NASA/JPL.
Dry Troposphere Range Correction	From ECMWF atmospheric pressures and model for S1 and S2 atmospheric tides
Wet Troposphere Range Correction from Model	From ECMWF model
Ionosphere correction from model	Based on Global Ionosphere TEC Maps from JPL
Sea State Bias Model	Empirical model derived from 3 years of MLE4 Jason-1 altimeter data with version "b" geophysical models.
Mean Sea Surface Model	CLS01
Mean Dynamic Topography Model	MDT_RIO_2005
Geoid	EGM96
Bathymetry Model	DTM2000.1
Inverse Barometer Correction	Computed from ECMWF atmospheric pressures after removing S1 and S2 atmospheric tides
Non-tidal High-frequency De-aliasing Correction	Mog2D high resolution ocean model on I/GDRs. None on OGDRs. Ocean model forced by ECMWF atmospheric pressures after removing S1 and S2 atmospheric tides.
Tide Solution 1	GOT00.2 + S1 ocean tide . S1 load tide ignored
Tide Solution 2	FES2004 + S1 and M4 ocean tides. S1 and M4 load tides ignored
Equilibrium long-period ocean tide model.	From Cartwright and Taylor tidal potential.
Non-equilibrium long-period ocean tide model.	Mm, Mf, Mtm, and Msqm from FES2004
Solid Earth Tide Model	From Cartwright and Taylor tidal potential.
Pole Tide Model	Equilibrium model
	.../...

Model	Product version "T" and "c"
Wind Speed from Model	ECMWF model
Altimeter Wind Speed	Wind speed table derived from Jason-1 data (Collard, [23]).

Table 4: *M*odels and standards adopted for the Jason-2 version "T" and "c" products. Adapted from [35]

Model	Product version "d"
Orbit	Based on Doris onboard navigator solution for OGDRS. DORIS tracking data for IGDRs (DORIS + SLR tracking for cycles 20 to 78) DORIS+SLR+GPS tracking data for GDRs. Using POE-D
Altimeter Retracking	"Ocean MLE4" retracking: MLE4 fit from 2nd order Brown analytical model: MLE4 simultaneously retrieves the 4 parameters that can be inverted from the altimeter waveforms: • Epoch (tracker range offset) → altimeter range • Composite Sigma → SWH • Amplitude → Sigma0 • Square of mispointing angle (Ku band only, a null value is used in input of the C band retracking algorithm) "Ocean MLE3" retracking: MLE3 fit from 1st order Brown analytical model: MLE3 simultaneously retrieves the 3 parameters that can be inverted from the altimeter waveforms: • Epoch (tracker range offset) → altimeter range • Composite Sigma → SWH • Amplitude → Sigma0 "Ice" retracking: Geometrical analysis of the altimeter waveforms, which retrieves the following parameters: • Epoch (tracker range offset) → altimeter range • Amplitude → Sigma0
	.../...

Model	Product version ”d”
Altimeter Instrument Corrections	Two sets: • on set consistent with MLE4 retracking • on set consistent with MLE3 retracking
Jason-2 Advanced Microwave Radiometer (AMR) Parameters	Using calibration parameters derived from long term calibration tool developed and operated by NASA/JPL.
Dry Troposphere Range Correction	From ECMWF atmospheric pressures and model for S1 and S2 atmospheric tides
Wet Troposphere Range Correction from Model	From ECMWF model
Ionosphere correction from model	Based on Global Ionosphere TEC Maps from JPL
Sea State Bias Model	Two empirical models: • MLE4 version derived from 1 year of MLE4 Jason-2 altimeter data with version ”d” geophysical models • MLE3 version derived from 1 year of MLE3 Jason-2 altimeter data with version ”d” geophysical models
Mean Sea Surface Model	MSS_CNES_CLS11
Mean Dynamic Topography Model	MDT_CNES-CLS09
Geoid	EGM96
Bathymetry Model	DTM2000.1
Inverse Barometer Correction	Computed from ECMWF atmospheric pressures after removing S1 and S2 atmospheric tides
Non-tidal High-frequency De-aliasing Correction	Mog2D high resolution ocean model on I/GDRs. None on OGDRs. Ocean model forced by ECMWF atmospheric pressures after removing S1 and S2 atmospheric tides.
Tide Solution 1	GOT4.8 + S1 ocean tide. S1 and M4 load tide included.
Tide Solution 2	FES2004 + S1 and M4 ocean tides. S1 and M4 load tides ignored
Equilibrium long-period ocean tide model.	From Cartwright and Taylor tidal potential.
	.../...

Model	Product version "d"
Non-equilibrium long-period ocean tide model.	Mm, Mf, Mtm, and Msqm from FES2004
Solid Earth Tide Model	From Cartwright and Taylor tidal potential.
Pole Tide Model	Equilibrium model
Wind Speed from Model	ECMWF model
Altimeter Wind Speed	Wind speed table derived from Jason-1 data (Collard, [23]). In addition, a calibration bias of 0.32 is applied to JA2 Ku-band sigma0 prior wind speed computation.
Rain flag	Derived from comparisons to thresholds of the radiometer-derived integrated liquid water content and of the difference between the measured and the expected Ku-band backscatter coefficient
Ice flag	Derived from comparison of the model wet tropospheric correction to a dual-frequency wet tropospheric correction retrieved from radiometer brightness temperatures, with a default value issued from a climatology table

Table 5: *M*odels and standards adopted for the Jason-2 version "d" products. Adapted from [35]

The differences between GDR-T and GDR-D products are listed in the table 6.

Model	Product Version "T"	Product Version "D"
Orbit	EIGEN-GL04S with time-varying gravity (annual and semi-annual terms up to deg/ord 50) + ITRF 2005 DORIS+SLR+GPS	EIGEN-GRGS_RL02bis_MEAN_FIELD with time-varying gravity (annual, semi-annual, and drifts up to deg/ord 50) + ITRF 2008 DORIS+SLR+GPS (increased weight for GPS)
		.../...

Model	Product Version "T"	Product Version "D"
Altimeter Retracking	MLE4 + 2nd order Brown model : MLE4 simultaneously retrieves the 4 parameters that can be inverted from the altimeter waveforms: epoch, SWH, Sigma0 and mispointing angle. This algorithm is more robust for large off-nadir angles (up to 0.8°).	Identical to version "T", in addition altimeter parameters are also available for MLE3 retracking
Altimeter Instrument Corrections	Consistent with MLE4 retracking algorithm.	One consistent with MLE4 retracking + One consistent with MLE3 retracking
Jason-2 Microwave Radiometer Parameters	Using calibration parameters derived from long term calibration tool developed and operated by NASA/JPL	Using calibration parameters derived from long term calibration tool developed and operated by NASA/JPL + enhancement in coastal regions + correction of anomaly in 34 GHz channel addition of radiometer rain and ice flag addition of radiometer 18.7 GHz/ 23.8 GHz/ 34 GHz antenna gain weighted land fraction in main beam
Dry Troposphere Range Correction	From ECMWF atmospheric pressures and model for S1 and S2 atmospheric tides.	Identical to version "T"
Wet Troposphere Range Correction from Model	From ECMWF model.	Identical to version "T"
Back up model for Ku-band ionospheric range correction.	Derived from JPL's Global Ionosphere Model (GIM) maps	Identical to version "T"
Sea State Bias Model	Empirical model derived from 3 years of Jason-1 MLE4 altimeter data with version "b" geophysical models	Empirical models derived from Jason-2 data (One consistent with MLE4 retracking + One consistent with MLE3 retracking)
Mean Sea Surface Model	CLS01	CNES_CLS_2011
Geoid	EGM96	Identical to version "T"
		.../...

Model	Product Version "T"	Product Version "D"
Bathymetry Model	DTM2000.1	Identical to version "T"
Mean Dynamic Topography	Rio 2005 solution	CNES_CLS2009 solution
Inverse Barometer Correction	Computed from ECMWF atmospheric pressures after removing model for S1 and S2 atmospheric tides.	Identical to version "T"
Non-tidal High-frequency De-aliasing Correction	Mog2D high resolution ocean model. Ocean model forced by ECMWF atmospheric pressures after removing model for S1 and S2 atmospheric tides.	Identical to version "T"
Tide Solution 1	GOT00.2 + S1 ocean tide . S1 load tide ignored.	GOT4.8 (S1 ocean tide and S1 load tide are included).
Tide Solution 2	FES2004 + S1 and M4 ocean tides. S1 and M4 load tides ignored	Identical to version "T"
Equilibrium long-period ocean tide model.	From Cartwright and Taylor tidal potential.	Identical to version "T"
Non-equilibrium long-period ocean tide model.	Mm, Mf, Mtm, and Msqm from FES2004.	Mm, Mf, Mtm, and Msqm from FES2004 + correction for a bug
Solid Earth Tide Model	From Cartwright and Taylor tidal potential.	Identical to version "T"
Pole Tide Model	Equilibrium model.	Equilibrium model + correction of error which was present over lakes and enclosed seas.
Wind Speed from Model	ECMWF model	Identical to version "T"
Altimeter Wind Speed	Table derived from Jason-1 GDR data.	Table is identical to version "T", but the inputs differ.
Altimeter Rain Flag	Set to default values	Derived from Jason-2 sigma naught MLE3 values
		.../...

Model	Product Version "T"	Product Version "D"
Altimeter Ice Flag	Flag based on the comparison of the model wet tropospheric correction and of a radiometer bi frequency wet tropospheric correction (derived from 23.8 GHz and 34.0 GHz), accounting for a backup solution based on climatologic estimates of the latitudinal boundary of the ice shelf, and from altimeter wind speed.	Identical to version "T"
Update of the altimeter characterization file		PRF value is no longer truncated (2058.513239 Hz) Bias of 18.092 cm applied for Ku- and C-band range (corrects the value of the distance between center of gravity and the reference point of the altimeter antenna) Antenna aperture angle (at 3 dB) changed to 1.29 deg MQE setting is applied during 20 Hz to 1 Hz compression Tracker_range_res at a more precise value
other	LTM calculated over 1 day	LTM calculated over 7 days (sliding window) and applied for one day. the origin of the constant part of the time tag bias was found and is directly corrected in the Gdr-D datation.

Table 6: *M*odels and standards adopted for the Jason-2 product version "T", and "D"

3. Data coverage and edited measurements

3.1. Missing measurements

3.1.1. Over land and ocean

Determination of missing measurements relative to the theoretically expected orbit ground pattern is an essential tool to detect missing telemetry or satellite events for instance. Applying the same procedure for Jason-1 and Jason-2, the comparison of the percentage of missing measurements has been performed. Jason-2 can use several onboard tracking modes: Split Gate Tracker (ie the Jason-1 tracking mode, and used for cycle 0 and half of cycle 1), Diode/DEM (used for cycles 3, 5, 7, and 34) and median tracker (used for the other cycles). These different tracking modes are described by [28]. Thanks to the new modes of onboard tracking (median tracker and Diode/DEM), the data coverage over land surface was dramatically increased in comparison with Jason-1 depending on the tracker mode and the period. Figure 1 shows the percentage of missing measurements for Jason-2 and Jason-1 (all surfaces) computed with respect to a theoretical possible number of measurements. Due to differences between altimeter tracking algorithms, the number of available data is greater for Jason-2 than for Jason-1. Differences appear on land surfaces as shown in figure 2. The missing data are highly correlated with the mountains location. The monitoring shows a slight annual signal. The slight increase of Jason-2 missing measurements end of 2008 (during cycle 16) is related to the correction of the low signal tracking anomaly (see section 8.1.).

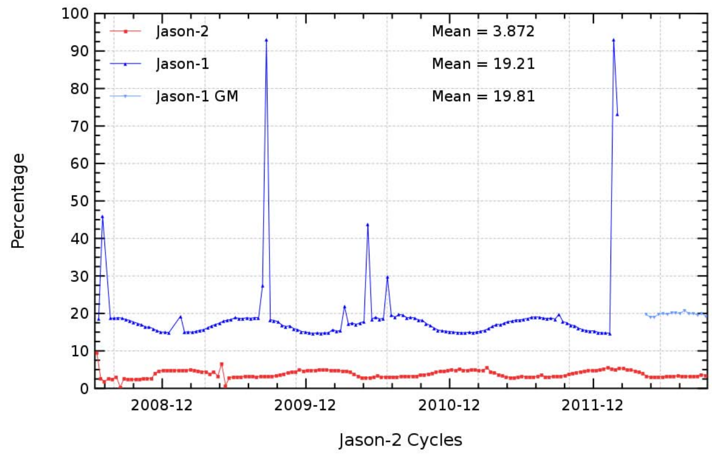

Figure 1: *Percentage of missing measurements over ocean and land for JA2 and JA1*

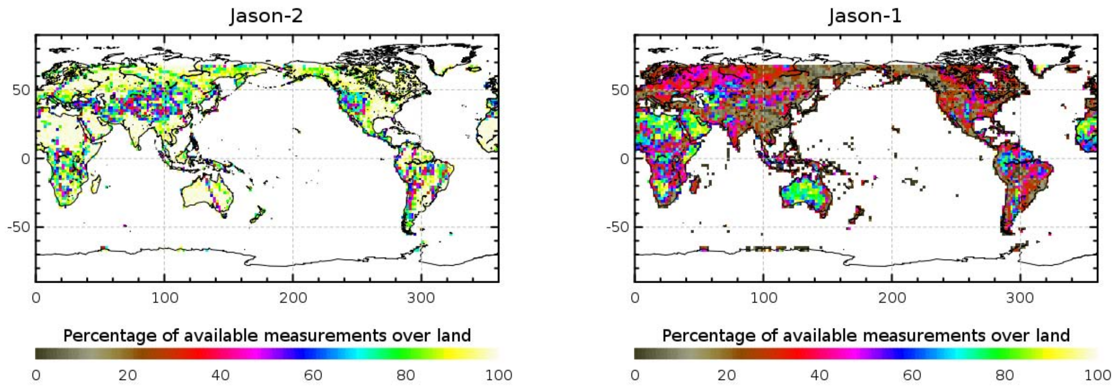

Figure 2: *Map of percentage of available measurements over land for Jason-2 on cycle 154 (left) and for Jason-1 on cycle 511 (right)*

3.1.2. Over ocean

When considering ocean surface, the same analysis method leads also to an improvement of Jason-2 data coverage, as plotted on the top left figure 3. It represents the percentage of missing measurements relative to the theory, when limited to ocean surfaces. The mean value is about 0.1% for Jason-2, 4.6% for Jason-1 on its repeat ground-track and 2.8% for Jason-1 on its geodetic ground-track. Note that since Jason-1 is on a geodetic ground-track, it is roughly once per month during about 2 h in INIT mode (no science data), due to Jason-2 overflight. Even if already very low, this figure of missing measurements is not significant due to several events where the measurements are missing. All these events are described on table 2.

On figure 3 on the top right, the percentage of missing measurements is plotted without taking into account the cycles where instrumental events or other big anomalies occurred. The mean value of missing measurements lowers down to 0.02% for Jason-2 and 1.9% (2.8%) for Jason-1 (Jason-1 geodetic). These additional Jason-1 missing measurements are mainly located over sea ice and near the coasts and are related to the altimeter tracking method. Indeed, selecting latitudes lower than 50° and bathymetry area lower than -1000m (see bottom of figure 3), the Jason-1 percentage becomes very weak (close to 0.02%) which represents less than 100 missing measurements per cycle over open ocean. For Jason-2, the same statistic is smaller with around 0.006% of missing measurements over open oean. This weak percentage of missing measurements is mainly explained by the rain cells and sigma0 blooms. These sea states can disturb significantly the Ku band waveform shape leading to an altimeter lost of tracking.

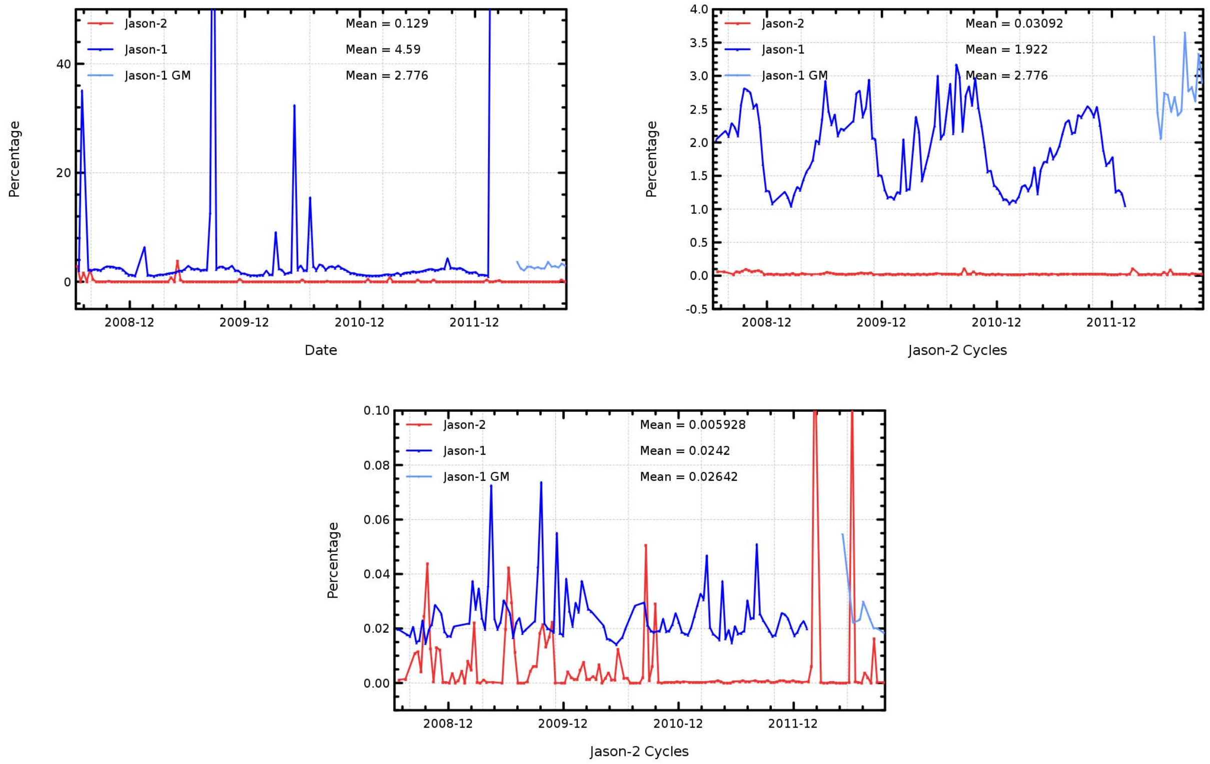

Figure 3: *Cycle per cycle percentage of missing measurements over ocean (top left), without anomalies (top right), without anomalies and with geographical selections (bottom).*

3.2. Edited measurements

3.2.1. Editing criteria definition

Editing criteria are used to select valid measurements over ocean. The editing process is divided into 4 parts. First, only measurements over ocean and lakes are kept (see section 3.2.2.). Second, some flags are used as described in section 3.2.3.. Note that though the altimeter rain flag is now available in the current release of GDR (D), it is not used hereafter in the editing procedure. But measurements corrupted by rain are well detected by other altimeter parameter criteria. Then, threshold criteria are applied on altimeter, radiometer and geophysical parameters and are described in the table 7. Except for the dual frequency ionosphere correction, only Ku-band measurements are used in this editing procedure, as they mainly represent the end user dataset. Moreover, a spline criterion is applied to remove the remaining spurious data. For each criterion, the cycle per cycle percentage of edited measurements has been monitored. This allows detection of anomalies in the number of removed data, which could come from instrumental, geophysical or algorithmic changes.

.../...

Parameter	Min thresholds	Max thresholds	mean edited

Parameter	Min thresholds	Max thresholds	mean edited
Sea surface height	$-130\,m$	$100\,m$	0.77%
Sea level anomaly	$-10\,m$	$10.0\,m$	1.02%
Number measurements of range	10	*Not applicable*	1.03%
Standard deviation of range	0	$0.2\,m$	1.40%
Squared off-nadir angle	$-0.2\,deg^2$	$0.64\,deg^2$	0.59%
Dry troposphere correction	$-2.5\,m$	$-1.9\,m$	0.00%
Inverted barometer correction	$-2.0\,m$	$2.0\,m$	0.00%
AMR wet troposphere correction	$-0.5m$	$-0.001\,m$	0.21%
Ionosphere correction	$-0.4\,m$	$0.04\,m$	1.18%
Significant wave height	$0.0\,m$	$11.0\,m$	0.65%
Sea State Bias	$-0.5\,m$	$0.0\,m$	0.62%
Number measurements of Ku-band Sigma0	10	*Not applicable*	1.02%
Standard deviation of Ku-band Sigma0	0	$1.0\,dB$	1.94%
Ku-band Sigma0 [1]	$7.0\,dB$	$30.0\,dB$	0.60%
Ocean tide	$-5.0\,m$	$5.0\,m$	0.01%
Equilibrium tide	$-0.5\,m$	$0.5\,m$	0.00%
Earth tide	$-1.0\,m$	$1.0\,m$	0.00%
Pole tide	$-15.0\,m$	$15.0\,m$	0.00%
Altimeter wind speed	$0\,m.s^{-1}$	$30.0\,m.s^{-1}$	1.02%
All together	-	-	3.24%

Table 7: *E*diting criteria

3.2.2. Selection of measurements over ocean and lakes

In order to remove data over land, a land-water mask is used. Only measurements over ocean or lakes are kept. This allows to keep data near the coasts and so to detect potential anomalies in these areas. Furthermore, there is no impact on global performance estimations since the most

[1] The thresholds used for the Ku-band Sigma0 are the same than for Jason-1 and T/P, but the same sigma0 bias as between Jason-1 and T/P (about 2.4 dB) is applied.

significant results are derived from analyzes in deep ocean areas. Figure 4 shows the cycle per cycle percentage of measurements eliminated by this selection. The signal shows mainly a seasonal cycle, due to changing properties of land reflection. But it also reveals the impact of the different altimeter tracking modes: SGT (split gate tracking), Median and DIODE/DEM (digital elevation model). SGT mode, the nominal mode for Jason-1, was used for Jason-2 during cycle 0 and half of cycle 1. This mode does not perform very well over land (as also depicted on right side of figure 2), therefore a comparable small percentage of measurements are edited over land for cycle 1 (approximately 24%). Most of Jason-2 cycles (cycles 2, 4, 6, 8 to 33, and onwards from cycle 35) were operated in Median mode (also used by Envisat). This mode is more adapted for tracking over land than SGT and provides therefore more measurements over land (as also seen on left side of figure 2) and so more measurements are edited (between 25.5% and 27% depending on season) due to the ocean/land criteria. A new tracking mode, DEM, was used during cycles 3, 5, 7, and 34. It has been designed to provide more data over inland water surfaces and coastal areas. It provides a continuous data set over land but some are not meaningful (in areas where the DEM is not accurate enough like in the major mountains). Therefore during these cycles, almost 29% of measurements are removed by the selection. Since 10th of December, 2008 the onbord altimeter configuration was modified to correct for the low signal tracking anomaly, which led to a more strict control of acquisition gain loop (to avoid the tracking of low signal anomalies). This explains the quite steep decrease of land measurements edited around cycle 16 (section 8.1.).

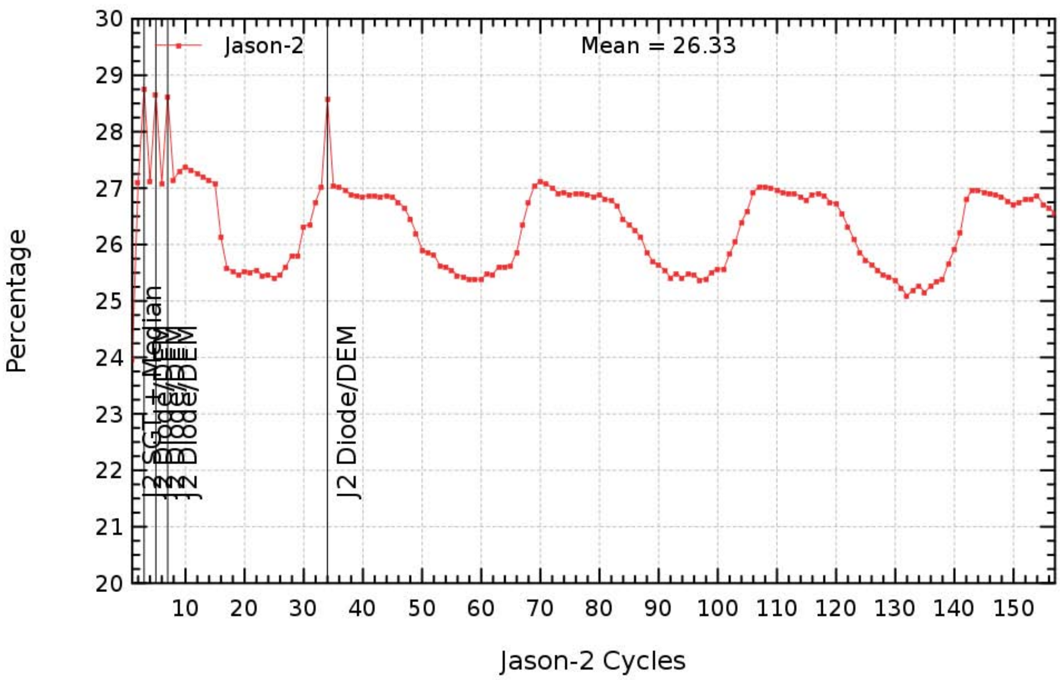

Figure 4: *Cycle per cycle percentage of eliminated measurements during selection of ocean/lake measurements.*

3.2.3. Flagging quality criteria: Ice flag

The ice flag is used to remove the sea ice data. Figure 5 shows the cycle per cycle percentage of measurements edited by this criterion. Over the shown period, no anomalous trend is detected (figure 5 left) but the nominal annual cycle is visible. Indeed, the maximum number of points over ice is reached during the southern winter (ie. July - September). As Jason-2 takes measurements between 66° north and south, it does not detect thawing of sea ice (due to global warming), which takes place especially in northern hemisphere over 66°N. The percentage of measurements edited by ice flag is plotted in the right of figure 5 for a period of 1 year.

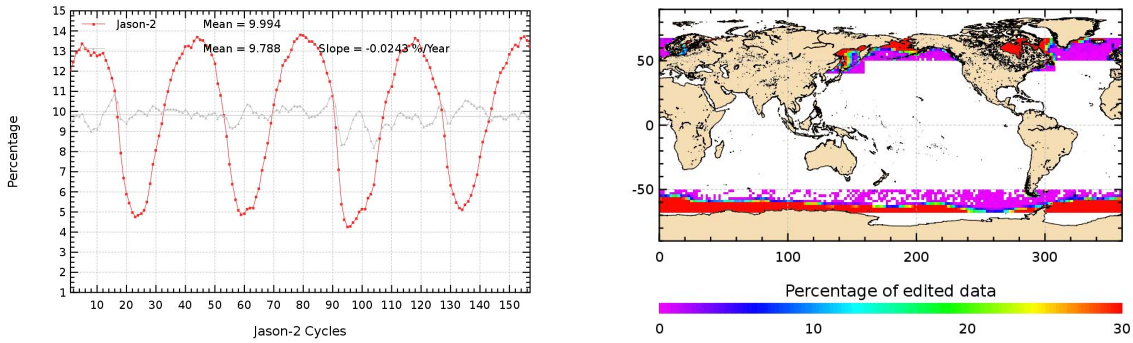

Figure 5: *Percentage of edited measurements by ice flag criterion. Left: Cycle per cycle monitoring. The gray curve shows the trend of edited measurements after adjusting for annual and semi-annual signals. Right: Map over a one year period (cycles 121to 157).*

3.2.4. Flagging quality criteria: Rain flag

Though the altimeter rain flag is now present in GDR-D release, it is not used hereafter during the editing procedure. The percentage of rain edited measurements is plotted in figure 6 over cycles 121 to 157 (covering 12 months). It shows that measurements are especially edited near coasts, but also in the equatorial zone and open ocean. The altimeter rain flag seems to be slightly too strict, using it would lead to edit 6.7% of additional measurements.

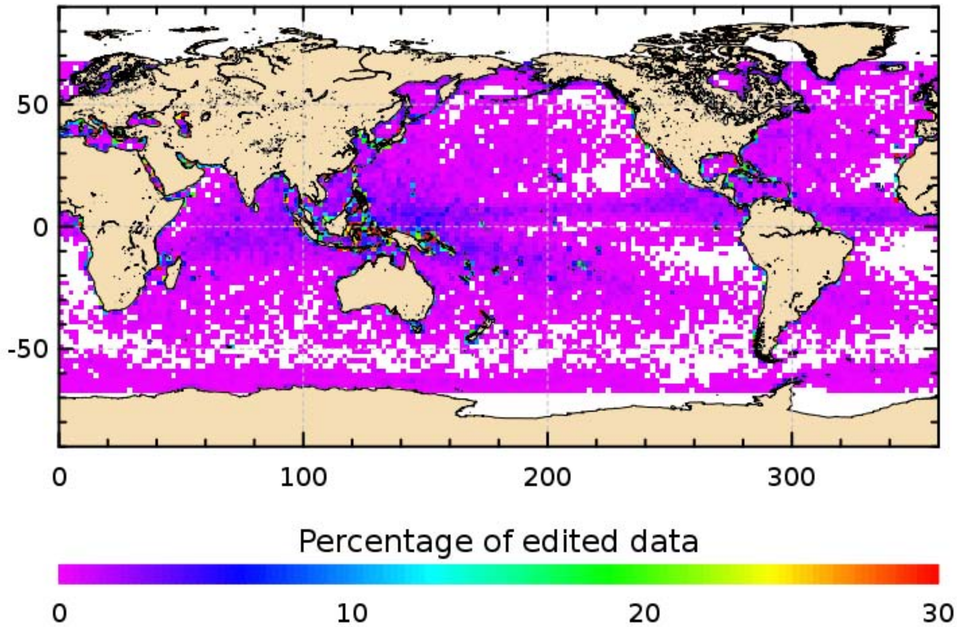

Figure 6: *Percentage of edited measurements by altimeter rain flag criterion. Map over a one year period (cycles 121to 157).*

3.2.5. Threshold criteria: Global

Instrumental parameters have also been analyzed from comparison with thresholds, after having selected only ocean/lakes measurements and applied flagging quality criteria (ice flag). Therefore measurements appear not as edited by thresholds, when they were already edited by land or sea ice flag. Note that no measurement is edited by the following corrections : dry troposphere correction, inverted barometer correction (including DAC), equilibrium tide, earth and pole tide. Indeed these parameters are only verified in order to detect data at default values, which might happen during a processing anomaly.
The percentage of measurements edited using each criterion is monitored on a cycle per cycle basis (figure 7). The mean percentage of edited measurements is about 3.2%. A small annual cycle is visible. The high percentage of edited measurements of cycle 019, is explained by an AMR anomaly, which resulted in defaulted radiometer values during several passes.

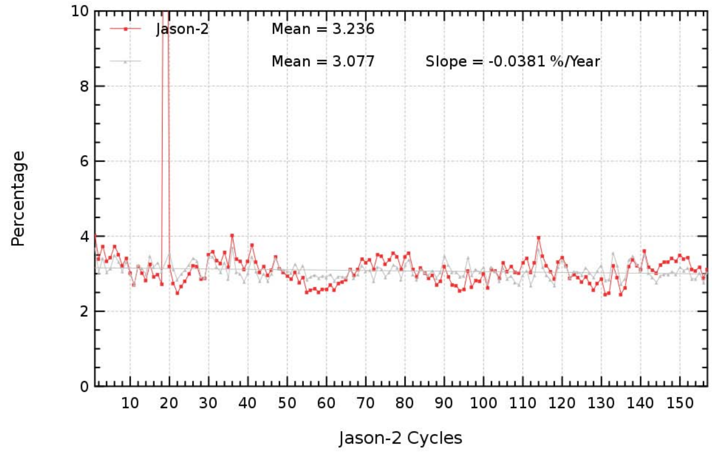

Figure 7: *Cycle per cycle percentage of edited measurements by threshold criteria. The gray curve shows the trend of edited measurements after adjusting for annual and semi-annual signals.*

3.2.6. Threshold criteria: 20-Hz measurements number

The percentage of edited measurements because of a too low number of 20-Hz measurements is represented on left side of figure 8. No trend neither any anomaly has been detected.
The map of measurements edited by 20-Hz measurements number criterion is plotted on right side of figure 8 and shows correlation with heavy rain and wet areas (in general regions with disturbed sea state). Indeed waveforms are distorted by rain cells, which makes them often meaningless for SSH calculation. As a consequence, edited measurements due to several altimetric criteria are often correlated with wet areas.

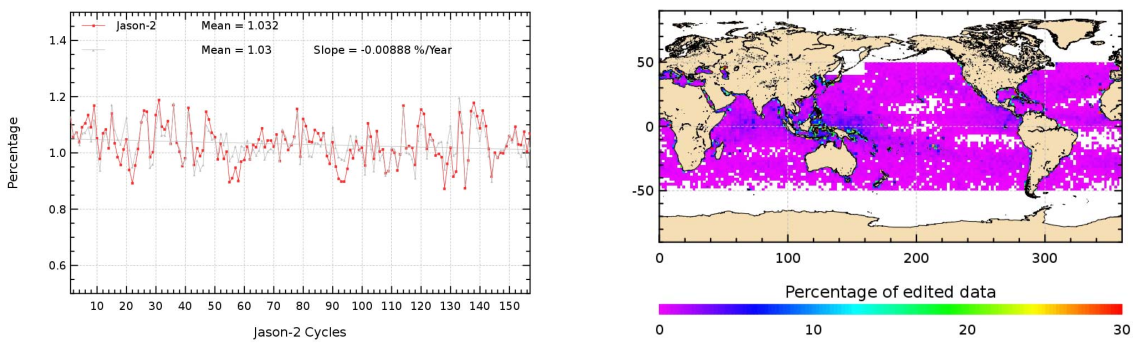

Figure 8: *Percentage of edited measurements by 20-Hz measurements number criterion. Left: Cycle per cycle monitoring. The gray curve shows the trend of edited measurements after adjusting for annual and semi-annual signals. Right: Map over a one year period (cycles 121to 157).*

3.2.7. Threshold criteria: 20-Hz measurements standard deviation

The percentage of edited measurements due to 20-Hz measurements standard deviation criterion is shown in figure 9 (left). During cycle 1, slightly more measurements are edited by 20-Hz measurements standard deviation criterion than during other cycles. This is likely due to low signal tracking anomaly which impacted especially this cycle. The right side of figure 9 shows a map of measurements edited by the 20-Hz measurements standard deviation criterion. As in section 3.2.6., edited measurements are correlated with wet areas.

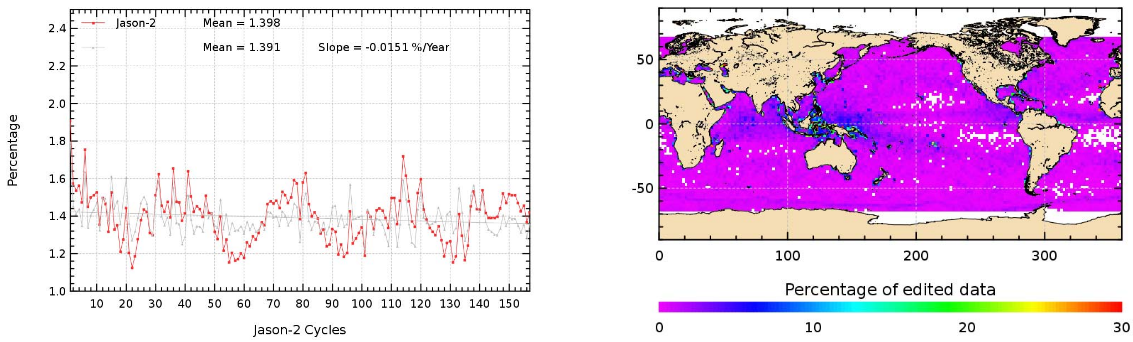

Figure 9: *Percentage of edited measurements by 20-Hz measurements standard deviation criterion. Left: Cycle per cycle monitoring. The gray curve shows the trend of edited measurements after adjusting for annual and semi-annual signals. Right: Map over a one year period (cycles 121to 157).*

3.2.8. Threshold criteria: Significant wave height

The percentage of edited measurements due to significant wave height criterion is represented in figure 10. It is about 0.65%. In the beginning of the mission, the curve of measurements edited by SWH threshold criterion is quite irregular, as low signal tracking anomalies occurred during SGT and Median tracking modes, whereas there are no low signal tracking anomalies during DEM tracking modes (cycles 3, 5, and 7). Indeed during periods of low signal tracking anomaly, parameters like significant wave height, backscattering coefficient and squared off-nadir angle from waveforms are out of thresholds and therefore edited (see section 8.1.). Figure 10 (right part) shows that measurements edited by SWH criterion are especially found near coasts in the equatorial regions and in the Mediterranean Sea.

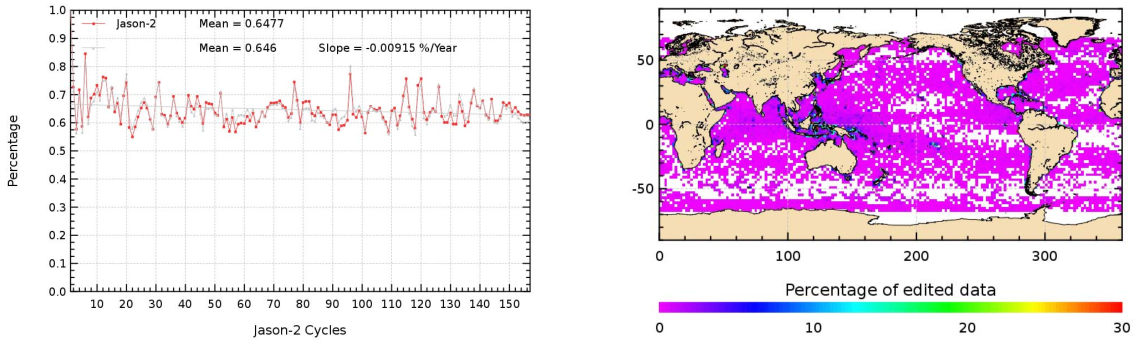

Figure 10: *Percentage of edited measurements by SWH criterion. Left: Cycle per cycle monitoring. The gray curve shows the trend of edited measurements after adjusting for annual and semi-annual signals. Right: Map over a one year period (cycles 121to 157).*

3.2.9. Backscatter coefficient

The percentage of edited measurements due to backscatter coefficient criterion is represented in figure 11. It is about 0.60% It is also impacted by low signal tracking anomalies, especially during cycle 1. The right part of figure 11 shows that measurements edited by backscatter coefficient criterion are especially found near coasts in the equatorial regions and enclosed sea (Mediterranean).

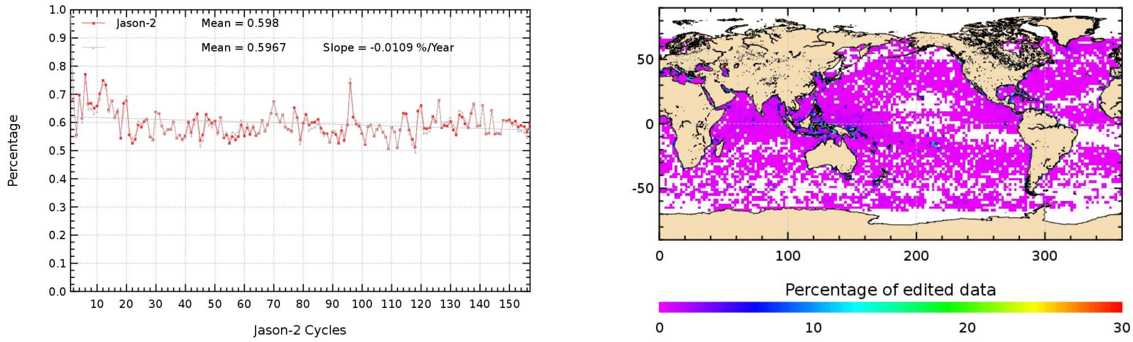

Figure 11: *Percentage of edited measurements by Sigma0 criterion. Left: Cycle per cycle monitoring. The gray curve shows the trend of edited measurements after adjusting for annual and semi-annual signals. Right: Map over a one year period (cycles 121to 157).*

3.2.10. Backscatter coefficient: 20 Hz standard deviation

The percentage of edited measurements due to 20 Hz backscatter coefficient standard deviation criterion is represented in figure 12. It is about 1.9%. The right part of figure 11 shows that measurements edited by 20 Hz backscatter coefficient standard deviation criterion are especially found in regions with disturbed waveforms.

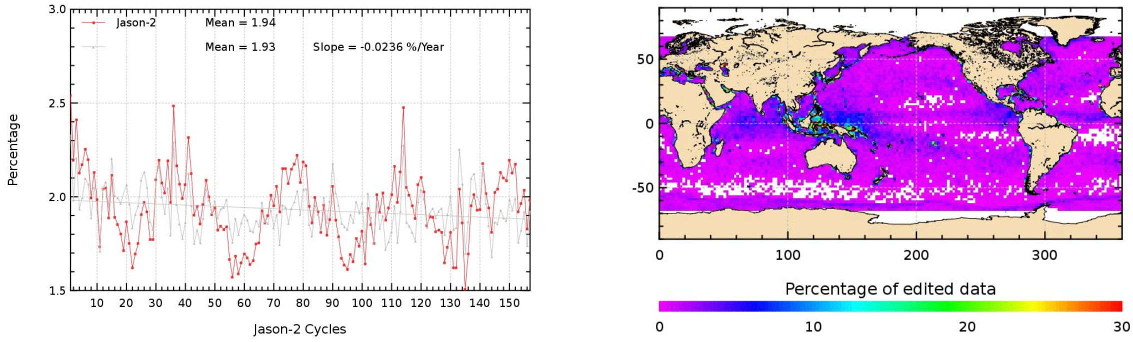

Figure 12: *Percentage of edited measurements by 20 Hz Sigma0 standard deviation criterion. Left: Cycle per cycle monitoring. The gray curve shows the trend of edited measurements after adjusting for annual and semi-annual signals. Right: Map over a one year period (cycles 121to 157).*

3.2.11. Radiometer wet troposphere correction

The percentage of edited measurements due to radiometer wet troposphere correction criterion is represented in figure 13. It is about 0.2%. When removing cycles which experienced problems, percentage of edited measurements drops to less than 0.1%. For cycle 19 the percentage of edited measurements is higher than usual. This is linked to radiometer wet troposphere correction at default value due to AMR unavailability.

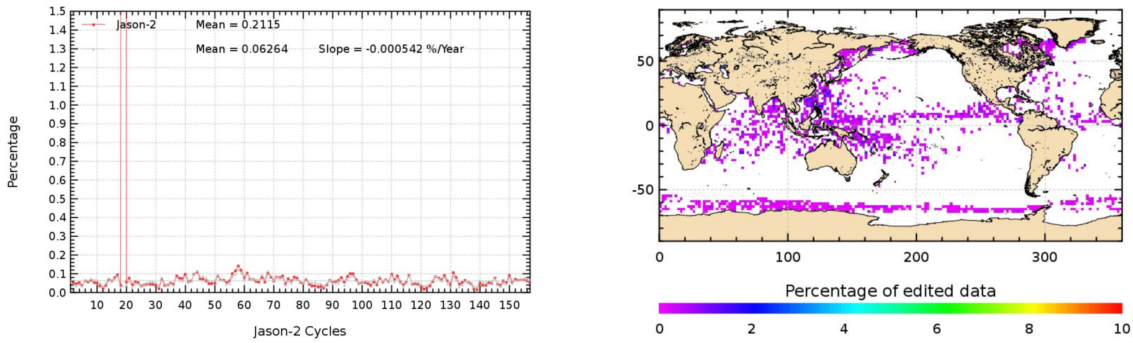

Figure 13: *Percentage of edited measurements by radiometer wet troposphere criterion. Left: Cycle per cycle monitoring. The gray curve shows the trend of edited measurements after adjusting for annual and semi-annual signals. Right: Map over a one year period (cycles 121to 157).*

3.2.12. Dual frequency ionosphere correction

The percentage of edited measurements due to dual frequency ionosphere correction criterion is represented in figure 14. It is about 1.2% and shows no drift. The map 14 shows that measurements edited by dual frequency ionosphere correction are mostly found in equatorial regions, but also near sea ice.

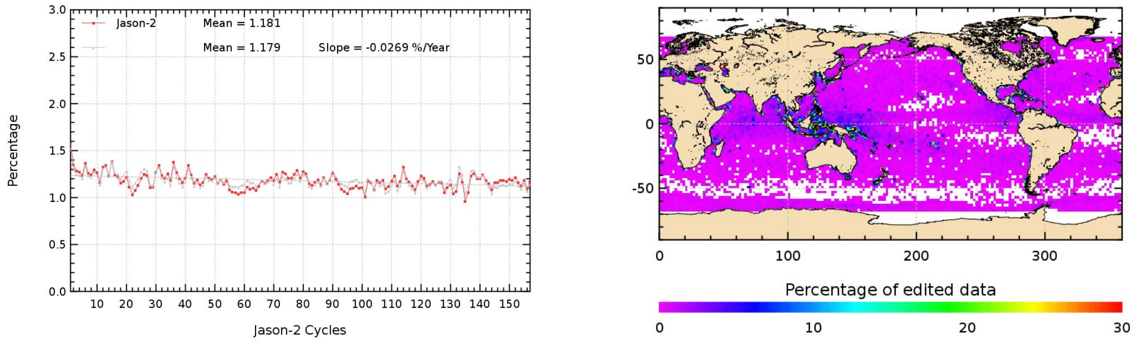

Figure 14: *Percentage of edited measurements by dual frequency ionosphere criterion. Left: Cycle per cycle monitoring. The gray curve shows the trend of edited measurements after adjusting for annual and semi-annual signals. Right: Map over a one year period (cycles 121to 157).*

3.2.13. Square off-nadir angle

The percentage of edited measurements due to square off-nadir angle criterion is represented in figure 15. It is about 0.6%. As for other parameters, impact of low signal tracking anomalies is visible in general for the first 16 cycles and especially for cycle 1. The map 15 shows that edited measurements are mostly found in coastal regions and regions with disturbed waveforms.

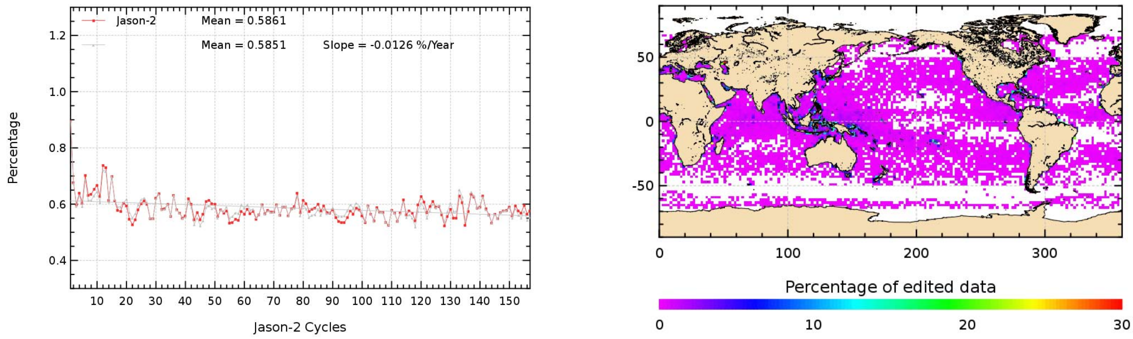

Figure 15: *Percentage of edited measurements by square off-nadir angle criterion. Left: Cycle per cycle monitoring. The gray curve shows the trend of edited measurements after adjusting for annual and semi-annual signals. Right: Map over a one year period (cycles 121to 157).*

3.2.14. Sea state bias correction

The percentage of edited measurements due to sea state bias correction criterion is represented in figure 16. The percentage of edited measurements is about 0.6% and shows no drift.
The map 16 shows that edited measurements are mostly found in equatorial regions near coasts.

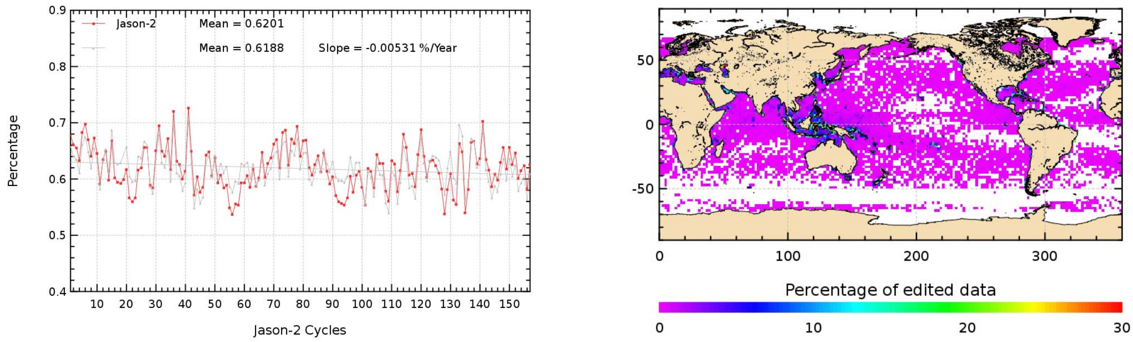

Figure 16: *Cycle per cycle percentage of edited measurements by sea state bias criterion (left). The gray curve shows the trend of edited measurements after adjusting for annual and semi-annual signals. Right: Map of percentage of edited measurements by sea state bias criterion over a one year period (cycles 121to 157).*

3.2.15. Altimeter wind speed

The percentage of edited measurements due to altimeter wind speed criterion is represented in figure 17. It is about 1.0%. The measurements are edited, because they have default values. This is the case when sigma0 itself is at default value, or when it shows very high values (higher than 25 dB), which occur during sigma bloom and also over sea ice. Indeed, the wind speed algorithm (which uses backscattering coefficient and significant wave height) can not retrieve values for sigma0 higher than 25 dB.
Wind speed is also edited, when it has negative values, which can occur in GDR products. Nevertheless, sea state bias is available even for negative wind speed values. Therefore, the percentage of edited altimeter wind speed is higher than that of edited sea state bias.

The map 17 showing percentage of measurements edited by altimeter wind speed criterion is correlated with maps 16 and 10.

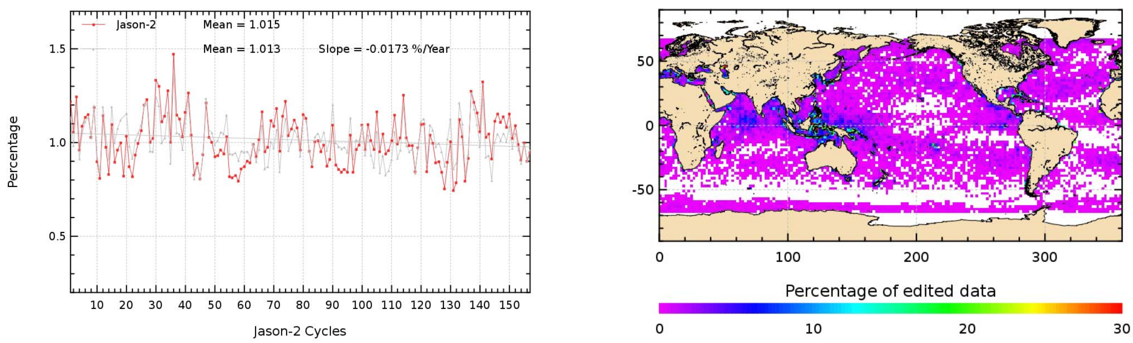

Figure 17: *Percentage of edited measurements by altimeter wind speed criterion. Left: Cycle per cycle monitoring.The gray curve shows the trend of edited measurements after adjusting for annual and semi-annual signals. Right: Map over a one year period (cycles 121to 157).*

3.2.16. Ocean tide correction

The percentage of edited measurements due to ocean tide correction criterion is represented in figure 18. It is less than 0.01% and is very stable. The ocean tide correction is a model output, there should therefore be no edited measurements. Indeed there are no measurements edited in open ocean areas, but only very few near coasts (Alaska, Kamchatka, Labrador). These measurements are mostly at default values.

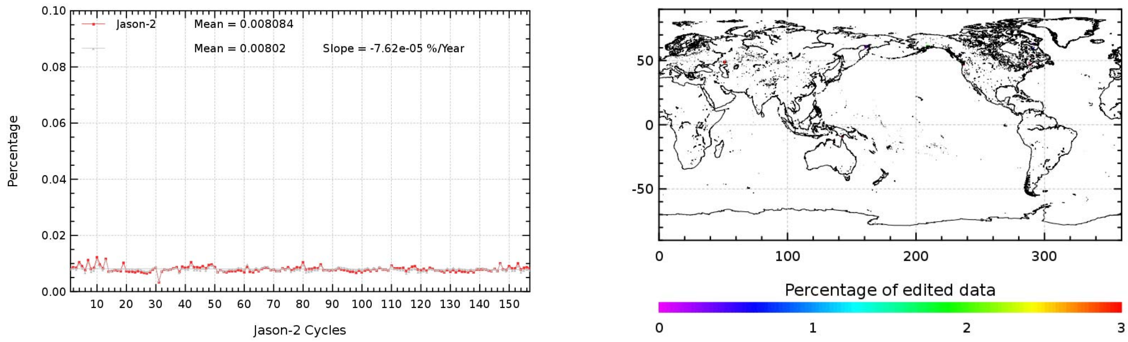

Figure 18: *Percentage of edited measurements by ocean tide criterion. Left: Cycle per cycle monitoring. The gray curve shows the trend of edited measurements after adjusting for annual and semi-annual signals. Right: Map over a one year period (cycles 121to 157).*

3.2.17. Sea surface height

The percentage of edited measurements due to sea surface height (orbit - ku-band range) criterion is represented in figure 19. It is about 0.77% and shows no drift. The measurements edited by sea surface height criterion are mostly found near coasts in equatorial regions (see map 19). The majority of the edited measurements has defaulted range values.

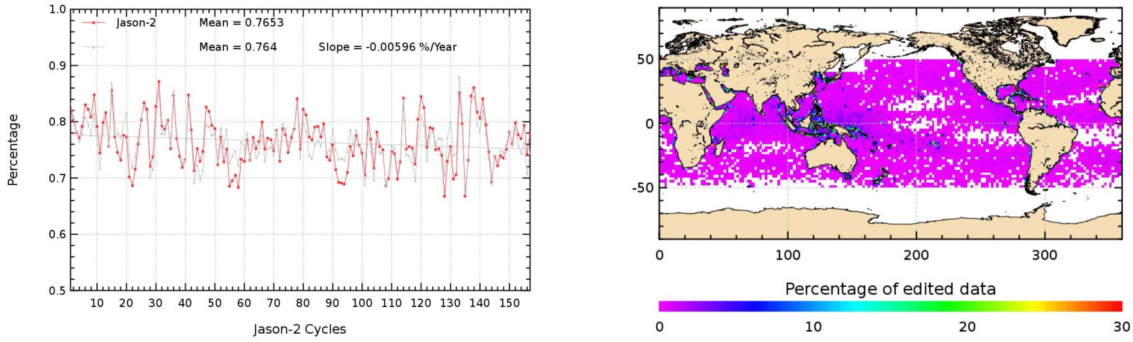

Figure 19: *Percentage of edited measurements by sea surface height criterion. Left: Cycle per cycle monitoring. The gray curve shows the trend of edited measurements after adjusting for annual and semi-annual signals. Right: Map over a one year period (cycles 121to 157).*

3.2.18. Sea level anomaly

The percentage of edited measurements due to sea level anomaly criterion is represented in figure 20. It is about 1.0% (0.9% without cycle 19) and shows no drift. The peak is related to AMR unavailability (see figure 13 (showing the percentage of measurements edited by AMR)), as the SLA clip contains, among other parameters, the radiometer wet troposphere correction.
Whereas the map in figure 20 allows us to plot the measurements edited due to sea level anomaly out of thresholds (after applying all other threshold criteria). There are only very few measurements, principally located in Caspian Sea.

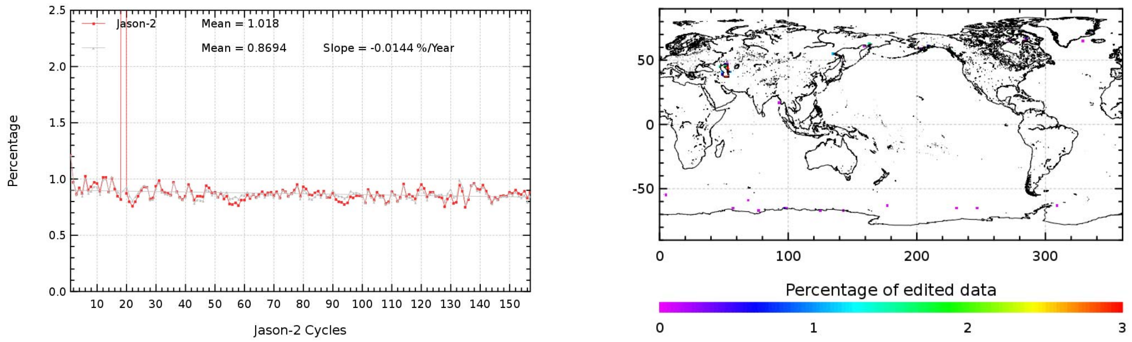

Figure 20: *Percentage of edited measurements by sea level anomaly criterion. Left: Cycle per cycle monitoring. The gray curve shows the trend of edited measurements after adjusting for annual and semi-annual signals. Right: Map over a one year period (cycles 121to 157).*

4. Monitoring of altimeter and radiometer parameters

4.1. Methodology

Both mean and standard deviation of the main parameters of Jason-2 (GDR-D) have been monitored since the beginning of the mission. Moreover, a comparison with Jason-1 parameters has been performed: it allows us to monitor the bias between the parameters of the 2 missions. Two different methods have been used to compute the bias:

- Till Jason-2 cycle 20, Jason-2 and Jason-1 are on the same ground track and are spaced out about 1 minute apart. The mean of the Jason-1 - Jason-2 differences can be computed using a point by point repeat track analysis.
- From Jason-2 cycle 21 (Jason-1 cycle 260), a maneuver sequence was conducted (from 26th of January to 14th of February 2009) to move Jason-1 to the new tandem mission orbit. Jason-1 has a repeat ground-track which is interleaved with Jason-2. It's the same ground-track as already used by Topex/Poseidon during its tandem phase with Jason-1, but there is a time shift of 5 days. Geographical variations are then too strong to directly compare Jason-2 and Jason-1 parameters on a point by point basis. Therefore day per day global differences have been carried out to monitor differences between the two missions. A filter over 11 days was applied. Nevertheless the differences are still quite noisy, especially for corrections which vary rapidly in time and space. Therefore occasional small jumps might be covered by the noise of the differences. Nevertheless it should be possible to detect drifts and permanent jumps. Jason-2 and Jason-1 were in this tandem phase from Jason-2 cycles 22 to 135 (Jason-1 cycles 262 to 374).

In February and March of 2012, Jason-1 experienced severals safe holds (anomaly on gyro3, double EDAC error in RAM memory). It was decided to move Jason-1 to geodetic orbit (more about the Jason-1 geodetic mission can be found in [7]). Science data on the geodetic orbit are available from 7th of May 2012. Note that the first cycle on the geodetic orbit starts with cycle 500 (this corresponds to end of Jason-2 cycle 141). The last (incomplete) cycle of Jason-1 on the repeat ground-track was cycle 374. As during the tandem phase, day per day global differences of the parameters have been carried out to monitor differences between the two missions.

Note that differences are done over Jason-2 cycles 1 to 157, corresponding to Jason-1 cycles 240 to 513/514.

4.2. 20 Hz Measurements

The monitoring of the number and standard deviation of 20 Hz elementary range measurements used to derive 1 Hz data is presented here. These two parameters are computed during the altimeter ground processing. For both Jason-1 and Jason-2, before performing a regression to derive the 1 Hz range from 20 Hz data, a MQE (mean quadratic error) criterion is used to select valid 20 Hz measurements. This first step of selection consists in verifying that the 20 Hz waveforms can be approximated by a Brown echo model (Brown, 1977 [16]) (Thibaut et al. 2002 [54]). Then, through an iterative regression process, elementary ranges too far from the regression line are discarded until convergence is reached. Thus, monitoring the number of 20 Hz range measurements and the standard deviation computed among them is likely to reveal changes at instrumental level.

The Jason-1 MQE threshold are not applicable to Jason-2, using those thresholds would edit more measurements than necessary. Therefore, for the first GDR release of Jason-2 (GDR-T), the MQE threshold had been set to default, leading to no editing based on MQE values. Note that for Jason-2 data in version GDR-D, specific Jason-2 MQE thresholds were computed and are applied.

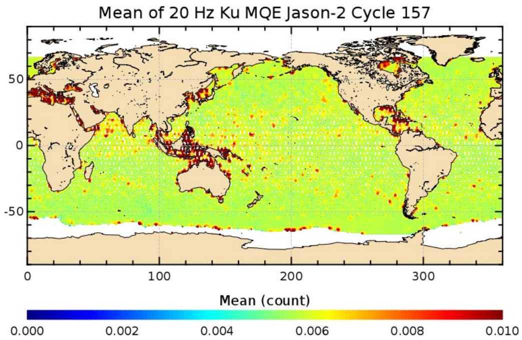

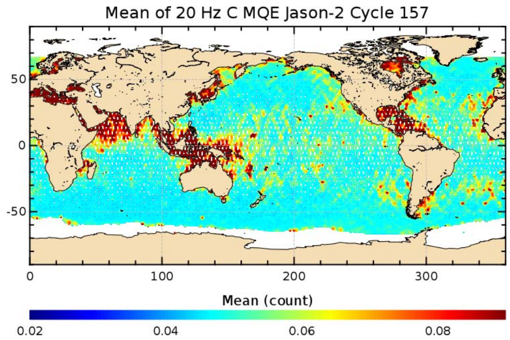

Figure 21: *Map of 20 Hz Ku-band (left) and C-band (right) MQE for Jason-2 cycle 157. Note that the color scales are different for the two maps.*

4.2.1. 20 Hz measurements number in Ku-Band and C-Band

GDR-D Jason-2 number of elementary 20 Hz range mesurements is very similar to Jason-1's (especially for C-band) with an average of 19.61 for Ku-band and 19.25 for C-band as shown on figure 22. For both satellites a slight annual signal is visible (especially for C-band). Figures 23 and 24 show on the left the daily monitoring of the mean and standard deviation of Jason-1 - Jason-2 differences of 20-Hz measurements number in Ku-Band and C-band during the formation flight phase. Besides a slight variation, they are quite stable and do not show any anomaly. Number of 20 Hz Ku-band range measurements is slightly higher for Jason-2 than for Jason-1, since mean of Jason-1 - Jason-2 difference is slightly negatif (-0.06 for Ku-band), whereas the difference for C-band is close to zero. The regions where Jason-1 has less elementary Ku-band range measurements are especially located around Indonesia, as shown on map of Jason-1 - Jason-2 differences (right side of figures 23). Indeed in regions of sigma bloom or rain, using a MQE criterion during the regression to derive 1Hz from 20Hz data, discards 20 Hz measurements and therefore reduces the value of number of the 20 Hz measurements used for the 1 Hz data. It is possible that diffrences in the tuning of the MQE criterion for Jason-1 and Jason-2 Ku-band explain what is observed on the right side of figure 23.

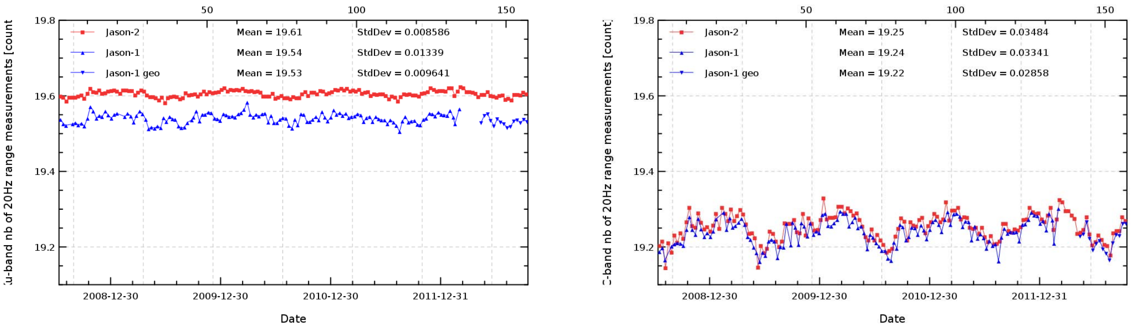

Figure 22: *Cyclic monitoring of number of elementary 20 Hz range measurements for Jason-1 and Jason-2 for Ku-band (left) and C-band (right).*

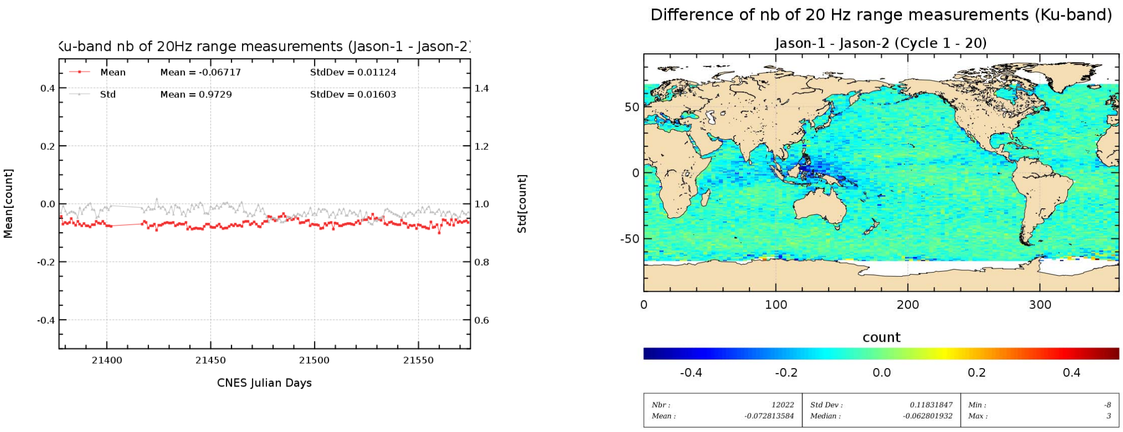

Figure 23: *Daily monitoring of mean and standard deviation of Jason-1 - Jason-2 differences for number of elementary 20 Hz Ku-band range measurements (left) and map showing mean of Jason-1 - Jason-2 differences over cycles 1 to 20.*

4.2.2. 20 Hz measurements standard deviation in Ku-Band and C-Band

Jason-2 standard deviation of the 20 Hz measurements is 8.0 cm for Ku-Band and 17.3 cm for C-Band (figure 25). It is very similar to Jason-1 data. Figure 26 and 27, showing daily monitoring of Jason-1 - Jason-2 difference of standard deviation of the 20 Hz measurements in Ku-Band and C-Band (on the left), reveal no trend neither anomaly. C-Band standard deviation of the 20 Hz measurements rms is noisier than those of Ku-Band. This is directly linked to the C-band standard deviation which is higher than the Ku, as the onboard averaging is performed over less waveforms (6 Ku for 1 C) leading to an increased noise.

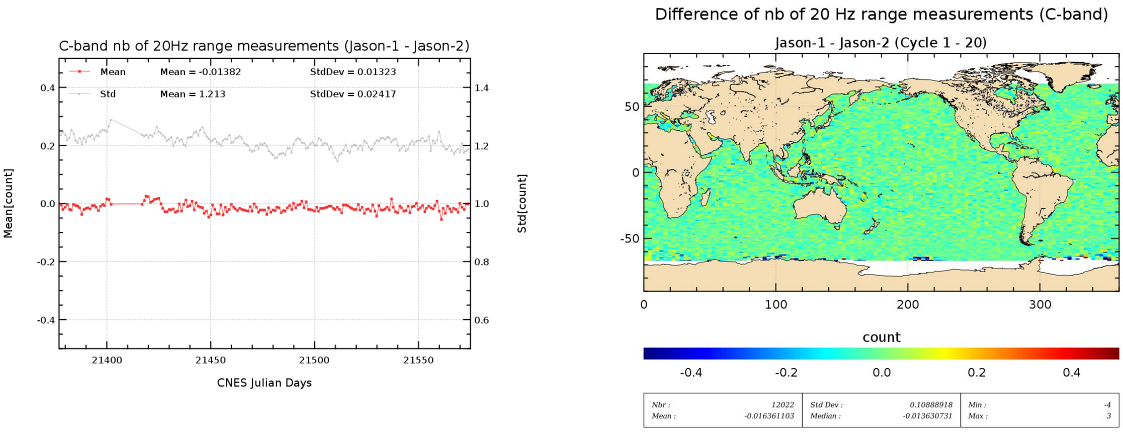

Figure 24: *Daily monitoring of mean and standard deviation of Jason-1 - Jason-2 differences for number of elementary 20 Hz C-band range measurements (left) and map showing mean of Jason-1 - Jason-2 differences over cycles 1 to 20.*

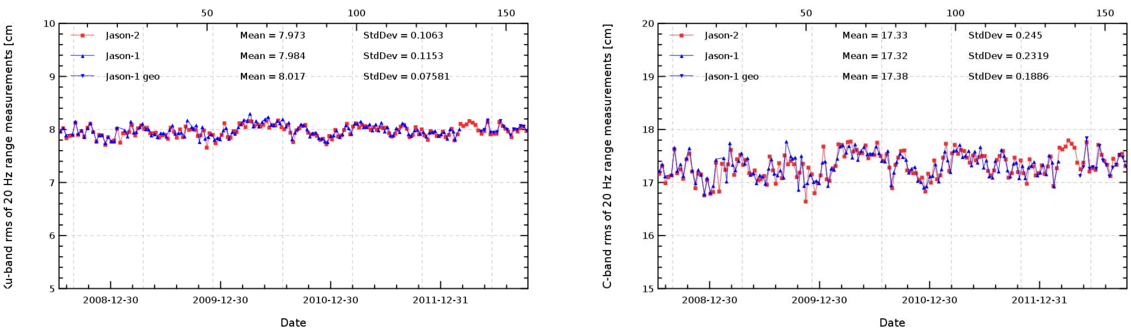

Figure 25: *Cyclic monitoring of rms of elementary 20 Hz range measurements for Jason-1 and Jason-2 for Ku-band (left) and C-band (right).*

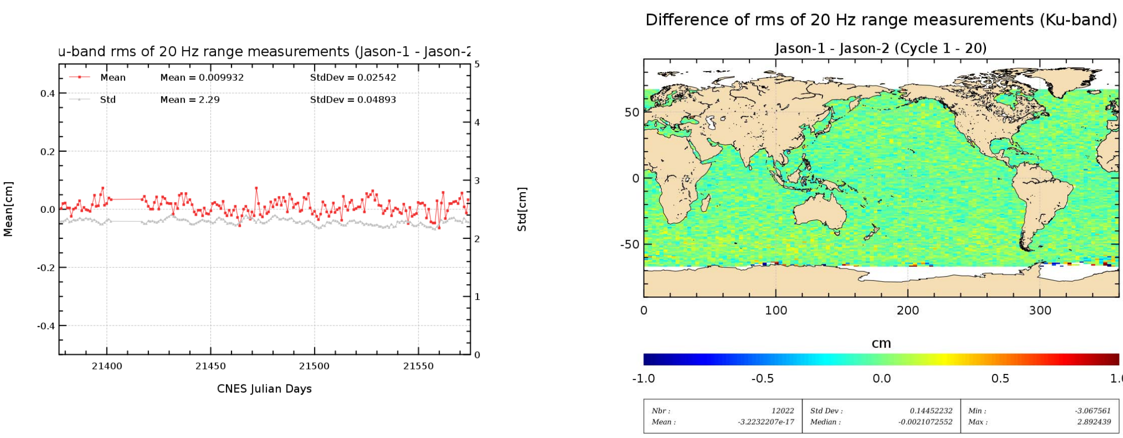

Figure 26: *Daily monitoring of mean and standard deviation of Jason-1 - Jason-2 differences for the rms of elementary 20 Hz Ku-band range measurements (left) and map showing mean of Jason-1 - Jason-2 differences over cycles 1 to 20 (right).*

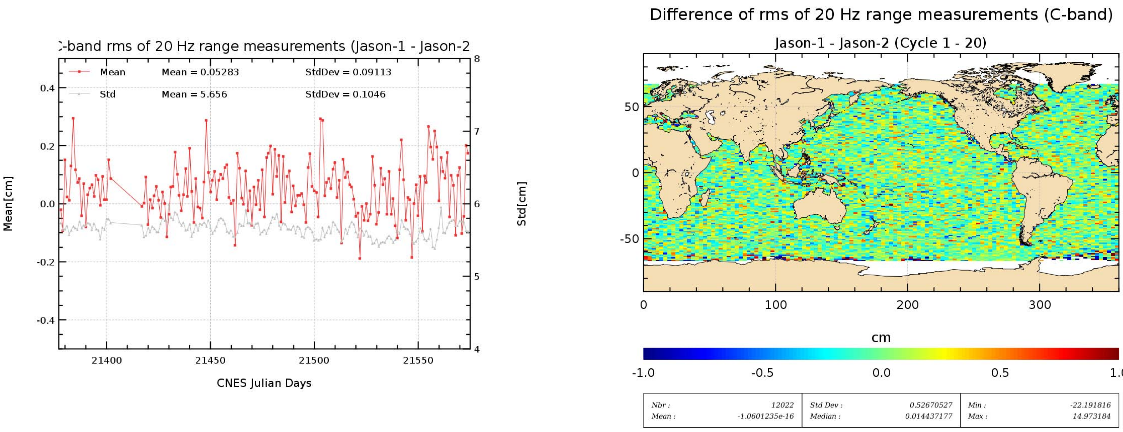

Figure 27: *Daily monitoring of mean and standard deviation of Jason-1 - Jason-2 differences for rms of elementary 20 Hz C-band range measurements (left) and map showing mean of Jason-1 - Jason-2 differences over cycles 1 to 20 (right).*

4.3. Off-Nadir Angle from waveforms

The off-nadir angle is estimated from the waveform shape during the altimeter processing. The square of the off-nadir angle, averaged on a daily basis, has been plotted for Jason-1 and Jason-2 on the left side of figure 28, whereas the right side shows the histograms over one cycle. For GDR-D Jason-2 the mispointing is very stable and very close to zero (though very slightly negative). Whereas Jason-1 may show higher values (related to the reduced tracking performance of both star trackers, especially during fixed-yaw). Jason-1 experienced especially during 2010 very high mispointing values, for more information see Jason-1 validation report [64]. Jason-1 mispointing situation has been highly improved since end of 2010.
Jason-2 GDR-T mispointing was slightly positive (see also reprocessing report ([10])), which was related to the antenna aperture values used for data processing (1.26° for GDR-T, 1.29° for GDR-D). Indeed [56] shows, that retracking with different values of antenna aperture, changes the mean value of Jason-2 mispointing (see figure 29). Note that for Jason-1 1.28° is used for the antenna aperture.

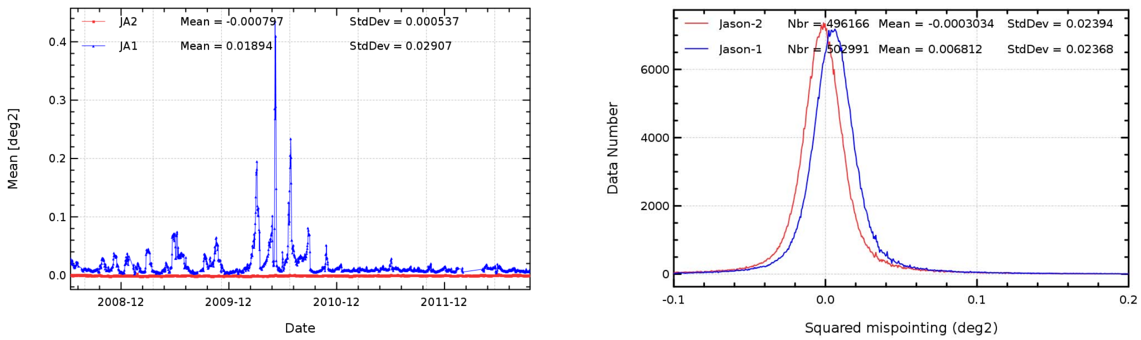

Figure 28: *Square of the off-nadir angle deduced from waveforms (deg^2) for Jason-1 and Jason-2: Daily monitoring (left), histograms for Jason-2 cycle 157 (Jason-1 cycle 513/514).*

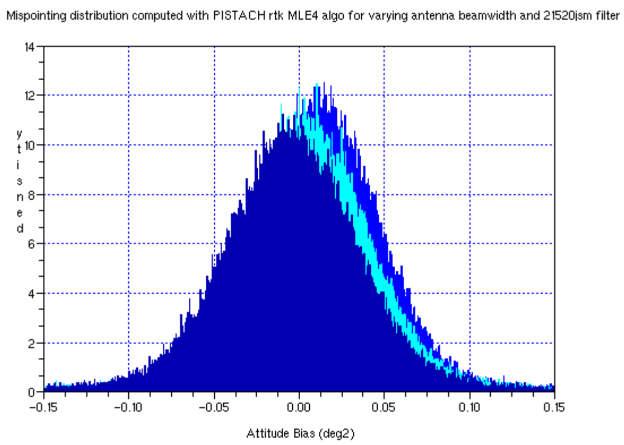

Figure 29: *Histograms of Jason-2 mispointing after retracking with different antenna beamwidth (from [56]): 1.26° (blue), 1.28° (light blue), 1.30° (dark blue).*

4.4. Backscatter coefficient

The Jason-2 Ku-band and C-band backscattering coefficient shows good agreement with Jason-1 as visible for cyclic monitoring in figure 30 (top left and right). Left sides of figures 31 and 32 show daily monitoring of mean differences during the formation flight phase. For Ku-band, a bias close to 0.3 dB is detected, it varies slightly (+/- 0.05 dB). This slight variation (± 0.05 dB) is related to Jason-1 backscattering coefficient which is slightly impacted by the higher off-nadir angles (due to low star tracker availability). Note that backscattering coefficients include instrumental corrections, which include also atmospheric attenuation which comes from the radiometer. Therefore differences between backscattering coefficients can also be partly due to differences between the atmospheric attenuation algorithms of Jason-1 and Jason-2. They main reasons for the differences (between Jason-1 and Jason-2 backscattering coefficients) are related to the antenna calibrations and to the internal calibrations of the altimeters (steps of numerical gain control).
The average standard deviation of both Sigma0 differences (measurements by measurements) is also very low around 0.15 dB rms. C-Band sigma0 differences indicate a small bias close to 0.16 dB. In the meantime, the map of mean differences (right side of figures 31 and 32) highlights very small differences. During the tandem phase (from Jason-2 cycle 21 onwards), mean differences continue to be calculated but comparing only the global day per day statistics (see bottom of figure 30). Although the statistic is calculated less accurately, a similar bias is observed as during the formation flight phase, and no significant drift is detected between both missions.

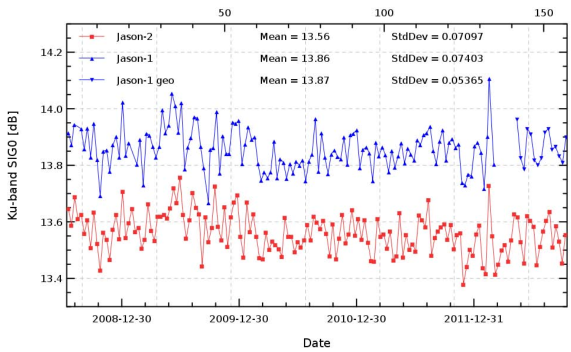

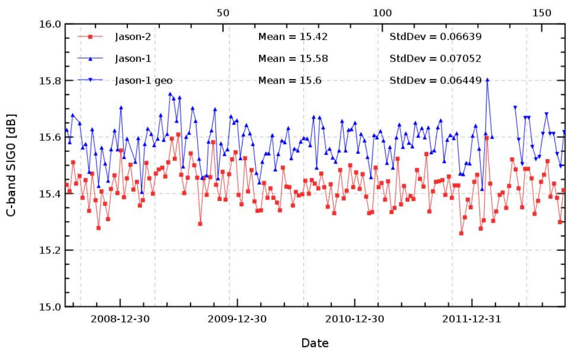

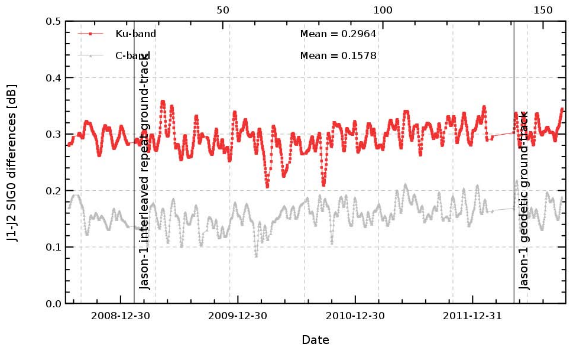

Figure 30: *Cyclic monitoring of Sigma0 for Jason-1 and Jason-2 for Ku-band (left) and C-band (right). Daily monitoring of Jason-1 - Jason-2 differences (bottom), a 10 day filter is applied.*

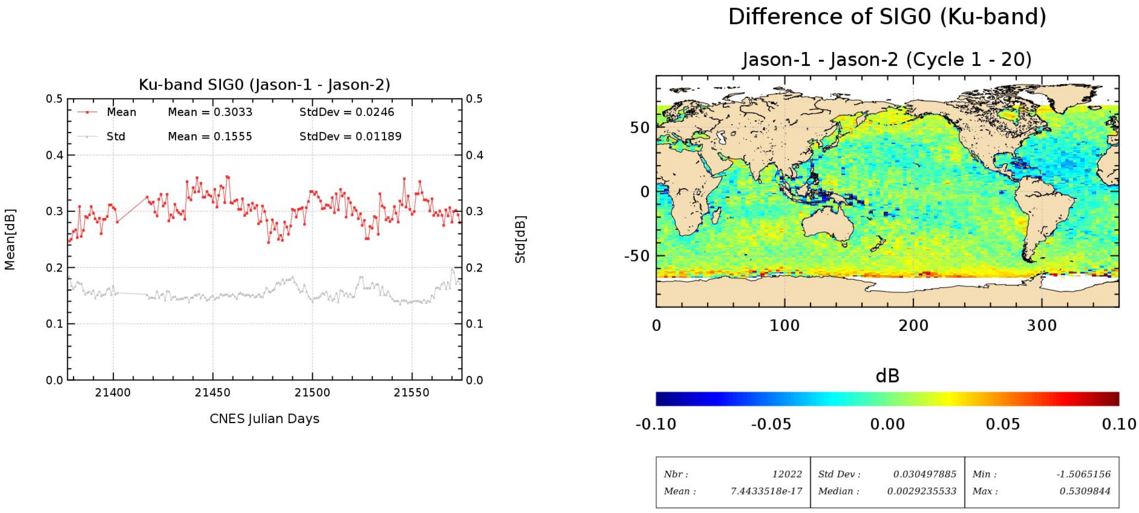

Figure 31: *Daily monitoring of mean and standard deviation of Jason-1 - Jason-2 differences for Ku-band Sigma0 (left) and map showing mean of Jason-1 - Jason-2 differences over cycles 1 to 20.*

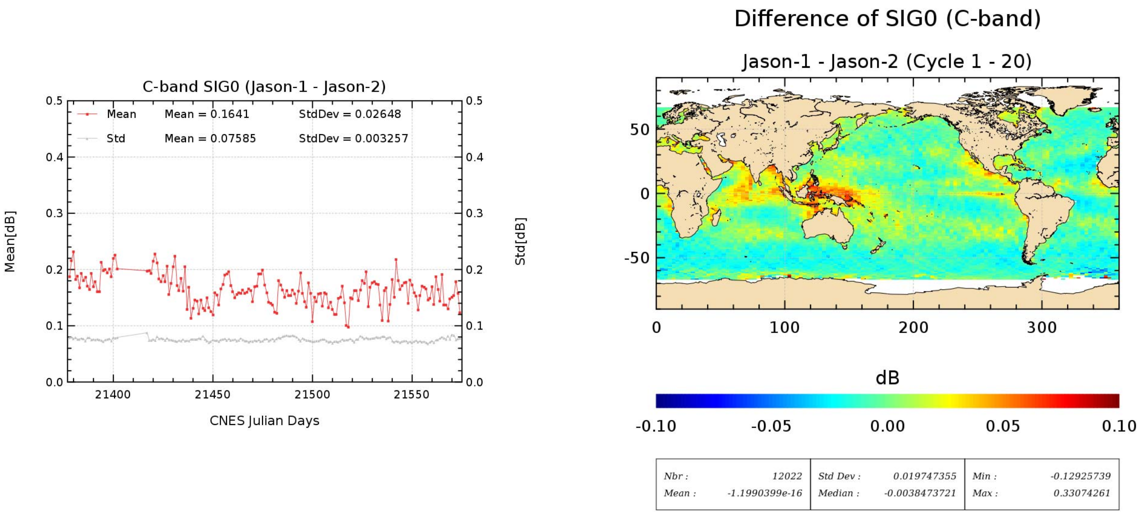

Figure 32: *Daily monitoring of mean and standard deviation of Jason-1 - Jason-2 differences for C-band Sigma0 (left) and map showing mean of Jason-1 - Jason-2 differences over cycles 1 to 20.*

4.5. Significant wave height

As for Sigma0 parameter, a very good consistency between both significant wave height is shown (see top left and right of figure 33). A small bias close to around -1.3 cm is calculated over the formation flight phase. It is close to -1.7 cm in C-band (see left side of figures 34 and 35). It is stable in time and space (see map of differences in right side of figures 34 and 35). These differences are too weak to impact scientific applications. They are probably due to ground processing differences between both missions. Differences are noisier for C-band. As previously, extending the monitoring of SWH bias during the tandem phase (bottom of figure 33) highlights larger variations since both satellites do not measure the same SWH. However bias is still stable and no drift is detected.

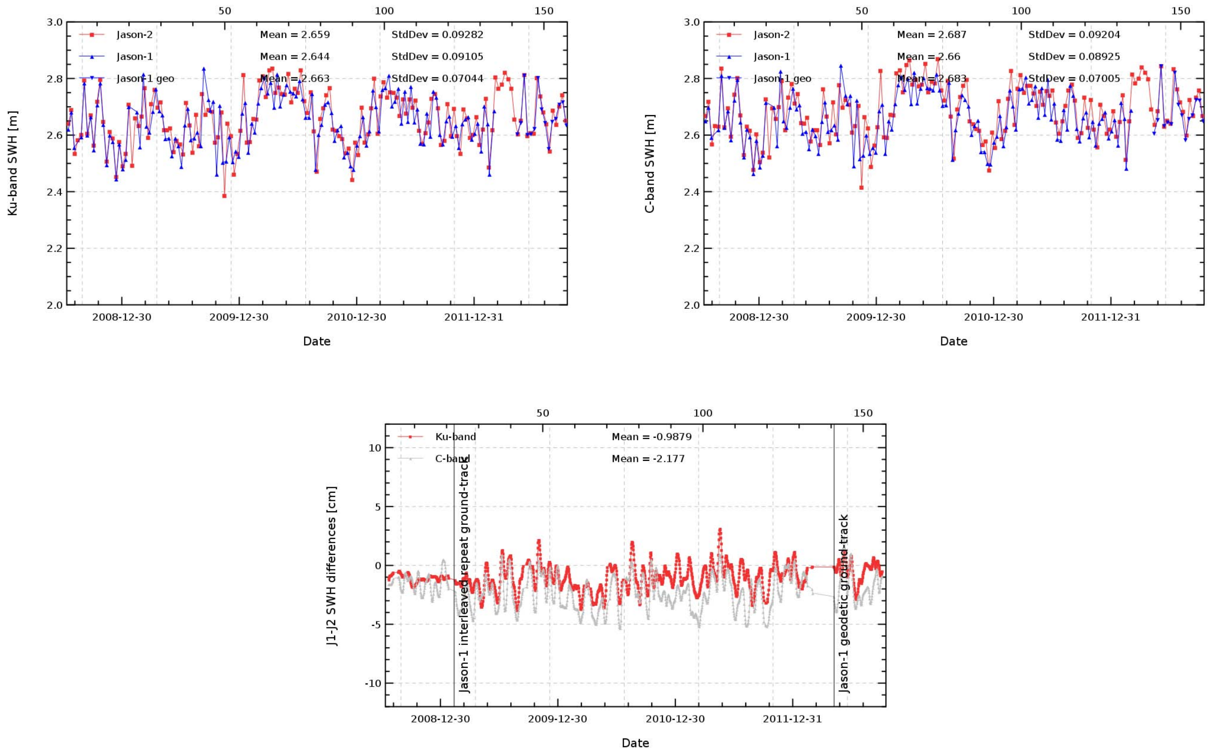

Figure 33: *Cyclic monitoring of SWH for Jason-1 and Jason-2 for Ku-band (left) and C-band (right). Daily monitoring of Jason-1 - Jason-2 differences (bottom), a 10 day filter is applied.*

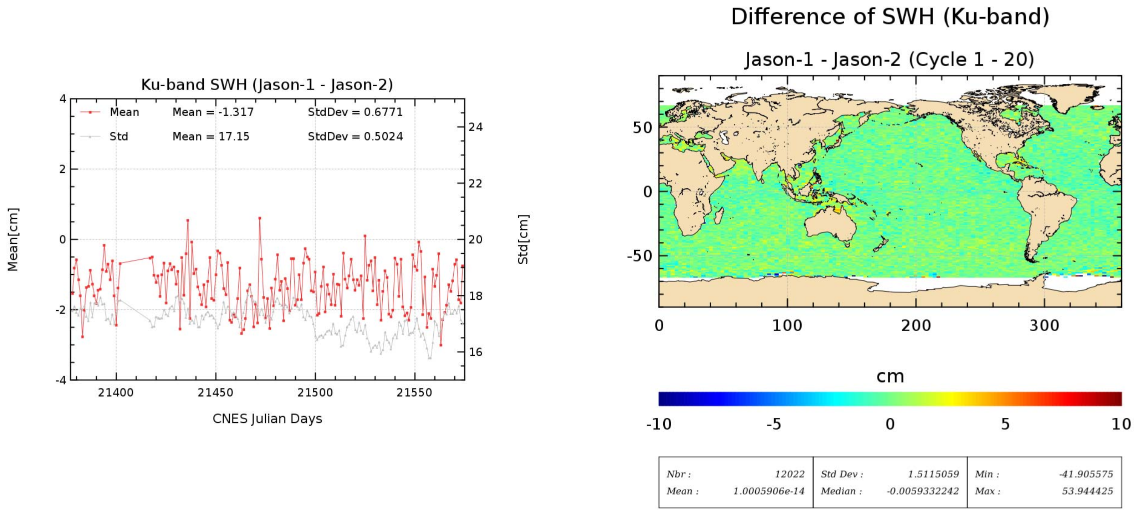

Figure 34: *Daily monitoring of mean and standard deviation of Jason-1 - Jason-2 differences for Ku-band SWH (left) and map showing mean of Jason-1 - Jason-2 differences over cycles 1 to 20.*

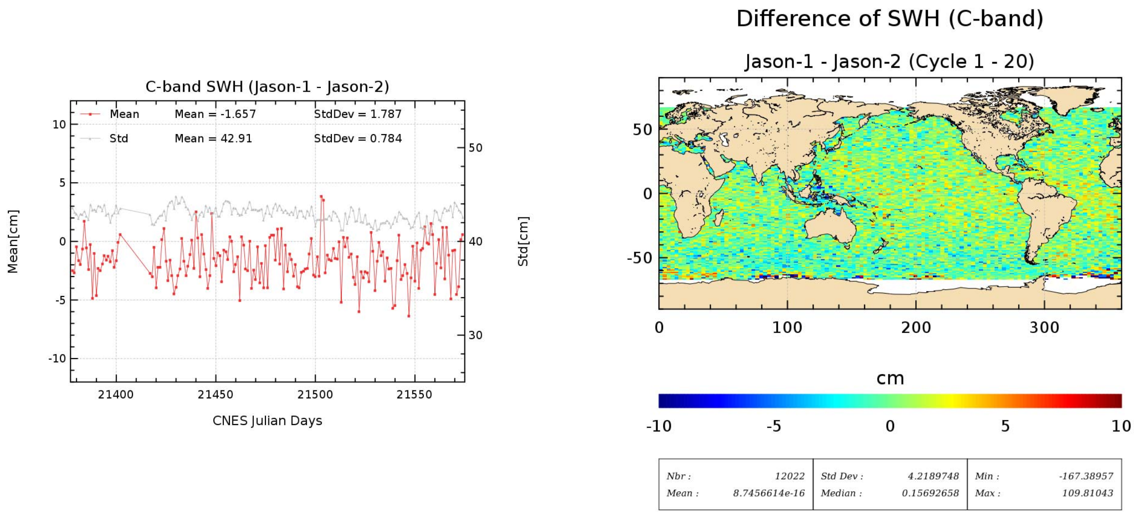

Figure 35: *Daily monitoring of mean and standard deviation of Jason-1 - Jason-2 differences for C-band SWH (left) and map showing mean of Jason-1 - Jason-2 differences over cycles 1 to 20.*

4.6. Dual-frequency ionosphere correction

The dual frequency ionosphere corrections derived from the Jason-2 and Jason-1 altimeters show a mean difference of about -0.3 cm (figure 36 (left)), with cycle to cycle variations lower than 1 mm. This bias is due to the relative Ku-band (-7.0 cm) and C-band (-2.2 cm) range difference between Jason-1 and Jason-2, as well as the relative Ku-band (-2.8 cm) and C-band (-6.0 cm) sea state difference between Jason-1 and Jason-2. As the dual-frequency ionosphere correction is derived from a combination of Ku and C band ranges (corrected for the corresponding sea state bias), a bias of -3 mm between Jason-1 and Jason-2 ionospheric corrections results. Apart from this bias, the two corrections are very similar and vary according to the solar activity. The map of local differences (figure 36 right) shows small regional differences.

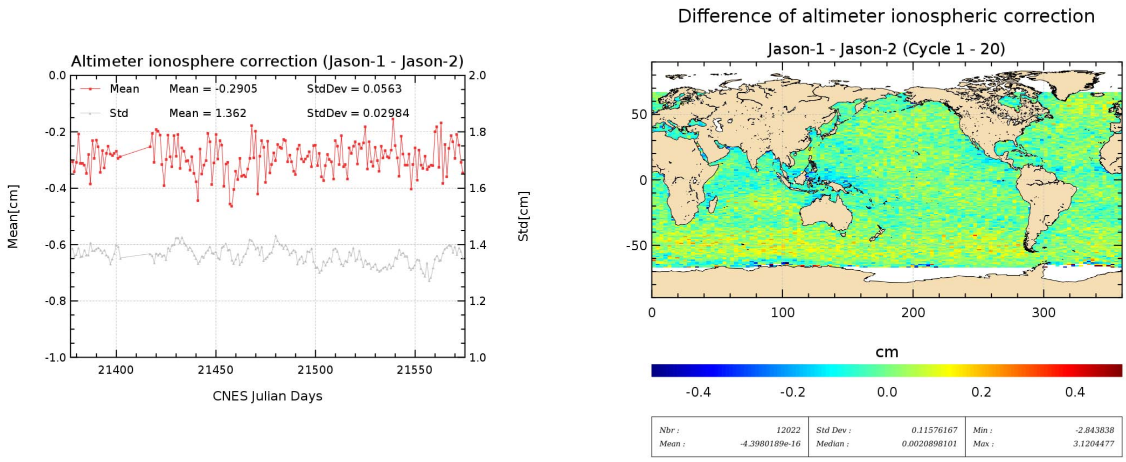

Figure 36: *Daily monitoring of mean and standard deviation of Jason-1 - Jason-2 differences for dual-frequency ionospheric correction (left) and map showing mean of Jason-1 - Jason-2 differences over cycles 1 to 20.*

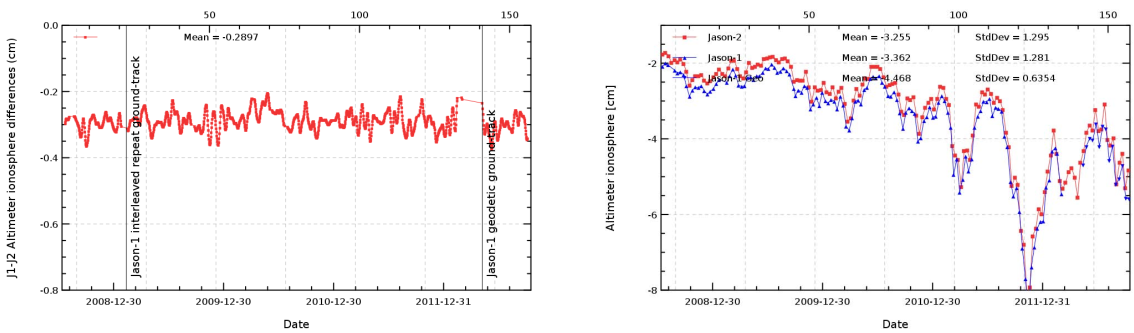

Figure 37: *Cyclic monitoring of dual-frequency ionosphere for Jason-1 and Jason-2 (right). Daily monitoring of Jason-1 - Jason-2 differences (left), a 10 day filter is applied.*

Notice that, as for TOPEX and Jason-1 (Le Traon et al. 1994 [40], Imel 1994 [38], Zlotnicky

1994 [65]), it is recommended to filter the Jason-2 dual frequency ionosphere correction before using it as a SSH geophysical correction (Chambers et al. 2002 [22]). A low-pass filter has thus been used to remove the noise of the correction in all SSH results presented in the following sections. Plotting difference of non-filtered ionospheric correction between Jason-1 and Jason-2 versus Jason-2 ionospheric correction shows an apparent scale error, which disappears when using filtered data (see figure 38). As in the beginnig of the Jason-2 mission, ionosphere correction was very low, the ionosphere noise is of the same order of magnitude as the ionosphere correction itself. Therefore plotting the difference of non-filtered dual-frequency ionospheric correction versus dual-frequency ionospheric correction induces an apparent scale error.

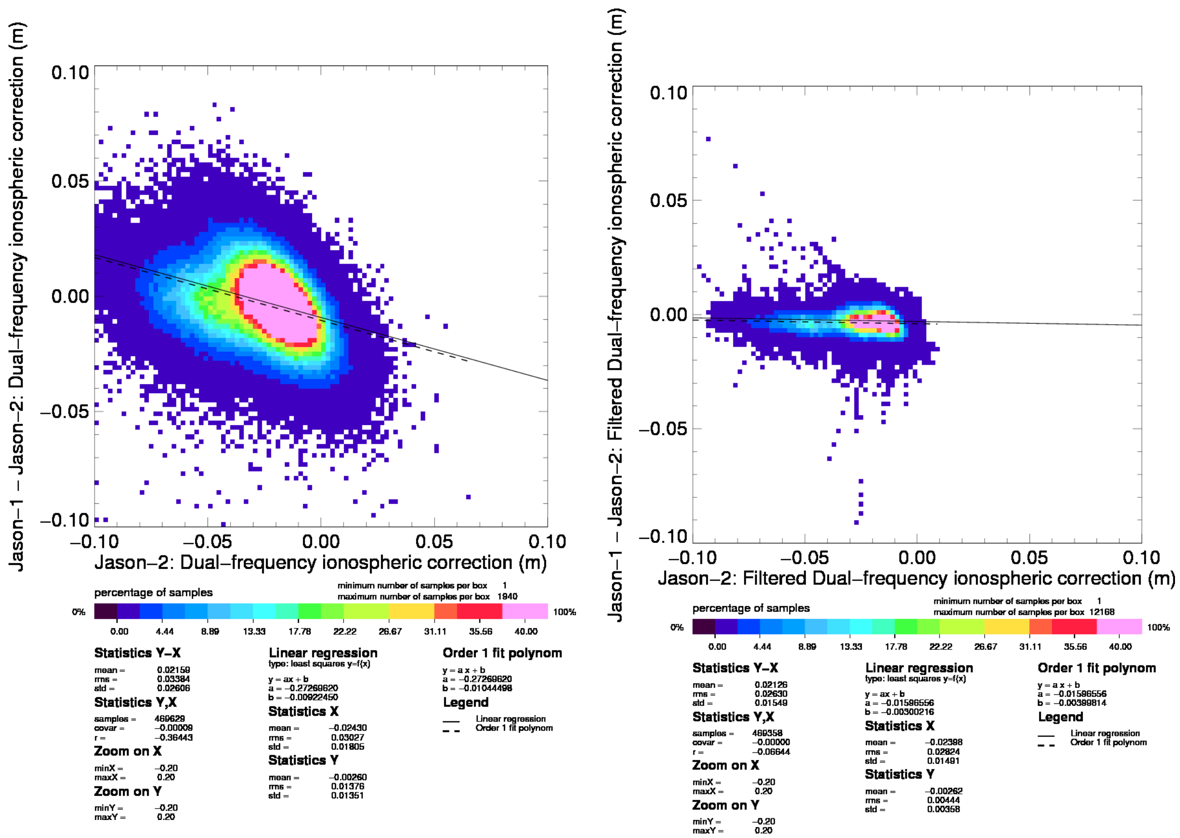

Figure 38: *Diagram of dispersion of Jason-1 - Jason-2 versus Jason-2 dual-frequency ionosphere correction for Jason-2 cycle 15. Left: non-filtered, right: filtered.*

During 2011, solar activity has increased and therefore also the absolute value of ionosphere correction (right part of figure 37).
When comparing altimeter ionosphere correction to GIM correction (figure 39), mean as well as standard deviation of this difference increases over 2011. This concerns both Jason missions. Figure 40 shows the mean difference between altimeter ionosphere and GIM correction after a one-year smooth for slots of local hours. Ionosphere differences between altimeter and GIM are higher for day time measurements than for night time measurements.

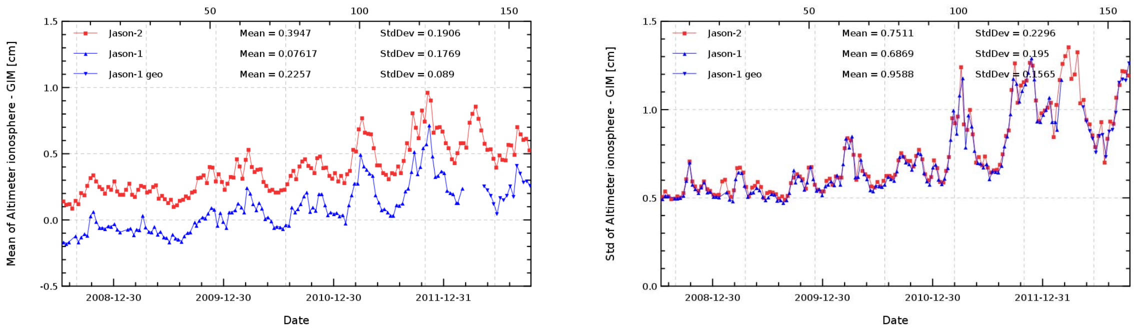

Figure 39: *Cycle per cycle monitoring of filtered altimeter ionosphere correction minus GIM ionosphere correction for Jason-1 and Jason-2. Left: Mean, right: standard deviation.*

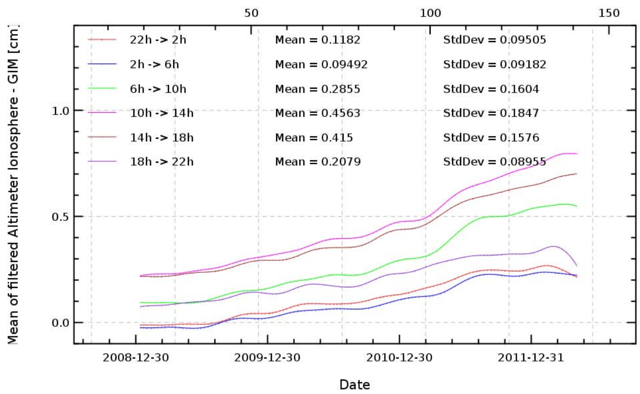

Figure 40: *Cycle per cycle monitoring of filtered altimeter ionosphere minus GIM correction computed per local hour time intervals. A one-year smooth is applied.*

4.7. AMR Wet troposphere correction

4.7.1. Overview

The Jason-2 radiometer wet troposphere correction available in GDR-D products contains beside the correction of the 34 GHz anomaly and the use of new calibration coefficients, an improved retrieval algorithm near coasts ([19]). Note that the GDR-D AMR radiometer wet troposphere correction has (according to S. Brown) several level of calibration:

- Cycles 1-113 - Climate data record quality calibration Cycles
- 114-140 - Intermediate quality calibration (somewhere between climate quality and operational(ARCS) quality)
- Cycle 141 onward - Operational(ARCS) quality calibration

Figure 41 shows on the left side the daily monitoring of the difference of radiometer wet troposphere correction between the two missions (JMR - AMR) during the formation flight phase. Note that for Jason-1 the JMR replacement product (which was available for cycles 228 to 259) was used. This corrects for stability problems of JMR which occured after the safehold in August 2008. For the other cycles the correction available in Jason-1 GDR-C is used. AMR is globally slightly dryer than JMR (-0.09 cm). But locally, especially near coasts (right side of figure 41), AMR is wetter than JMR. This is related to the fact that the Jason-2 correction uses improved retrieval algorithm in coastal areas, whereas this is not the case for Jason-1. The daily monitoring is very stable, except for julian day 21556 (2009-01-07), where the difference between the two radiometers shows a drop of 3 mm. This is related to the JMR replacement, which is for this day about 3 mm wetter than usually.

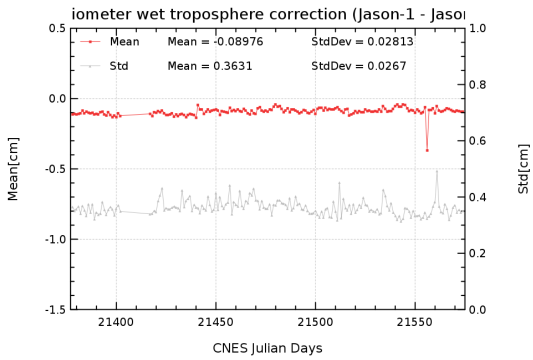

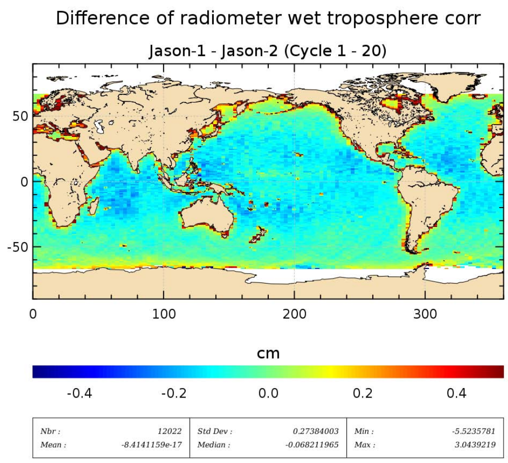

Figure 41: *Daily monitoring of mean and standard deviation (left) of Jason-1 - Jason-2 radiometer wet troposphere correction. Map showing mean of Jason-1 - Jason-2 differences over cycles 1 to 20.*

4.7.2. Comparison with the ECMWF model

The ECWMF wet troposphere correction has been used to check the Jason-1 and Jason-2 radiometer corrections. Daily differences are calculated and plotted in figure 43. It clearly appears (on left side of figure 43) that Jason-2 radiometer correction (AMR) from GDR products is much more stable than for Jason-1 (JMR), especially at the beginning of Jason-2 period where large oscillations (up to 7mm) are observed between JMR (from GDR-C product) and model. Indeed after the safehold mode of Jason-1 in August 2008 (corresponding to Jason-2 cycle 4), JMR experienced some thermal instability. In addition, small differences linked to yaw-dependent effects (as also observed on TOPEX radiometer (Dorandeu et al., 2004, [30])) are visible (yaw maneuvers are indicated as gray lines on left side of figure 43). In order to take into account these effects, new JMR calibration coefficients are provided and updated at each Jason-1 GDR reprocessing campaign. Using the JMR replacement (available for Jason-1 cycles 228 to 259) product corrects for the instabilities during August 2008 (Brown et al. 2009, [18]). Now, thanks to the new ARCS (Autonomous Radiometer Calibration System) (Brown et al. 2009, [18]) calibration system set up for Jason-2, AMR radiometer correction is calibrated at each GDR cycle and the calibration coefficients are modified if necessary. On right side of figure 43 the black lines indicate, each time a modification of the calibration coefficients were necessary. The lines are only drawn from cycle 114 onwards.
During 2011, the frequency of application of new calibration coefficients has increased, especially during summer 2011. The AMR wet troposphere correction shows jumps and drifts in the IGDRs. The calibrations applied for the GDRs correct most of these anomalies, nevertheless small jumps persist. There are also small drifts visible within a cycle (for exemple cycle 111 and 112), as the ARCS corrections apply a discret value to correct a drift. Furthermore, the AMR comparison with model highlights also long-term signals with Jason-2 not clearly observed with Jason-1. As a result of a poor confidence in stability of just one radiometer, Envisat wet troposphere correction (MWR) is also compared to the ECMWF model in the same figure 43 (left side). Sometimes MWR and JMR show similar differences, sometimes AMR and JMR show similar differences. For AMR, there might be a risk that real geophysical signals are absorbed by the calibration method used. Finally, the cross-comparison between all radiometers and models available is necessary to analyze the stability of each wet troposphere correction. An overview of the wet troposphere correction importance for mean sea level is given in Obligis et al. [42].

Figure 42 shows mean and standard deviation for cycle per cycle differences between Jason-2 radiometer and ECMWF model wet troposphere corrections for several data types. As previously mentionned, OGDR and IGDR radiometer data are more subject to drifts and jumps. The mean of OGDR and IGDR wet troposphere differences is quite similar, but the standard deviation is higher for OGDR than for IGDR, as OGDR contain predicted model fields instead of analysed model field (for IGDR and GDR products).

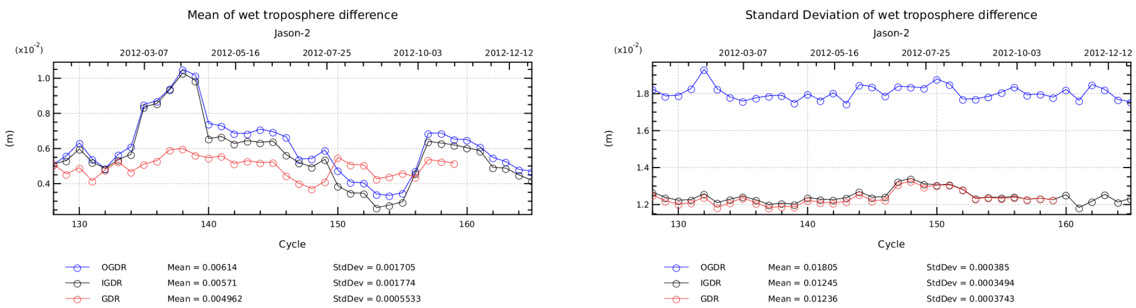

Figure 42: *Cycle per cycle monitoring of mean (left) and standard deviation (right) of radiometer minus ECMWF model wet troposphere correction over 2012 for Jason-2 O/I/GDR.*

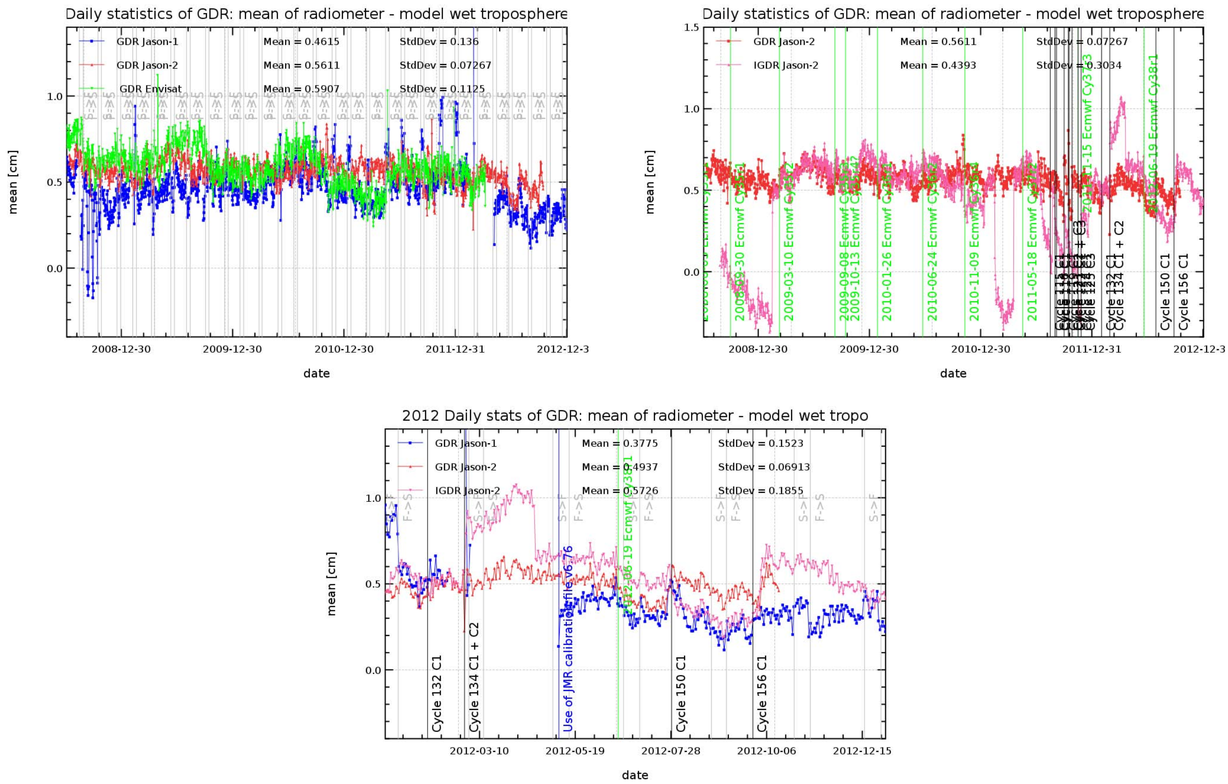

Figure 43: *Daily monitoring of radiometer and ECMWF model wet troposphere correction differences for Jason-1 (blue), Jason-2 (red) and Envisat (green) limited to 66° latitude. Vertical gray lines correspond to yaw maneuvers on Jason-2. Right: daily monitoring for Jason-2 GDRs (red) and IGDRs (pink). Vertical green lines correspond to ECMWF model version changes, black lines correspond to AMR calibration coefficients changes on GDR products also impacting IGDR product (but latter). Bottom: Daily monitoring for Jason-2 GDRs (red) and IGDRs (pink), as well as Jason-1 GDRs (blue) for 2012. Vertical green lines correspond to ECMWF model version changes, black lines correspond to AMR calibration coefficients changes on GDR products. They impact also IGDR products (but later).*

4.8. Altimeter wind speed

Figure 44 shows on the left side the daily monitoring of the difference of altimeter wind speed between the two missions. Before the Jason-2 reprocessing, there was a difference of about -0.4 m/s between Jason-1 and Jason-2. This is also shown on figure 45 displaying wind speed histograms. Note that the histograms of Jason-2 GDR-T and Jason-1 have different shapes. Using GDR-D data, the mean difference between Jason-1 and Jason-2 altimeter wind speed is reduced to 0.05 m/s, and the shapes of the histograms are also much more closer. Finally the regional differences are also reduced. Locally (right side of figure 44), altimeter wind speed from Jason-1 is higher than from Jason-2. The signal visible on daily monitoring, is anti-correlated to the signal visible on daily monitoring of backscattering coefficient (see figure 31), as wind speed computation uses principally backscattering coefficient. This signal is related to events of high mispointing of Jason-1.

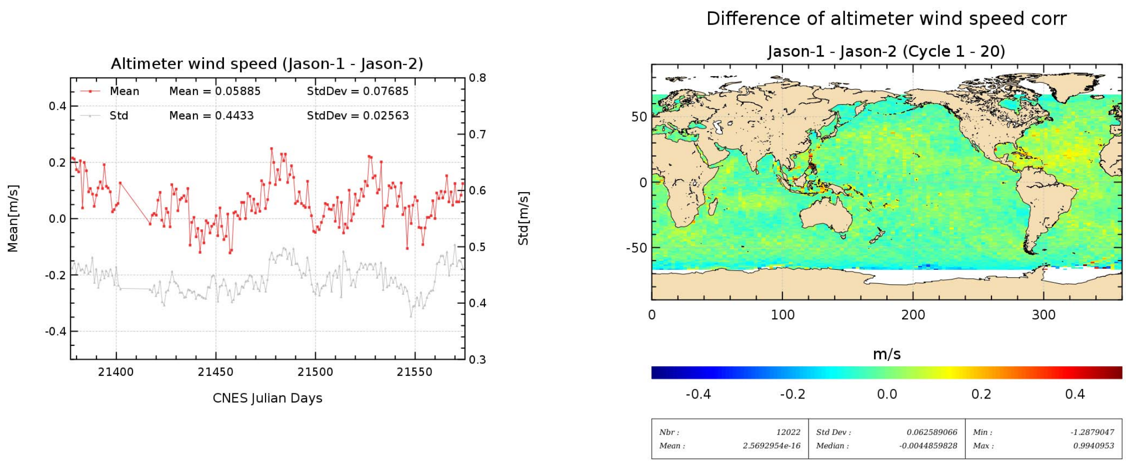

Figure 44: *Daily monitoring of mean and standard deviation (left) of Jason-1 - Jason-2 altimeter wind speed. Map showing mean of Jason-1 - Jason-2 differences over cycles 1 to 20.*

For Jason-1 Gdr-C release, the wind speed is calculated with an algorithm based on ([34]), fitted on Jason-1 Sigma0 (Collard algorithm). It is the same algorithm applied for Jason-2 now. As there is a bias between Jason-1 and Jason-2 Ku-band backscattering coefficients, prior to the altimeter wind speed computation of GDR-D, a calibration bias of 0.32 dB has been added to the Ku-band backscattering coefficient.
Thanks to the altimetry standard improvements since Jason-1 launch ([48], [24]), the error budget of SSH calculation has been reduced. Through the sea state bias correction, the Sigma0 bias uncertainty has thus become not inconsiderable as shown in recent study ([58], [2]). Indeed an error of 0.1 dB on the backscattering coefficient has an impact of about 0.5 m/s on the altimeter wind speed, which in turn has an impact of about 1.6 mm on the sea state bias correction.

Figure 46 shows mean and standard deviation for cycle per cycle altimeter wind speed for several data types of Jason-2. Note that the curve of GDR is in version D (as they were reprocessed), whereas IGDR switched to standard D from cycle 150 onwards, and OGDR switched to standard D around pass 078 of cycle 150. This explains the higher values of IGDR and OGDR wind speeds before cycle 150. From cycle 151 onwards, the altimeter wind speed of the different data types is

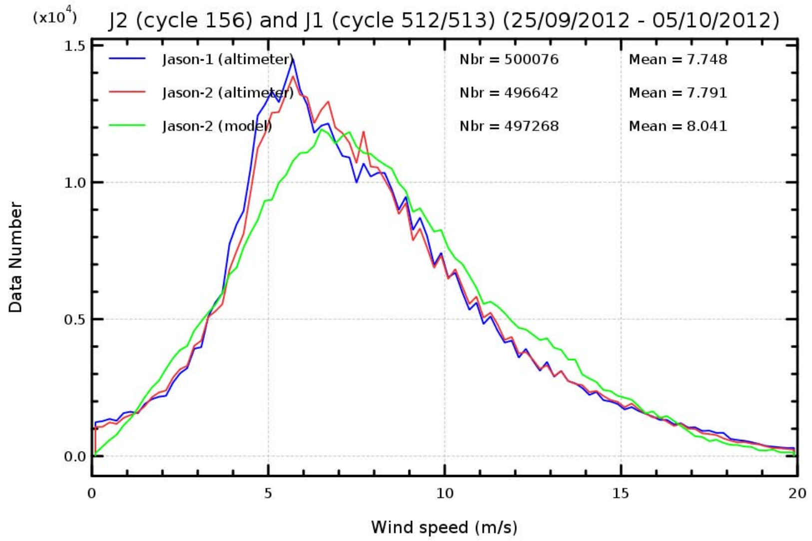

Figure 45: *Histogram of altimeter (Jason-1 in blue, Jason-2 in red) and model wind speed (green) for a 10 day period.*

coherent.

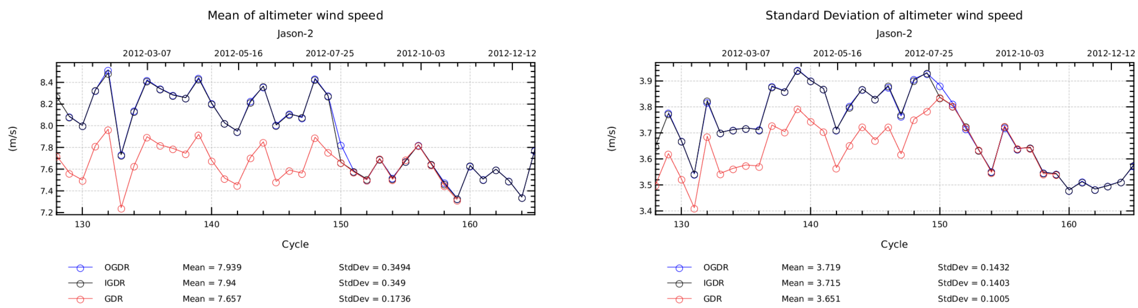

Figure 46: *Cycle per cycle monitoring of mean (left) and standard deviation (right) of altimeter wind speed over 2012 for Jason-2 O/I/GDR.*

4.9. Sea state bias

A new sea state bias look-up table was provided for the GDR-D reprocessing. It was computed using Jason-2 data from internal reprocessing which were as close as possible to the GDR-D standards. The GDR-D sea state bias differs by about 3 cm from the GdrT sea state bias (which used the same look up table as used in Jason-1 GdrC), see also report of reprocessing ([10]). Therefore differences between Jason-1 and Jason-2 are about -3 cm (left of figure 47).

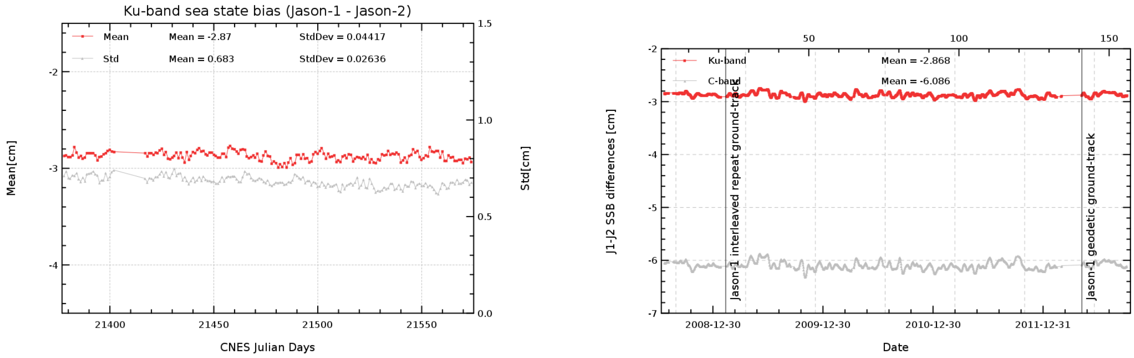

Figure 47: *Daily monitoring of mean and standard deviation (left) of Jason-1 - Jason-2 sea state bias over cycles 1 to 20. Daily monitoring of Jason-1 - Jason-2 differences (right), a 10 day filter is applied.*

This difference is not a bias, as can be seen from the maps of the Jason-1 - Jason-2 sea state bias difference (figure 48). Differences between Jason-1 and Jason-2 sea state bias increase using Jason-2 GdrD (top of figure 48), as the methods (as well as data) used for the SSB model computation are different. In the case of top left side of figure 48, the SSB model was the same for Jason-1 GDR-C and Jason-2 GDR-T data, only the input values (altimeter wind speed and significant wave height) differed. For the top right side of figure 48, the input values (wind, wave) have evolved for Jason-2 (from GDR-T to GDR-D version). Furthermore the method of computing the SSB model has also changed (see [58]). Indeed, GDR-D sea state model is calculated with a different approach of low sea states. In these areas, the editing method has changed so that differences are mainly observed here.
At OSTST 2012 meeting, Tran et al. [60] presented a new SSB model computed using one year of GDR-D data. This model seems better than the SSB model used for the GDR-D product. Though the SSB model used for the GDR-D products was computed on Jason-2 data from an internal reprocessing which was as close as possible to the GDR-D standard, there were nevertheless some differences with the GDR-D data. Indeed, the wind speed (necessary for SSB computation) from the internal reprocessing was tuned with a preliminary bias on sigma0, whereas the wind speed of the GDR-D product uses a fine-tuned bias (takes into account additionally a correction from LTM and corrected atmospheric correction from S. Brown in sigma0).

When using the updated sea state bias proposed by Tran et al. [60] for both missions, the Jason-1 minus Jason-2 differences are much more homogeneous (see bottom right of figure 48). Note that this homogenization is mainly due to the updated Jason-2 SSB and to a lesser extent due to the updated Jason-1 SSB.

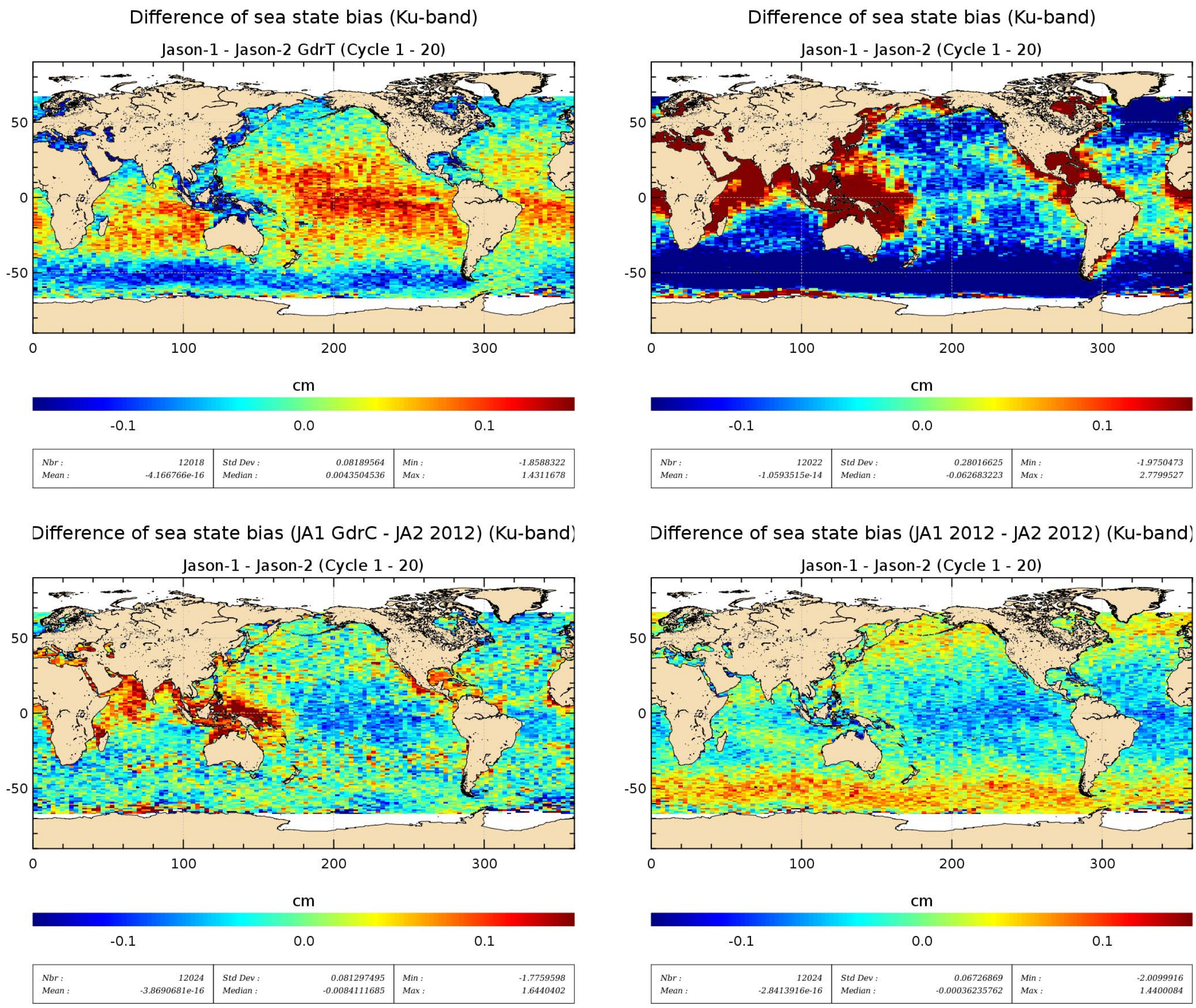

Figure 48: *Map showing mean of Jason-1 - Jason-2 sea state bias differences over cycles 1 to 20. Top left: using SSB from Jason-1 GDR-C and Jason-2 GDR-T (map centered around 0.158cm). Top right: using SSB from Jason-1 GDR-C and Jason-2 GDR-D (map centered around -2.82 cm). Bottom left: using SSB from Jason-1 GDR-C and updated (2012) SSB for Jason-2 (map centered around -0.31 cm). Bottom right: using updated (2012) SSB for both Jason-1 and Jason-2 (map centered around 0.13 cm).*

5. SSH crossover analysis

5.1. Overview

SSH crossover differences are the main tool to analyze the whole altimetry system performances. They allow us to analyze the SSH consistency between ascending and descending passes. However in order to reduce the impact of oceanic variability, we select crossovers with a maximum time lag of 10 days. Mean and standard deviation of SSH crossover differences are computed from the valid data set to perform maps or a cycle by cycle monitoring over all the altimeter period. In order to monitor the performances over stable surfaces, additional editing is applied to remove shallow waters (bathymetry above -1000m), areas of high ocean variability (variability above 20 cm rms) and high latitudes ($> |50| deg$). SSH performances are then always estimated with equivalent conditions.
The main SSH calculation for Jason-2 and Jason-1 are defined below.

$$SSH = Orbit - Altimeter\ Range - \sum_{i=1}^{n} Correction_i$$

with $Jason-1/Jason-2\ Orbit = CNES\ orbit$ for GDR products, and

$$\begin{aligned}
\sum_{i=1}^{n} Correction_i &= Dry\ troposphere\ correction \\
&+ Dynamical\ atmospheric\ correction \\
&+ Radiometer\ wet\ troposphere\ correction \\
&+ Dual\ frequency\ ionospheric\ correction\ (filter\ 250\ km) \\
&+ Non\ parametric\ sea\ state\ bias\ correction \\
&+ Ocean\ tide\ correction\ (including\ loading\ tide) \\
&+ Earth\ tide\ height \\
&+ Pole\ tide\ height
\end{aligned}$$

In order to allow better comparisons between Jason-1 and Jason-2, some standards of Jason-1 GDR-C were updated.

Parameter	Jason-1 GDR-C	Jason-1 GDR-C with updates
Orbit	CNES POE-C	CNES POE-D
radiometer wet troposphere correction	JMR	JMR replacement product for period which corresponds to Jason-2 cycles 001 to 020
		.../...

Parameter	Jason-1 GDR-C	Jason-1 GDR-C with updates
Global ocean tide	GOT00V2	GOT 4.8
Mean Sea Surface	CLS_2001	CNES_CLS_2011

Table 8: *u*pdated standards of Jason-1 for comparison with Jason-2

Note that from 7th of May 2012 (Jason-1 cycle 500, which corresponds to end of Jason-2 cycle 141), Jason-1 is on a geodetic ground-track. The Jason-1 GDR-C product contains from cycle 500 onwards already the POE-D solution and the MSS CNES_CLS_2011.

Concerning Jason-2 data, if not otherwise mentionned, GDR-D products are used.

5.2. Mean of SSH crossover differences

The cycle by cycle mean of SSH differences is plotted in figure 50 for Jason-2 and Jason-1 (using standards from Jason-1 GDR-C products and updated standards). The curves are very similar and do not highlight any anomaly. However, a small 120 day signal is visible for Jason-2 GDR-D data. It is increased for updated Jason-1 products (compared to Jason-1 GDR-C products). Note that for Jason-2 GDR-T data (right of figure 50) the 120 day signal was even more important. Furthermore the GDR-T curve had noticeable negative values (-0.67 cm for Jason-2 GDR-T compared to -0.1 cm for Jason-2 GDR-D) indicating a systematic ascending/descending SSH bias. The map of SSH differences calculated over all the Jason-2 GDR-T period in right side of figure 49, shows that this bias was not spatially homogenous with a negative structure reaching -2 cm in the southern Atlantic, east of the southern Pacific, and west of the Indian Ocean and tropical Pacific. In inverse, a positive patch close to +2 cm is observed in the northern Atlantic. Although orbit was fully compliant with mission requirements, orbit calculation (as well as a small time tag bias) is the main source to explain these discrepancies between ascending and descending passes since they are significantly reduced using other orbits than those available in GDR-T products, such as orbits based only on GPS solutions provided by CNES ([20]) or JPL ([5]). The map of mean SSH crossover differences plotted in left side of figure 49 was calculated using Jason-2 GDR-D products (which contain POE-D standard). The geographically correlated patterns are strongly reduced. Futhermore the North/South hemispheric signal has disappeared. This signal (which is no longer an issue for GDR-D) came from a small pseudo time tag bias (approximatly -0.28 ms) as explained further in chapter 5.5..

Further studies concerning orbit solutions from different orbit centers can be found in chapter 8.4..

Mean of SSH differences at crossovers for Jason-2 IGDR products (using MOE orbits) were even more negative (in average) than GDR-T products before the switch to standard D (from cycle 150 onwards), as can be seen on figure 51. Since the switch to standard D, mean of IGDR SSH differences at crossovers are more centered, but a strong 120 day signal seems to appear. SSH differences of OGDR products (using Doris/Diode navigator orbit) show stronger variations. But since the use of the recent Doris version 11 (from 2012-09-19 onwards), the mean of OGDR SSH crossover differences is much more homogeneous (though again negative).

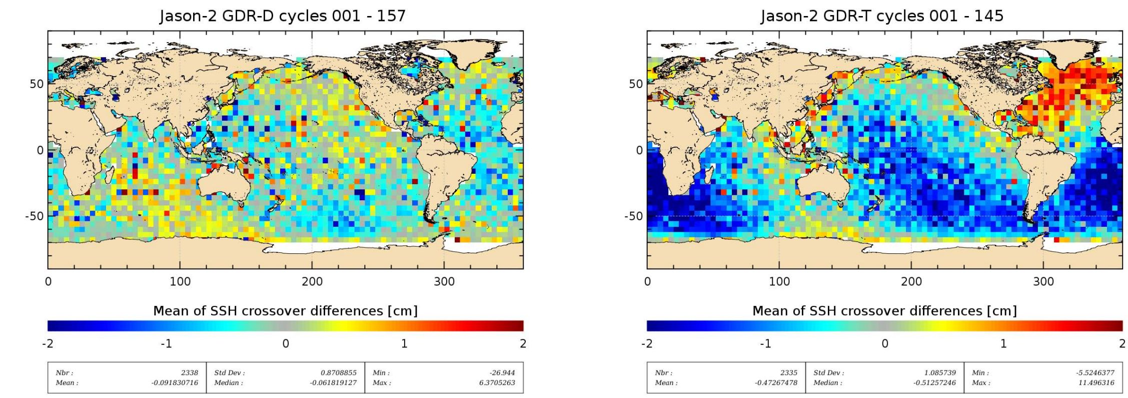

Figure 49: *Map of mean of SSH crossovers differences for Jason-2 cycle 1 to 157(using GdrD data) on the left. For GdrT (cycles 001 to 145) on the right.*

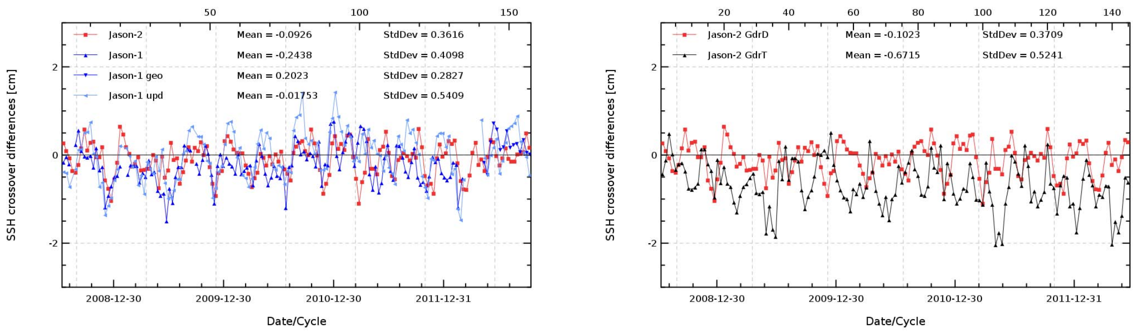

Figure 50: *Monitoring of mean of SSH crossover differences for Jason-2 and Jason-1. Left: using Jason-2 GdrD (red), Jason-1 GdrC (blue), Jason-1 GdrC Upd with GOT4V8 + POE-D + JMR replacement (light blue). Right: Jason-2 GdrD (red), Jason-2 GdrT (black).*

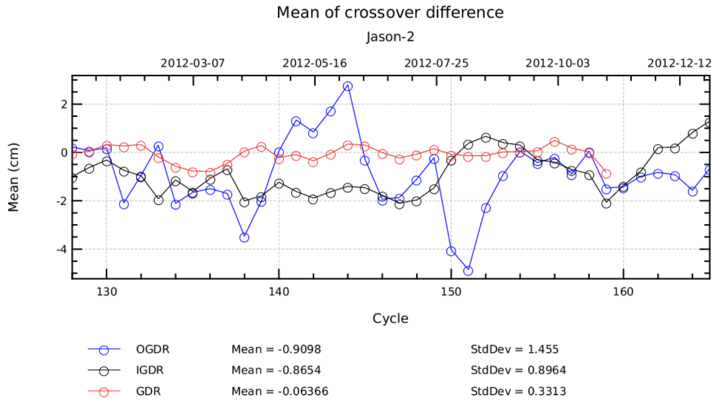

Figure 51: *Monitoring over 2012 of mean of SSH crossover differences for different data types of Jason-2: OGDR (blue), IGDR (black), GDR-D (red). Note that IGDR switched to standard D from cycle 150 onwards and OGDR from cycle 150 pass 078 onwards.*

5.3. Mean of SSH crossover differences between Jason-2 GDR-D and other missions

Dual-mission crossover performances are computed between Jason-2 and Jason-1, as well as Jason-2 and Envisat. Jason-1 GDR-C data were used with updated standards (see table 8). Mean SSH differences at Jason-2/Jason-1 crossovers (shown on left side of figure 52) have a bias of about 10 cm (JA1-JA2). This bias is mostly due to the range differences between the two satellites, but also due to different sea state bias models. The map shows small regional structures of about ±1 cm, especially in southern Pacific, but also around Indonesia and in the Mediterranean Sea. These structures are stronger than those observed between Jason-2 GDR-T and Jason-1 GDR-C (see Jason-2 annual report 2011 [[8]]). This difference comes mainly from the different sea state biases used for Jason-1 GDR-C and Jason-2 GDR-D (see also chapter 4.9.). Using updated sea state bias (presented at 2012 OSTST by Tran et al. [[60]]) for both Jason-2 and Jason-1 data, reduces most of the geographical pattern (right of figure 52). A small pattern remains. This structure was also seen during the flight formation phase, when differences without applying geophysical corrections were possible. It is dependant on orbit solutions, as it is strongly reduced when using GSFC orbit solutions for both missions ([4], see also bottom of figure 58).

For comparisons with Envisat, reprocessed V2.1 Envisat data were used, in addition GOT4.8 global ocean tide was updated. Though Jason-2 GDR-T and Envisat V2.1 are using CNES produced POE (POE-C standard), a large east/west bias is observed on the left side of figure 53, see also [29]. This is also seen on Jason-1/Envisat crossovers, especially since 2007 (see [32]). This behaviour is related to the gravity field used during orbit computation. When using Jason-2 GDR-D, as well as POE-D for Envisat (POE-D is based on EIGEN-GRGS_RL02bis_MEAN-FIELD gravity fiels), this east/west biased disappears, as shown on right side of figure 53 (see also annual report of Envisat 2011 [45]). The remaining structure is partly due to the different SSB models, especially in South Pacific and Mediterranean Sea, as these differences are decreased using OSTST 2012 sea state model for both satellites (as shown on bottom of figure 53). The remaining differences could be due to the ionosphere correction (as the dual-frequency ionosphere correction is no longer available

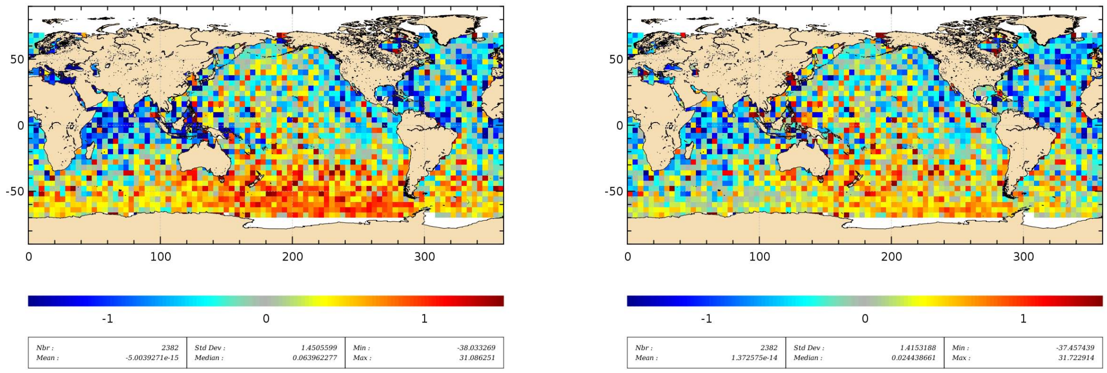

Figure 52: *Map of mean of SSH crossovers differences between Jason-2 and Jason-1 (JA1-JA2) for 2011 using POE-D orbit (left). The map is centered around the mean (10.06 cm). Right: same as left, but using 2012 sea state biais for both satellites. The map is centered around the mean (7.09 cm).*

for this period on Envisat) or other differences. Note that comparison between Envisat and Jason-1 show similar structure, as shown in Envisat annual report 2012 ([9]).

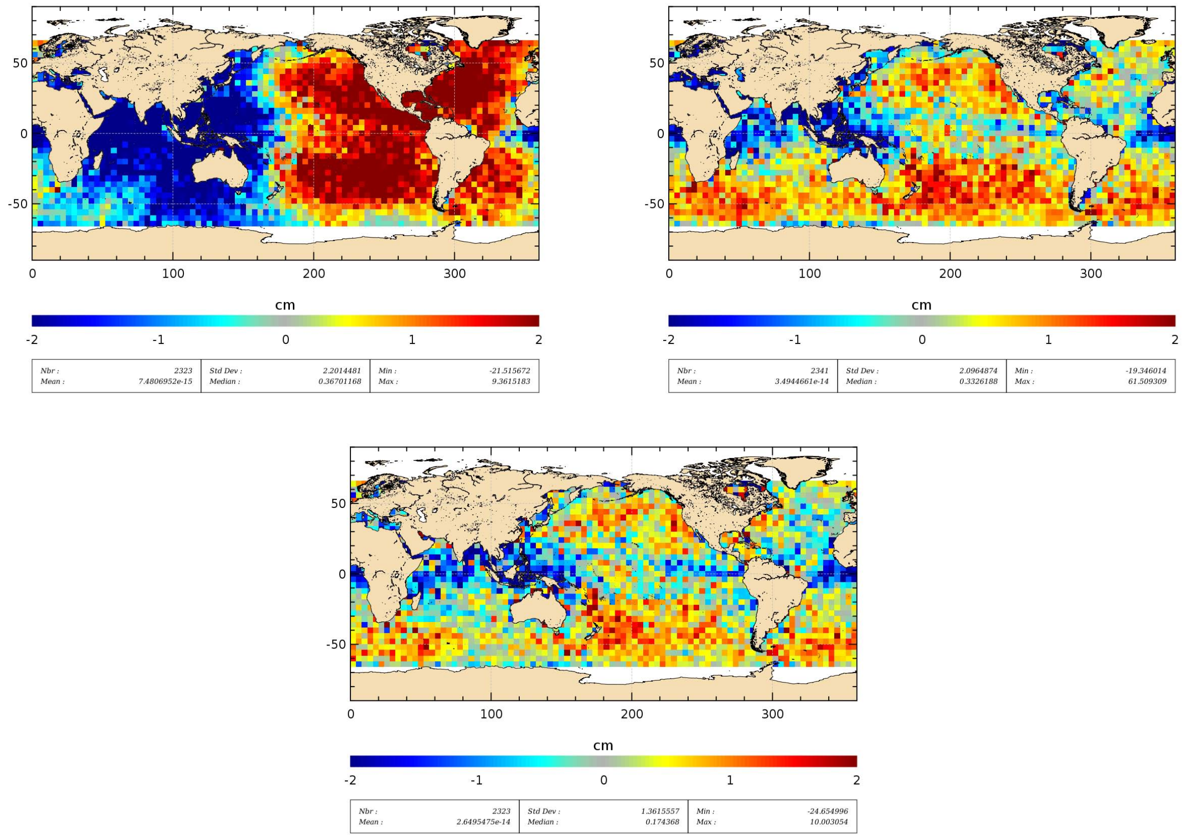

Figure 53: *Map of mean of SSH crossovers differences between Jason-2 and Envisat (EN-JA2) for 2011 using model wet troposphere correction. Left: Jason-2 GdrT (POE-C already included) and Envisat V2.1 data (POE-C already included). The map is centered around the mean of 28.64 cm. Right: Jason-2 GdrD (POE-D already included) and Envisat V2.1 data + POE-D standard. The map is centered around the mean of 46.18 cm. Bottom: Jason-2 GdrD and Envisat V2.1 data + POE-D standard + OSTST 2012 sea state bias (for both missions). The map is centered around 44.74 cm.*

5.4. Standard deviation of SSH crossover differences

The cycle by cycle standard deviation of SSH crossovers differences are plotted for Jason-2 and Jason-1 in figure 54 after applying geographical criteria (bathymetry, latitude, oceanic variability) as defined previously (chapter 5.1.). Both missions show very good performances, very similar and stable in time. No anomaly is detected (the value above 6 cm for Jason-1 is related to degraded orbit quality due to several inclination maneuvers during Jason-1 cycle 315). The average figure is 5.1 cm rms for Jason-1, 5.0 for updated Jason-1, and 4.9 cm rms for Jason-2 data. Keeping in mind that during the Jason-1/TOPEX formation flight phase in 2002, the same statistic using Jason-1 GDR-A products was close to 6.15 cm (see [30]). This illustrates the improvements performed in the altimetry ground processing since the Jason-1 launch especially thanks to new retracking algorithms, new geophysical corrections (oceanic tidal, dynamic atmospheric correction, ...) and new orbit calculations implemented first in GDR-B and later in GDR-C release (see [48] concerning impact of GDR-B/GDR-A, [24] concerning impact of GDR-C/GDR-B). The reprocessing of Jason-

2 in GDR-D also improved the performance at crossover points. The variance of SSH crossover differences was reduced by 1.7 cm2 when switching from GDR-T to GDR-D standards, as shown on figure 55. The main contributors to this improvement are the POE-D orbit standard and the GOT4.8 global ocean tide. The new ocean tide model reduces the variance especially for regions of continental shelfs, where the water depth is less important than elsewhere (note the strong variance reductions for example east of Argentina on right of figure 55).
Though Jason-1 and Jason-2 show very good performances and are within the mission specifications, their standard deviation of SSH differences at crossovers is sometimes higher than usual.

When comparing the performances of the different Jason-2 data types (OGDR, IGDR, GDR) over 2012 (right of figure 54), OGDR have the highest standard deviation with 6.6 cm, though this value is already extremely good considering that OGDR have a latency of about 3h, recalling that Jason-1 GDR-A products had a standard deviation of 6.15 cm. IGDR data have a standard deviation of 5.2 cm over 2012. Note that IGDR switched to standard D from cycle 150 onwards, which reduces the standard deviation.

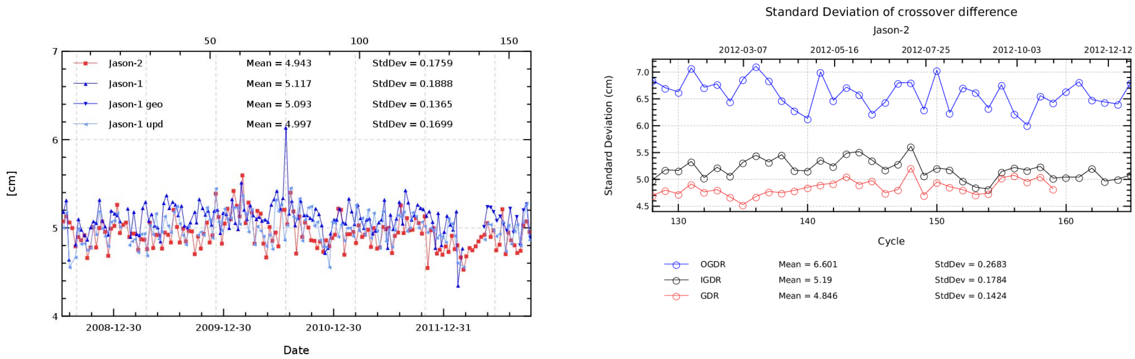

Figure 54: *Cycle by cycle standard deviation of SSH crossover differences for Jason-2 and Jason-1. Only data with abs(latitude) < 50°, bathymetry < -1000m and low oceanic variability were selected.*

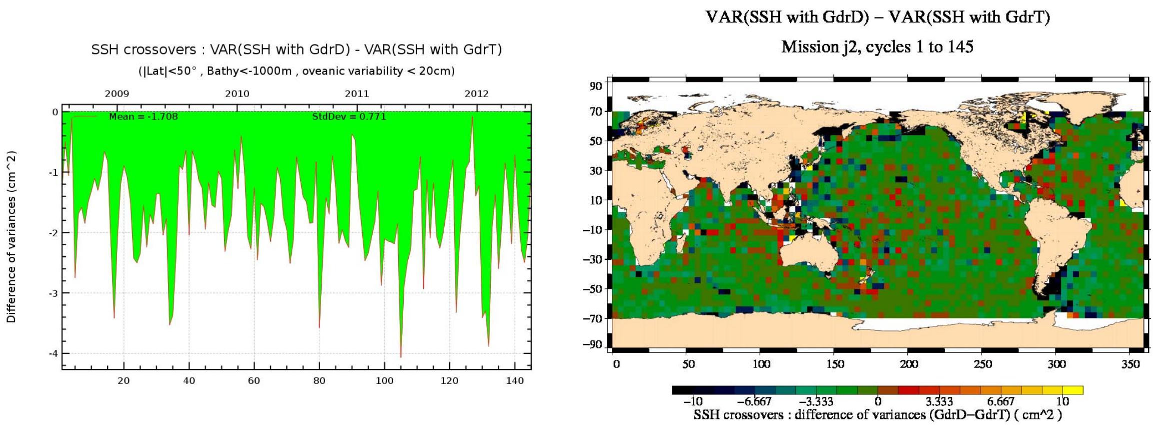

Figure 55: *Left: Difference of SSH variance at crossovers between GdrD and GdrT. Crossovers are only selected for open ocean (latitude less than ± 50°, bathymetry less than -1000 m and oceanic variability less than 20 cm). Right: Map of difference of SSH variances (variance SSH_{GdrD} - variance SSH_{GdrT}).*

5.5. Estimation of pseudo time-tag bias

The pseudo time tag bias (α) is found by computing at SSH crossovers a regression between SSH and orbital altitude rate ($\dot{H}$), also called satellite radial speed:

$$SSH = \alpha \dot{H}$$

This empirical method allows us to estimate the potential real time tag bias but it can also absorb other errors correlated with $\dot{H}$. Therefore it is called "pseudo" time tag bias. The monitoring of this coefficient estimated at each cycle is performed for Jason-1 and Jason-2 in figure 56. Both curves are very similar highlighting an almost 59-day signal with almost no bias (close to 0.01 ms for Jason-1 and -0.02 ms for Jason-2). Before the Jason-2 reprocessing the GDR-T showed a bias of -0.29 ms. As mentioned just previously, this bias directly explained the small hemispheric differences observed at GDR-T SSH crossover differences with maximal differences close to 8 mm where $\dot{H}$ is maximal (15 $m.s^{-1}$) at medium latitudes ($\pm 50^{\circ}$). Recently, the origin of this pseudo time tag bias was found by CNES [15], nevertheless the 59 day-signal is still unexplained. The constant part of the datation bias is corrected in the Jason-2 GDR release (see also the Jason-2 handbook [35]). Therefore the datation of Jason-2 GDR-T and GDR-D is not the same. For Jason-1 GDR-C products ([3], an empirical correction containing $\alpha \dot{H}$ has been already added to improve the Jason-1 SSH calculation.

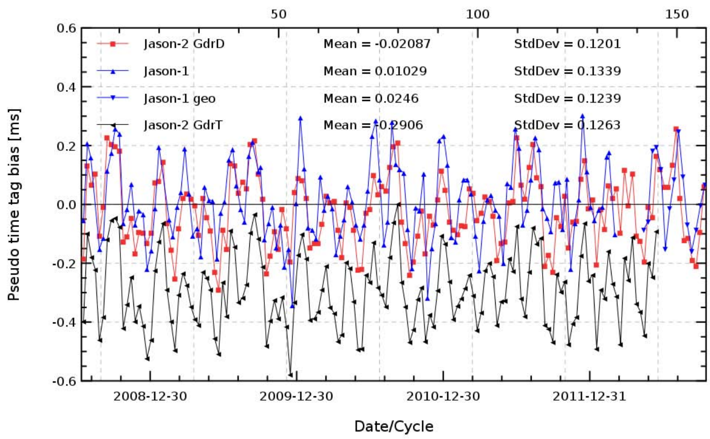

Figure 56: *Monitoring of pseudo time-tag bias estimated cycle by cycle from GDR products for Jason-2 and Jason-1*

6. Sea Level Anomalies (SLA) Along-track analysis

6.1. Overview

The Sea Level Anomalies (SLA) are computed along track from the SSH minus the mean sea surface with the SSH calculated as defined in previous section 5.1. :

$$SLA = SSH - MSS(CNES/CLS2011)$$

Note that Jason-2 GDR-D products contain MSS_CNES_CLS_2011. For better comparison with Jason-1, in this study MSS 2011 was also updated on Jason-1 data (in addition to the other updates: POE-D, GOT4.8, JMR replacement product).

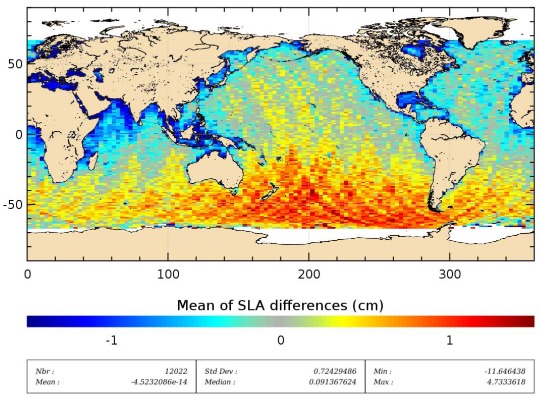

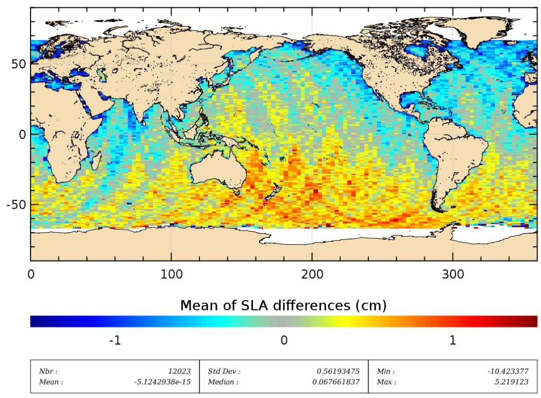

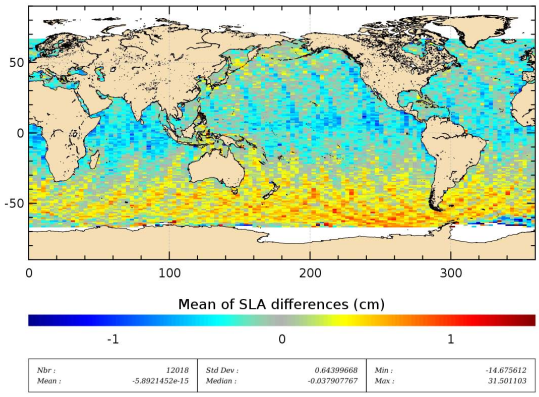

Figure 57: *Maps of SLA (orbit - range - geophysical corrections - MSS2011) mean differences between Jason-1 and Jason-2 during formation flight phase (cycles 1 to 20). Top left: using Jason-2 GDR-D and Jason-1 updated GDR-C (the map is centered around the mean of 10.24 cm). Top right: same as left, but in addition using for both satellites OSTST 2012 sea state bias (the map is centered around the mean of 7.26 cm). Bottom: using Jason-2 GDR-T and Jason-1 GDR-C products (the map is centered around the mean of -7.47 cm).*

SLA analysis is a complementary indicator to estimate the altimetry system performances. It allows us to study the evolution of SLA mean (detection of jump, abnormal trend or geographical correlated biases), and also the evolution of the SLA variance highlighting the long-term stability of the altimetry system performances. In order to take advantage of the Jason-2/Jason-1 formation flight phase (cycles 1 to 20), we performed direct SLA comparisons between both missions during this period.

There are geographically correlated structures of up to ± 1.5 cm amplitude between Jason-2 GDR-D and updated Jason-1 GDR-C data (see left of figure 57). This is particularly the case for regions with low, but also high significant wave height. Most of this difference comes from the still different sea state bias models used on both satellites (see also chapter 4.9.). Updating both satellites with the OSTST 2012 sea state bias strongly reduces the differences, as shown on right side of figure 57. The remaining differences are due to orbit differences (though for both POE-D orbit standard was used), as shown on figure 58. Note that differences between Jason-2 GDR-T and Jason-1 GDR-C were slightly smaller, but also related to the orbit standards used.

Corrections applied in SSH calculation are theoretically the same for Jason-1 and Jason-2 since both satellites measure the same ocean. Thus, it's possible to not apply them in order to obtain directly information on the altimeter range and the orbit calculation differences. However, as the repetitivity of both ground passes is not exact (± 1 km cross-track distance), SLA measurements have to be projected and interpolated over the Jason/TOPEX theoretical ground pass after applying the MSS in order to take into account cross-track effects on SSH.

$$\Delta SLA_{J1-J2} = [(Range_{Ku} - Orbite - MSS)_{J1}]_{\bar{T}} - [(Range_{Ku} - Orbite - MSS)_{J2}]_{\bar{T}}$$

This allows us also to select the intersection of both datasets and compare exactly the same data. After Jason-1 ground track change, direct SLA comparisons are no more possible. Thus, global statistics computed cycle by cycle are just basically compared.

6.2. Mean of SLA differences between Jason-2 and updated Jason-1

Spatial uncorrected SLA (orbit - range - MSS) differences (only during the Jason-1 formation flight phase) between both missions as plotted in left side of figure 58 show a weak hemispheric bias lower than 1 cm. In addition, positive differences are stronger in South Pacific and negative differences are stronger in North Atlantic. These differences are in relationship with orbit calculation differences. Though for both satellites POE-D was used, there are some differences between Jason-1 POE-D and Jason-2 POE-D, for Jason-1 orbit computation the GPS data are no longer available, whereas they are used for the Jason-2 POE computation. Jason-2 POE-D is therefore based on three orbit determination techniques (Doris, GPS, Laser), whereas Jason-1 POE (over the Jason-2 period) is only based on two orbit determination techniques (Doris and Laser). On the right of figure 58 the difference between Jason-1 and Jason-2 uncorrected SLA is shown using for Jason-2 also a Doris/Laser orbit (instead of an Doris/GPS/Laser orbit). They hemispheric differences seems to be more homogeneous, but are still present. When using GSFC std 0905 orbits for both satellites (bottom of figure 58) the hemispheric bias disappears. This is under investigation on CNES POD side.

The cycle by cycle monitoring of mean SLA differences between updated Jason-1 data and Jason-2 is plotted in figure 59 over all the Jason-2 period. During the formation flight phase, the SSH bias is computed with and without the SSH corrections. During this period, both types of curves are very similar and stable in time with variations close to 1 mm rms. They are spaced out by a 3.3

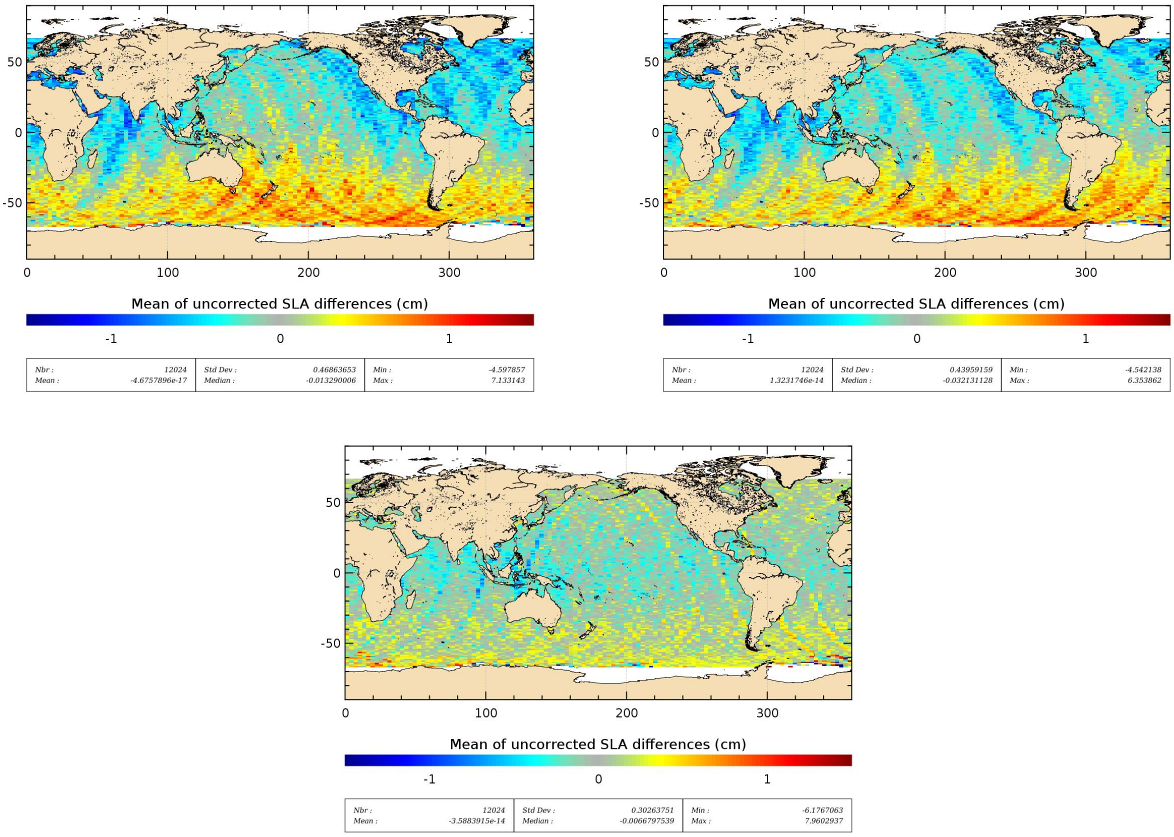

Figure 58: *Maps of SLA (orbit - range - MSS2011) mean differences between Jason-1 and Jason-2 during formation flight phase (cycles 1 to 20). Top left: using POE-D orbits. Top right: using POE-D orbit for Jason-1 and Doris/Laser POE-D orbit for Jason-2. Bottom: using GSFC09 orbits.*

cm bias (3.2 cm when using ECMWF model wet troposphere correction) resulting from differences between Jason-1 and Jason-2 sea state bias model used, and to a small amount due to ionosphere correction differences. The global average SSH bias is close to 10.3 cm using SSH corrections (10.2 cm when using ECMWF instead of radiometer wet troposphere correction) and 7.1 cm without. Previously, using Jason-2 GDR-T data, a bias of -8.3 cm (without corrections) was found. Investigations by CNES presented at Seattle OSTST in June 2009 [Zaouche, 2009], [Desjonqueres, 2009] explained the origin of most of the bias between both altimeters. The authors explain that there are 2 origins. Firstly the use of a truncated altimeter PRF (Pulse repetition frequency) in the Jason-1 and Jason-2 ground segments leads to a Jason-1 minus Jason-2 difference of 2.15 cm, and secondly a difference in the characterization parameter (on Jason-1) set for Ku-band leads to a difference of -11.70 cm, combining to a Jason-1 minus Jason-2 bias of -9.5 cm. This was very close to the observed bias of -8.3 cm before the reprocessing. Furthermore it was discovered, that for computation of the Jason-2 range, a wrong antenna reference point was used. For GDR-D reprocessing this antenna reference point issue, as well as the precise altimeter PRF were taken into account. This increased the Jason-2 range by about 15.5 cm for the GDR-D. The remaining differences between Jason-1 and Jason-2 are therefore a small bias due to troncated altimeter PRF (-0.316 cm), the characterization file (-11.7 cm) and the antenna reference point (+18.09 cm), which sums up to a difference of 6.1 cm. This is quite close to the curently observed value of 7.1 cm. However, the more

crucial point for scientific applications is to insure that there is no drift between both missions, since the global bias can be easily corrected a fortiori. The extension of the monitoring of the SSH bias after the Jason-1 ground track change is precisely a good way to check the long-term Jason-1 and Jason-2 stability. It is plotted over 157 cycles in figure 59. The curve using radiometer wet troposphere correction seems to show a small drift before the end of the Jason-1 repeat mission. This is not the case when using ECMWF model wet troposphere correction.
When Jason-1 was moved to a geodetic ground track, a jump is visible. It is slightly smaller when using ECMWF model wet troposphere correction than when using radiometer wet troposphere correction. Indeed from Jason-1 cycle 500 (geodetic ground-track) onwards, a new JMR calibration file was used, accounting for a bias of 1 to 2 mm. Furthermore, since the geodetic ground-track, Jason-1 PRF is no longer truncated (as it was previously). This accounts for a bias of 3.16 mm. Nevertheless a small part of the jump remains unexplained.

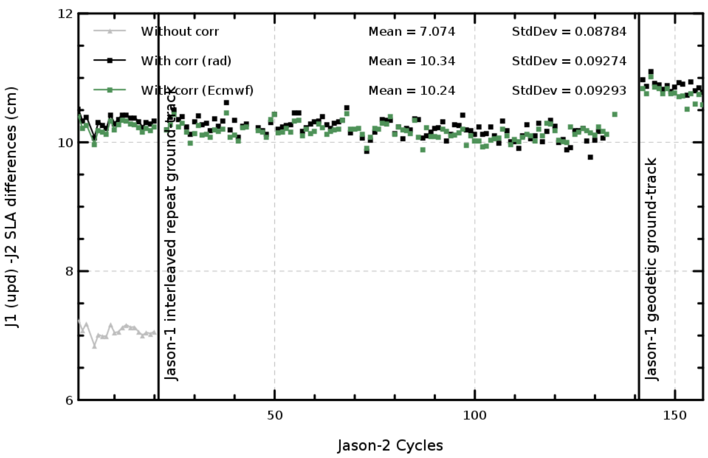

Figure 59: *Cycle by cycle monitoring of SSH bias between Jason-1 and Jason-2 before and after Jason-1 ground-track change (black curve and dots) and SSH bias without applying corrections in SSH calculation for both missions only during the formation flight phase (gray curve).*

6.3. Standard deviation of SLA differences between Jason-2 and Jason-1

The monitoring of SLA standard deviation has been computed for both missions, as well as updated Jason-1 standards over the whole data set (plotted in figure 60). The curves are very well correlated during the formation flight phase, as well as after Jason-1 moved to the geodetic ground-track. For the geodetic ground-track Jason-1 GDR-C contain the MSS CNES/CLS 2011 which is improved compared to the 2001 MSS ([36]) especially for ground-tracks outside the historical T/P-Jason ground track. During the Jason-1 interleaved repetitive ground-track (from Jason-2 cycle 21 to 134), Jason-1 standard deviation increases by 3 cm rms in average: 11.06 cm rms for Jason-1 instead of 10.61 cm rms for Jason-2. Similar feature was observed comparing Jason-1 and TOPEX performances after T/P satellite was moved on its new ground track in August 2002 ([30]). The new MSS CNES/CLS 2011 ([52]), using all the satellite tracks including the interleaved T/P and Jason-1 ground tracks - which was computed in the frame of the SLOOP project ([31]) - improves the SLA calculation also for the interleaved ground tracks. Cartography of standard deviation of spatial Jason-1 minus Jason-2 SLA differences (not shown here) does not show any anomaly. It varies indeed in function of noise on measurements, which is dependant on significant wave height. Therefore, standard deviation of SLA differences is higher in regions with important significant wave heights.

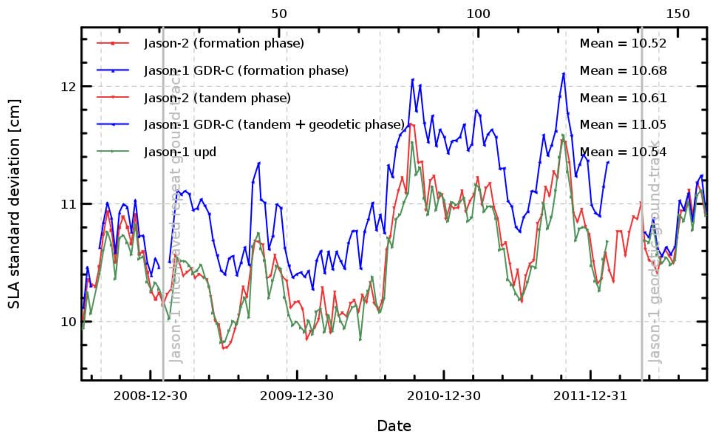

Figure 60: *Cycle by cycle monitoring of SLA standard deviation for Jason-1 and Jason-2.*

7. Mean Sea Level (MSL) calculation

7.1. Altimeter Mean Sea Level evolution

7.1.1. Mean sea level (MSL) calculation of reference time serie

The global mean level of the oceans is one of the most important indicators of climate change. Precise monitoring of changes in the mean level of the oceans, particularly through the use of altimetry satellites, is vitally important, for understanding not just the climate but also the socioeconomic consequences of any rise in sea level. Thanks to the T/P, Jason-1 and now Jason-2 altimetry missions, the global MSL has been calculated on a continual basis since January 1993 (figure 61) highlighting a trend of 3.16 mm/yr (see http://www.aviso.oceanobs.com/msl). We connect Topex/Poseidon and Jason-1 at Jason-1's cycle 11 (May 2002) by applying a bias of 8.45 cm to Jason-1's MSL. We replaced Jason-1 by Jason-2 in the MSL time data series at Jason-2 cycle 11 (October 2008) applying a SSH bias between both missions of -10.67 cm as calculated previously (in addition to the bias between Jason-1 and Topex/Poseidon). The altimeter standards used are described on Aviso website (http://www.aviso.oceanobs.com/en/news/ocean-indicators/mean-sea-level/processing-corrections.html). Note that Jason-2 GDR-D data and Jason-1 GDR-C data (only updated for GOT4.7 and JMR replacement product (cycles 228 to 259)) were used. To calculate a precise MSL rate, it is essential to link accurately time data series together (see also chapter 8.5.). A study ([1]) showed the uncertainty on the global MSL trend resulting from the impact of MSL bias uncertainties between TOPEX-A and TOPEX-B (due to altimeter change in February 1999) and between TOPEX-B and Jason-1 (in May 2002) is close to 0.2 mm/yr from 1993 onwards. As we showed just previously, the SSH consistency between Jason-1 and Jason-2 is very good in space and stable in time during the formation flight phase, the SSH bias uncertainty is consequently very weak and close to 0.5 mm. It is lower than between T/P and Jason-1 (estimated close to 1 mm ([1])). Its impact on global MSL trend error budget is thus very weak: lower than 0.05 mm/yr.
Notice, that MSL decreased in 2010/2011, similar, but much stronger to what was already observed in 2007. According to Boening et al. ([14]) the global mean sea level drop of 5 mm between beginning 2010 and mid-2011 is due to a decline of ocean mass coinciding with an equivalent increase in terrestrial water storage (primary over Australia, northern South America and Southeast Asia). The authors write, that this temporally shift of water from ocean to land is closely related to the transition from El Niño conditions in 2009/2010 to a strong 2010/2011 La Niña which affected precipitation patterns world wide.

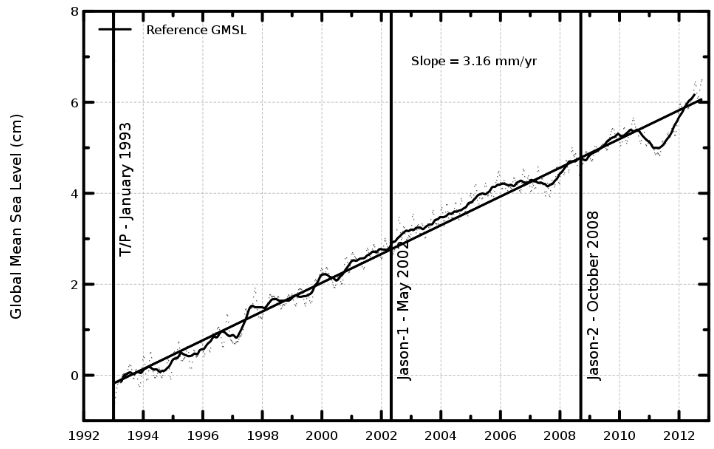

Figure 61: *MSL evolution calculated from T/P, Jason-1 and using Jason-2 data from october 2008 onwards. GIA (-0.3 mm/yr, [47]) is applied.*

7.1.2. Regional and global mean sea level trend for Jason-2

Although, 4 years of Jason-2 is still a short time period for MSL trend calculation, it is possible to compute a MSL trend. Nevertheless, slope values are to be taken with caution and are rather used to compare between several standards. Due to the short period, slope values change much when passing from one period to another period. Using radiometer wet troposphere correction increases for Jason-2 GDR-D data the slope by around 0.35 mm/yr (left side of figure 62). Separating in ascending and descending passes, shows very similar slopes thanks to the POE-D standard (see right of figure 62). The amplitude of the MSL curve computed from descending passes is higher than for ascending passes (for GDR-D). The difference between ascending and descending passes shows for GDR-D a signal of a period around 120 days (see also chapter 5.2.). Note that for GDR-T data there was a slope difference between ascending and descending passes of 0.7 mm/yr (bottom of figure 62).

The regional MSL trends over the Jason-2 period (figure 63) show similar behaviour for Jason-1 and Jason-2, with a small increase in western tropical pacific and a small decrease in eastern tropical pacific. This is probably influenced by the La Niña or neutral conditions which occured before mid-2009 and after mid-2010 ([61],[62]).

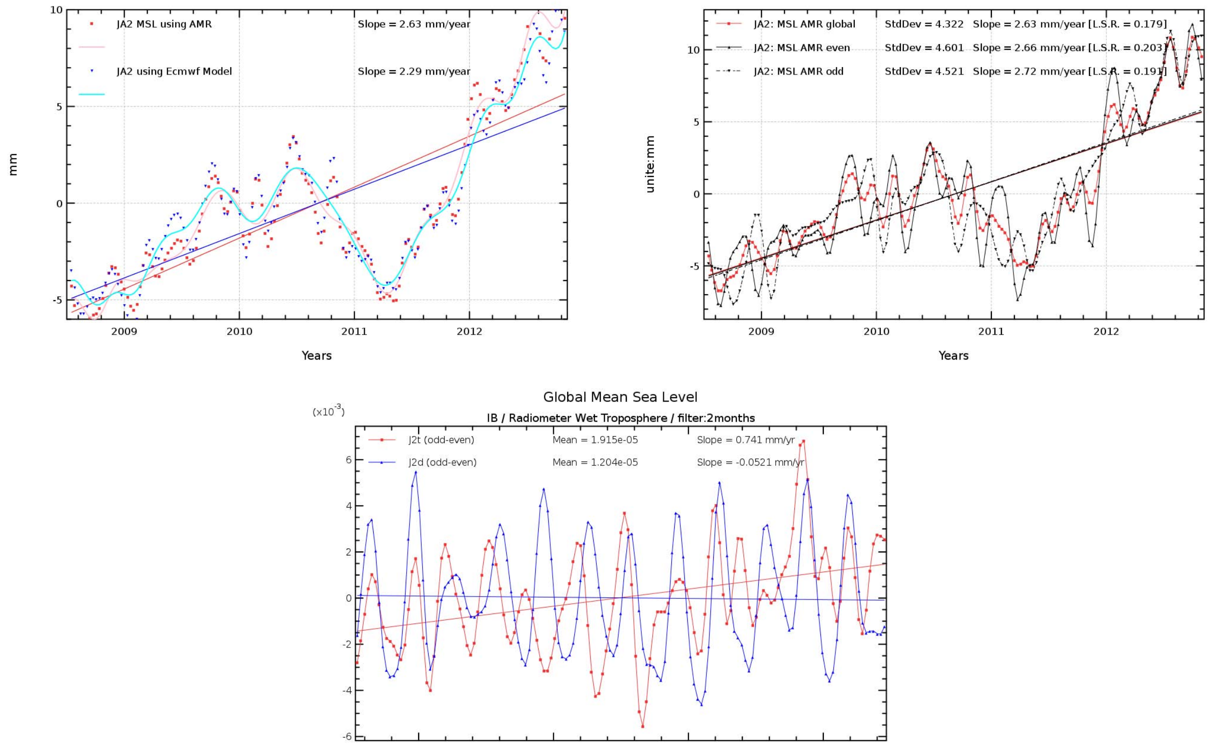

Figure 62: *Global MSL trend evolution calculated for Jason-2 (left). MSL trend evolution when separating in ascending and descending passes (right). Bottom: Difference of MSL slopes (MSL ascending passes - MSL descending passes) for Jason-2 GDR-T and GDR-D. Slopes are computed for 2 month filtered data. Seasonal signal (annual and semi-annual) is adjusted. GIA correction is not applied.*

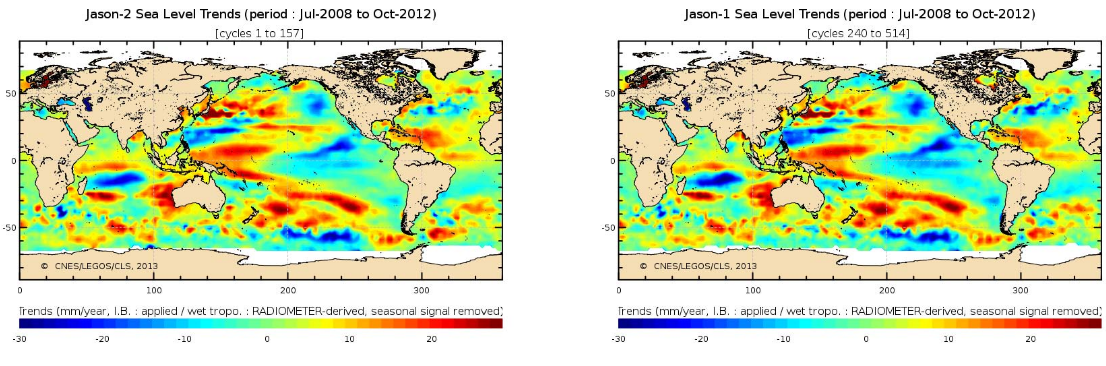

Figure 63: *Maps of regional MSL slopes for Jason-2 and Jason-1, seasonal signal removed.*

7.2. External data comparisons

In order to assess the global MSL trend, comparisons to independent in-situ datasets are of great interest. Two methods have been developed in the frame of in-situ Calval studies and thoroughly described in annual reports ([12] and [13]).

7.2.1. Comparison with tide gauges

Firstly, Jason-2 altimeter data is compared with tide gauge measurements thanks to a dedicated method which aims at detecting potential drifts in sea surface heights (SSH). The tide gauge network processed is the GLOSS/CLIVAR "fast" sea level database, formerly known as the WOCE network. For more information on the method and more detailed results, please refer to the 2012 report of comparison between altimeter data and tide gauges ([12]).

From these comparison methods, SSH bias monitorings have been computed and are shown on figure 64. Looking at the Jason-2/tide gauges residual signals superimposed with Jason-1, the 2 cm amplitude and periodic signals of the global data time series differences are in good agreement on the same time period. However, trend differences are slightly different with Jason-1s between 2008 and 2012 (-0.8 mm/yr for Jason-1, -0.3 mm/yr for Jason-2 GDR-T and 0.1 mm/yr for Jason-2 GDR-D). Although the GDR-D result seems to be in better agreement, the formal adjustment error is still very high (close to 0.5 mm/yr) due to the short period considered.

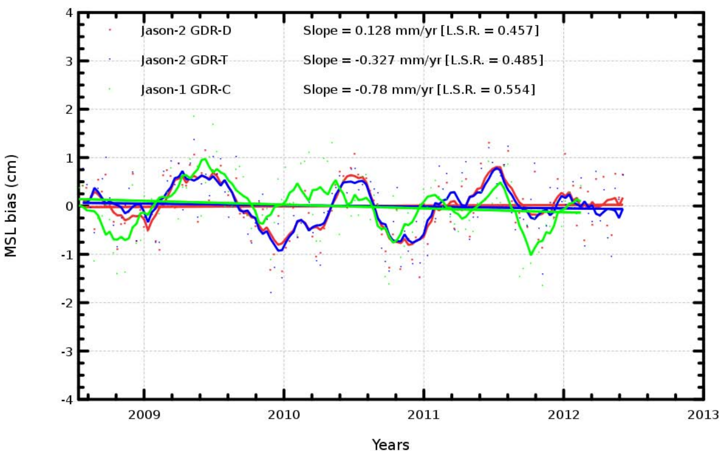

Figure 64: *Jason-2 and Jason-1 altimeter MSL drift compared with tide gauges measurements*

7.2.2. Inter annual evolution of the altimeter residuals compared with Argo T/S profiles

The Argo network provides a coverage of almost the whole global ocean with Temperature and Salinity (T/S) profiles.
About 100 000 profiles per year are available for recent years and the Dynamic Height Anomalies derived from these profiles are used as a reference to analyze the inter-annual evolution of the altimeter residuals (difference between altimeter data and the steric Dynamic Heights Anomalies from Argo T/S profiles and the mass contribution to the sea level from GRACE data).

Figure 65 shows the sea level differences for 3 different missions over the Jason-2 period. Without annual and semi-annual signals, the amplitude of the remaining inter-annual signals ranges within

± 5 mm and a good coherence is observed between the three missions. The sea level differences obtained with Envisat are more different than both Jason differences which are more similar to each other. This is associated with the differences of altimeter standards and corrections (USO, PTR). Note that the 3.5 years period analyzed here remains short to allow the analysis of inter annual signals whose signature is detected at 3 to 5 years minimum.
For further analysis concerning comprison between altimeter and T/S profiles please refer to 2012 report ([13]).

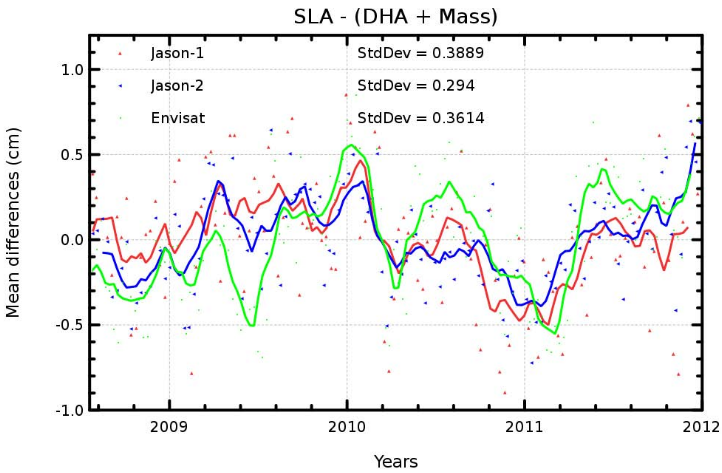

Figure 65: *Monitoring of the altimeter sea level differences compared with Argo and GRACE data for Jason-1, Jason-2 (GDR-D) and Envisat over the Jason-2 altimeter period. Annual and semi-annual signals are removed and data are 2-month filtered.*

8. Particular Investigations

This sections contains some investigations led on Jason-2 data. Some, such as investigation on the low signal tracking anomaly and investigation on radiometer wet troposphere correction, were already presented in previous annual reports. They are maintained in this report, as the features described are still present in the current GDR-D version.
Furthermore, results from preliminary GDR-D products and orbits are also presented.

8.1. Low signal tracking anomaly (AGC anomaly)

During SGT and also Median tracking mode, Jason-2 altimeter could track during several minutes low signal echoes with "Brown like" but "distorted" shape (see [27]). This concerned less than 0.5% of ocean measurements. An example of waveforms during such an anomaly is visible in [55]. This anomaly was especially noticeable over ocean. These measurements were edited by several parameters out of threshold: mispointing, backscattering coefficient, significant wave height. They also showed a drop in AGC (automatic gain control). These anomalies were called "low signal tracking anomaly" or "AGC anomaly". An example of low signal tracking anomaly is shown in figure 66.
Low signal tracking anomaly were especially severe (several tens of minutes) during SGT mode, they were shorter in median mode (at worst a couple of minutes) and never appeared during DEM modes. During cycle 16, on 10th of December 2008, a correction for the low signal tracking anomaly (AGC anomaly) was uploaded (during pass 73). Till cycle 16 pass 70, AGC anomalies were still detected, but no further AGC anomaly (on ocean) has occurred since the upload of the correction. The correction for the low signal tracking anomaly consists in more strict criteria for acquisition (to avoid that low signal echoes are tracked). This has no impact for the quantity of ocean measurements as shown on figure 67 where cycle 15 (before upload of correction for low signal tracking anomaly) and 18 (after upload of correction) show equivalent number of measurements. But number of tracked measurements over land has decreased (see figure 68 and 69).

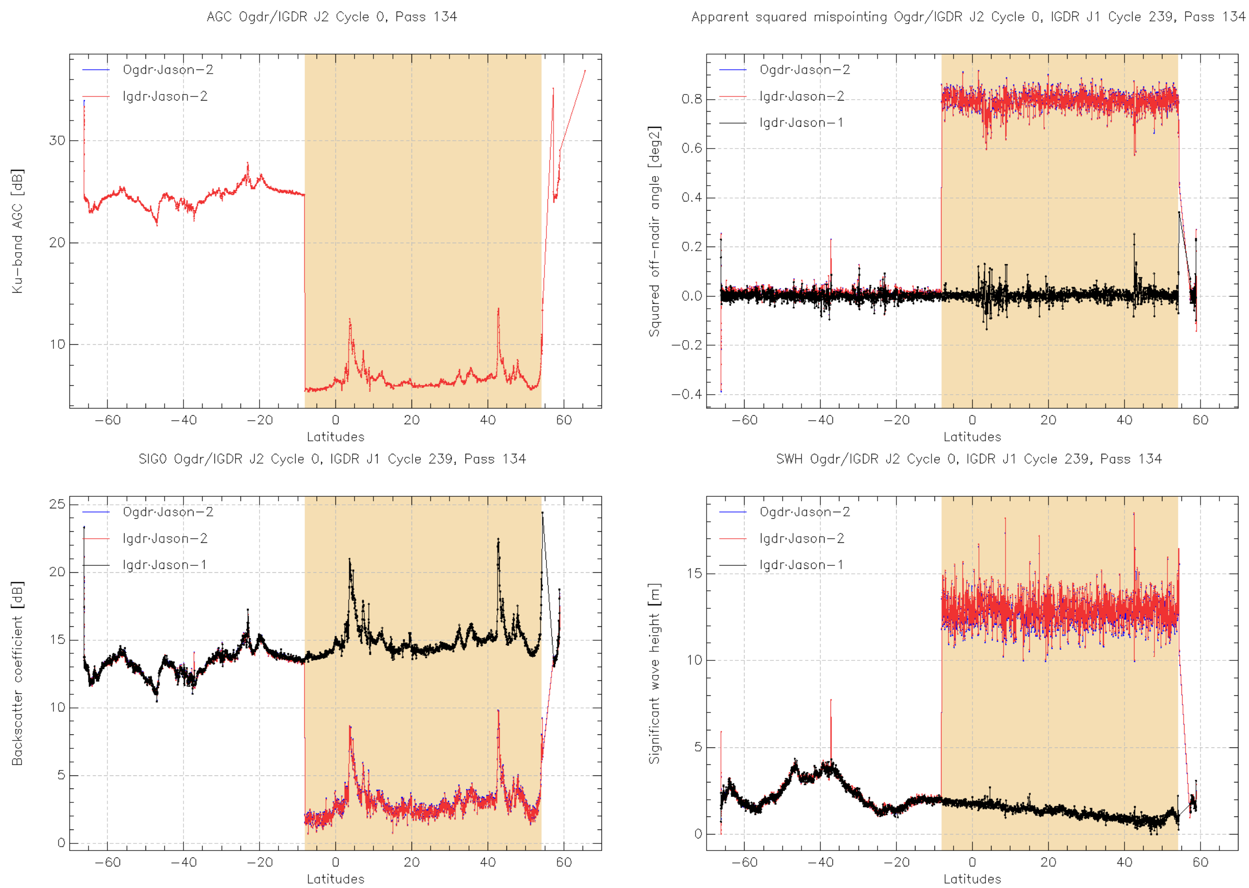

Figure 66: *Example of low signal tracking anomaly for pass 134, Jason-2 cycle 0. Several parameters are shown: AGC (top left), apparent squared mispointing (top right), Sigma0 (bottom left), and SWH (bottom right). Period of anomaly colored.*

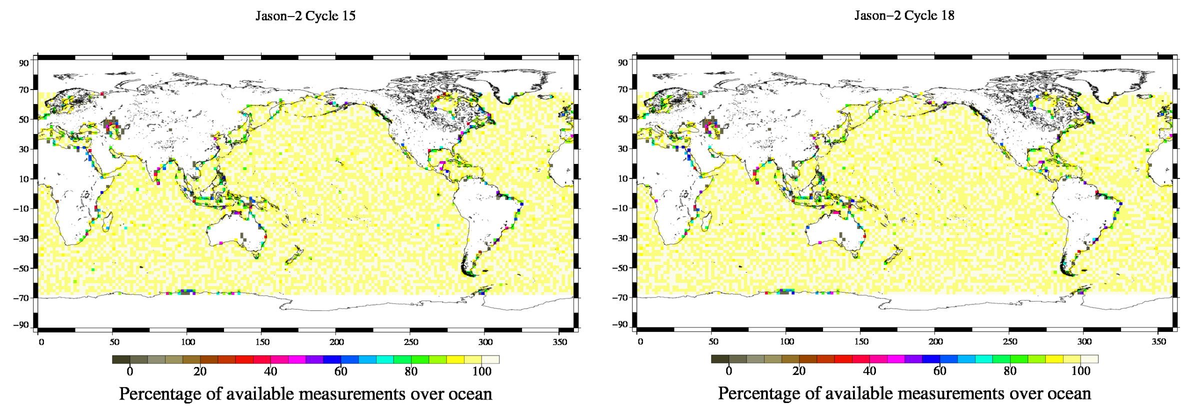

Figure 67: *Percentage of available measurements over ocean for Jason-2 cycle 15 (left) and 18 (right).*

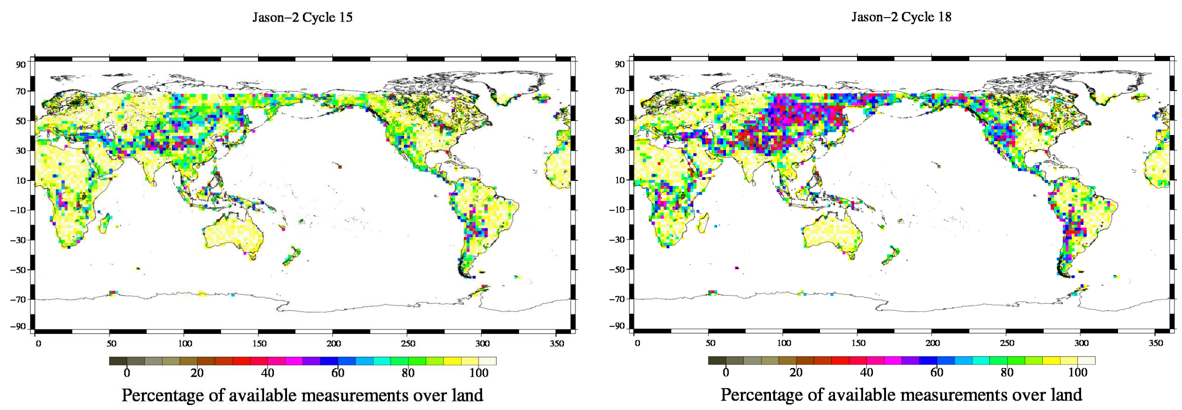

Figure 68: *Percentage of available measurements over land for Jason-2 cycle 15 (left) and 18 (right).*

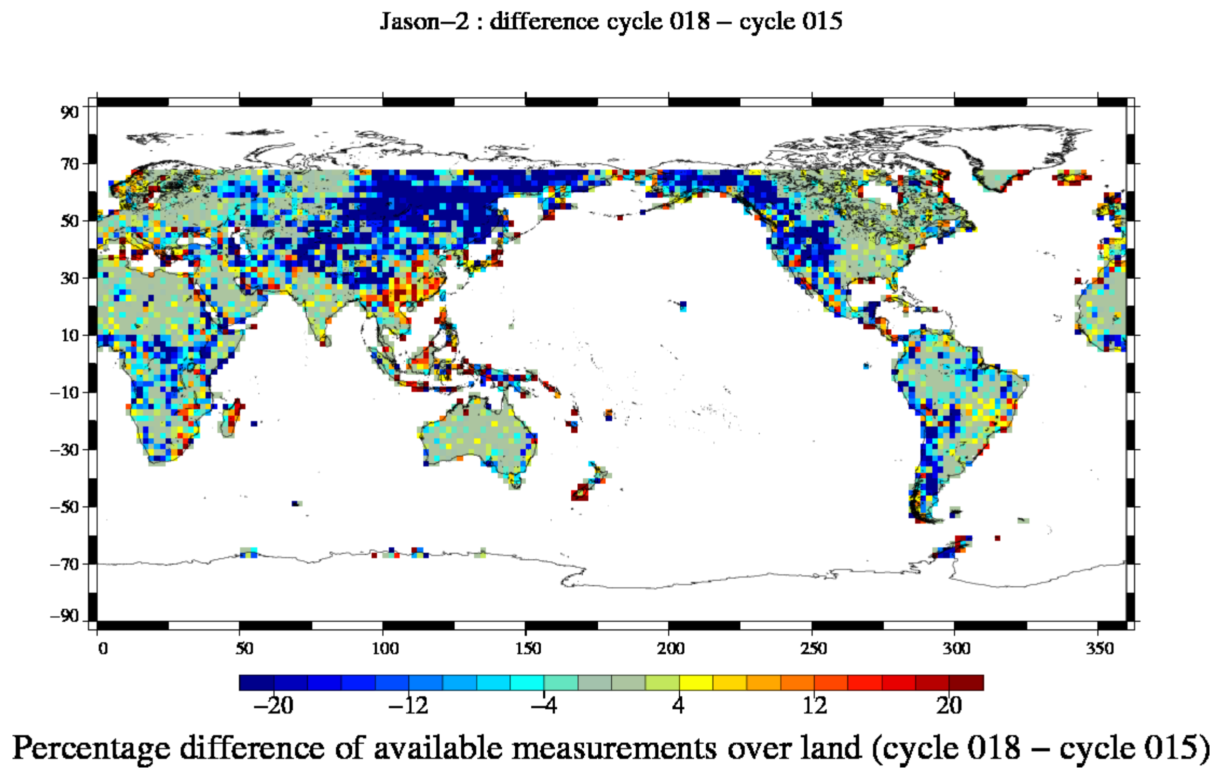

Figure 69: *Percentage difference of available measurements over land for Jason-2. Cycle 018 (after correction) - cycle 015 (before correction).*

8.2. AMR incident during cycle 19

During cycle 19, brightness temperatures and radiometer wet troposphere correction were at default values during two times:

- from 2009-01-07 11:00:35 to 2009-01-08 03:23:34 impacting passes 24 to 42
- from 2009-01-11 03:56:38 to 2009-01-12 19:26:14 impacting passes 119 to 161

The first time brightness temperatures went to default values on pass 24 at land/ocean transition, the second time on pass 119 over pacific ocean (figure 70). Both times, brightness temperatures did not show any anomaly before going to default values, as visible on figure 71, where Jason-2 and Jason-1 34 GHz brightness temperature are shown.

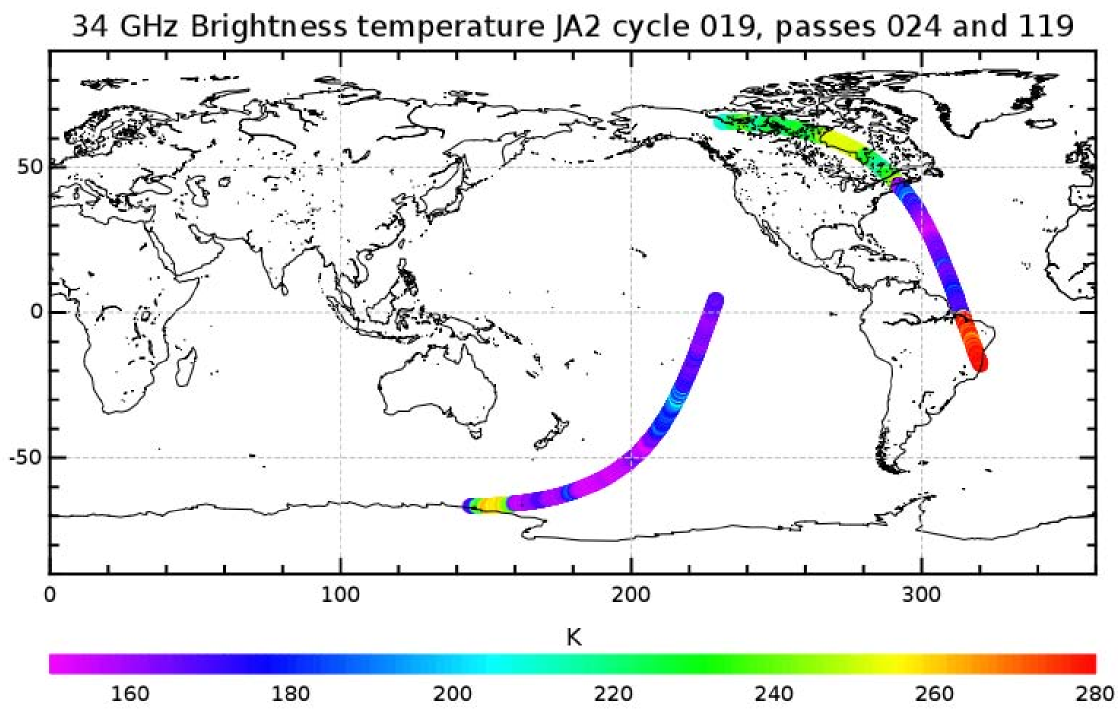

Figure 70: *Map of 34 GHz brigthness temperature for Jason-2 cycle 19 showing location of passes 24 and 119 (passes where incidents started).*

Note that the unavailability of AMR has also a small impact on editing of measurements, other than radiometer wet troposphere correction. Indeed, ice flag also uses brightness temperatures. When they are at default value, a backup is used (based on climatological data). This backup is the same ice flag as used in GDRs version "b" of Jason-1 data. It has the drawback to never detect ice in the far left side of Hudson bay. This also happens on figure 72 for the passes with brightness temperatures at default value. Nevertheless, these measurements - due to their non-ocean waveforms - are edited by other criteria, such as number of elementary 20 Hz measurements, backscattering coefficient, ocean tide, orbit minus range, ... Therefore for cycle 19, percentage of edited measurements is higher than usual for several threshold criteria (see section 3.2.).

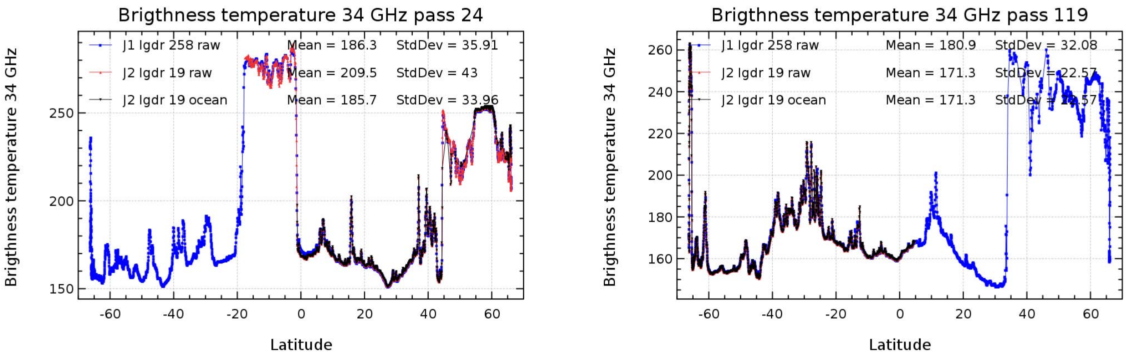

Figure 71: *34 GHz brigthness temperature for Jason-2 in red and black (and Jason-1 in blue) cycle 19 along passes 24 (left) and 119 (right).*

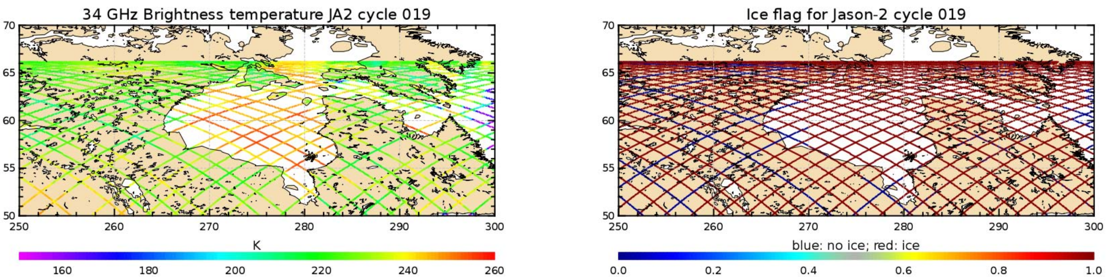

Figure 72: *Map of 34 GHz brightness temperature (left) and map of ice flag (right) in Hudson bay for Jason-2 cycle 19.*

8.3. High Radio-Frequency Interference during cycle 110 pass 47

During routine Cal/Val an anomaly was noticed for pass 047 of cycle 110. Several minutes of non-consecutive open ocean (Pacific) measurements were edited by the radiometer wet troposphere correction (see figure 73).

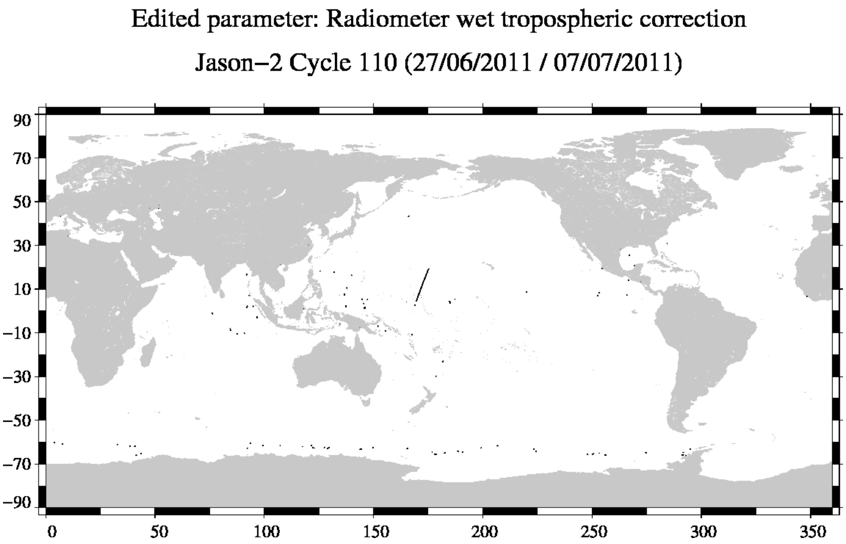

Figure 73: *Map of Jason-2 cycle 110 measurements edited by radiometer wet troposphere correction.*

The radiometer wet troposphere correction is edited as it is either at default value or with zero value. The radiometer and ECMWF wet troposphere corrections are very different during a period of about 10 minutes (between 0˚N and 25˚N). The radiometer correction is very noisy with several default values and zero values.
Regarding brightness temperatures, the 34 GHz channel is also very noisy. Furthermore, for several short periods, it is at default value. At the same time, the 18.7 GHz and 23.8 GHz brightness temperature seem to saturate at respectively 290K and 305K (see figure 74).

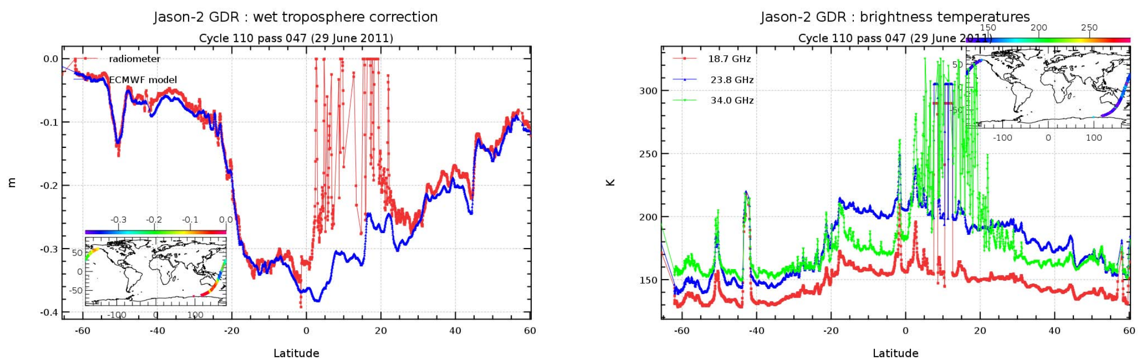

Figure 74: *Jason-2 cycle 110 pass 047: radiometer and ECMWF model wet troposphere correction (left) and brightness temperatures (right).*

Cycle 110 pass 47 was the first time that the radiometer wet troposphere correction was edited

over a relatively long time (a couple of minutes), except of course for cycle 19, when AMR was unavailable.
On other cycles, very small portions (generally less than 1 minute) of the radiometer wet troposphere correction are often edited over ocean, but generally that is due to rain. Furthermore, the brightness temperatures do not show the saturation as on cycle 110 pass 047.

Example: *radiometer wet troposphere correction edited due to rain*
Figure 75 shows the brightness temperatures for pass 162 cycle 32. A small portion is edited by the wet troposphere correction, because it is less (wetter) than -0.5m at about 20° South. The brightness temperatures are high. The map on the right side (Tropical Rainfall Measuring Mission) shows indeed for this region rain.

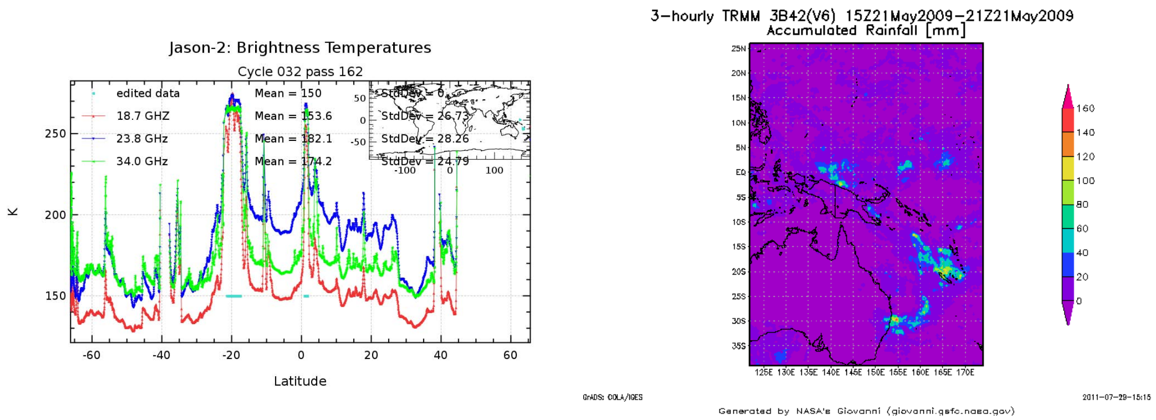

Figure 75: *Jason-2 cycle 032 pass 162: brightness temperatures (left). Map of 3-hourly precipitation products (right).*

Nevertheless, a couple of cases (over very short periods, each time for pass 112) can be found, where the brightness temperatures from 18.7 and 23.8 GHz channels saturate around respectively 290 K and 305 K (as it is the case for cycle 110 pass 047).
These examples of saturated brightness temperatures are pass 112 for cycles 047,048 and 051. The radiometer wet troposphere correction is edited, because it is at default value. Each time it happens near a small island. There seems to be no rain over the island itself. Apart from the saturation, the brightness temperatures seems to behave normally (see figure 76).

Investigations on JPL side, concluded that this unusual behaviour of brightness temperatures and radiometer wet tropopshere correction on pass 047 of Cycle 110 was "due to a very high level of radio-frequency interference from a ground based source. The radiometer behaved as expected during this interference and is healthy" (email from S. Brown).

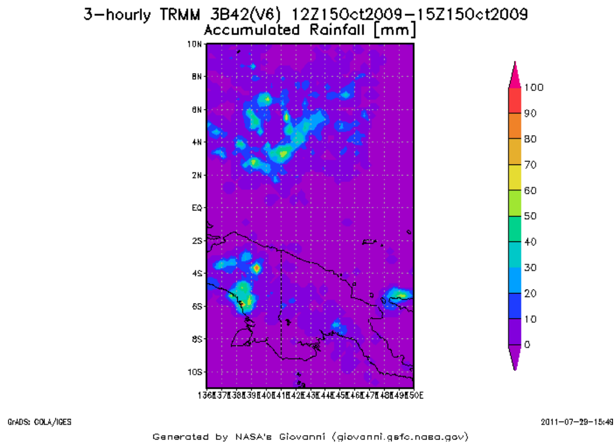

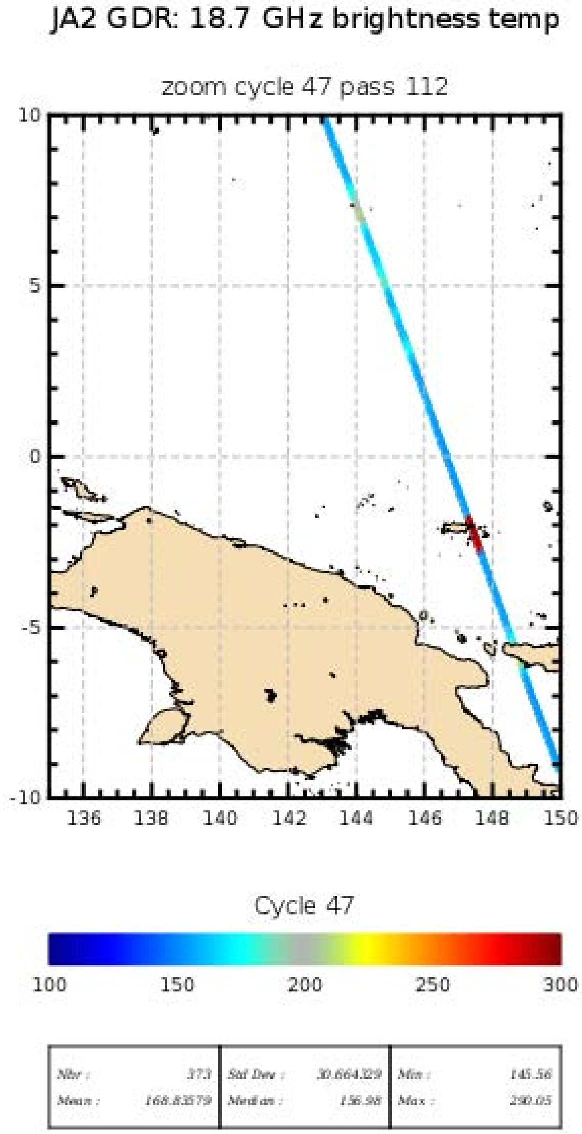

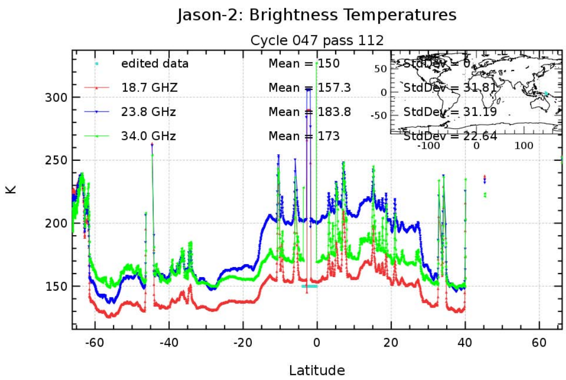

Figure 76: *Map of 3-hourly precipitation products (top left) and map of region where brightness temperatures are at default value (top right). Brightness temperatures for Jason-2 cycle 047 pass 112 (bottom).*

8.4. Comparison between several Jason-2 orbits (JPL, GSFC, POE-C, POE-D)

POE orbit solution from several productions centers (CNES, GSFC, JPL), using different technics, are tested for Jason-2 data (resumed in table 9) in order to study the impact on mean SSH differences at ascending/descending crossovers. Figure 77 shows maps of SSH differences at crossovers for different orbit solutions.
For all figures shown in this chapter Jason-2 GDR-T products were used, only the orbit solution was exchanged. Note that GDR product version and CNES orbit solution version coincide not necessarily, e.g. Jason-2 GDR-T products contained the POE-C standard.

Orbit	Type	Cycles used for figures	ITRF	Gravity field
JPL_RLSE11A (reduced dynamic)	using GPS only	1 to 144	IGS08 (co-eherent to ITRF2008)	GGM02Cs
GSFC_STD1201	using Doris only	1 to 144	2008	GOCO2S_fit
POE CNES standard GDR-T (called POE-C in this part)	using Doris, GPS and Laser	1 to 144	2005	EIGEN-GL04S
POE CNES standard GDR-D (called POE-D in this part)	using Doris, GPS and Laser	1 to 144	2008	EIGEN-GRGS_RL02bis_MEAN-FIELD

Table 9: *U*sed orbits

Orbits of Jason-2 GDR-T products are fully compliant with requirement. Nevertheless, small geographically correlated patterns of amplitudes up to ± 2 cm (positive in North-Atlantic and South-Pacific, negative in South-Atlantic and North-Pacific) are visible on maps of mean SSH differences at crossovers (see bottom left of figure 77). Using orbits based on a new version of gravity field reduces these small geographically correlated pattern (see figure 77). Moreover, note that for all tested orbits, data were corrected for a pseudo datation bias (-0.28ms) following the discovery of an anomaly in the ground processing software (see also chapter 5.5.). So, a small hemispheric signal of about 1 cm between northern and southern hemisphere disappears when correcting for pseudo datation bias.

Figure 78 shows temporal evolution of mean SSH differences at crossovers. It shows a 120 day signal (related to β' angle) for most orbit solutions. JPL_RLSE11A and POE-D orbits seem less impacted than GSFC_STD1201 and POE-C orbits. POE-C orbit solutions show a strong ascending/descending SSH differences (as also shown on figure 77). All tested orbits show an improvement versus POE-C, as it is more centered and particularly POE-D and JPL_RLSE11A orbits (see left of figure 78).
Figure 79 shows differences of SSH variances (test orbit variance - POE-D orbit variance). Negative values indicate a variance reduction (hence an improvement) of the test orbit in comparison to the POE-D orbit. JPL_RLSE11A orbit solution shows clearly an improvement versus the POE-D orbit

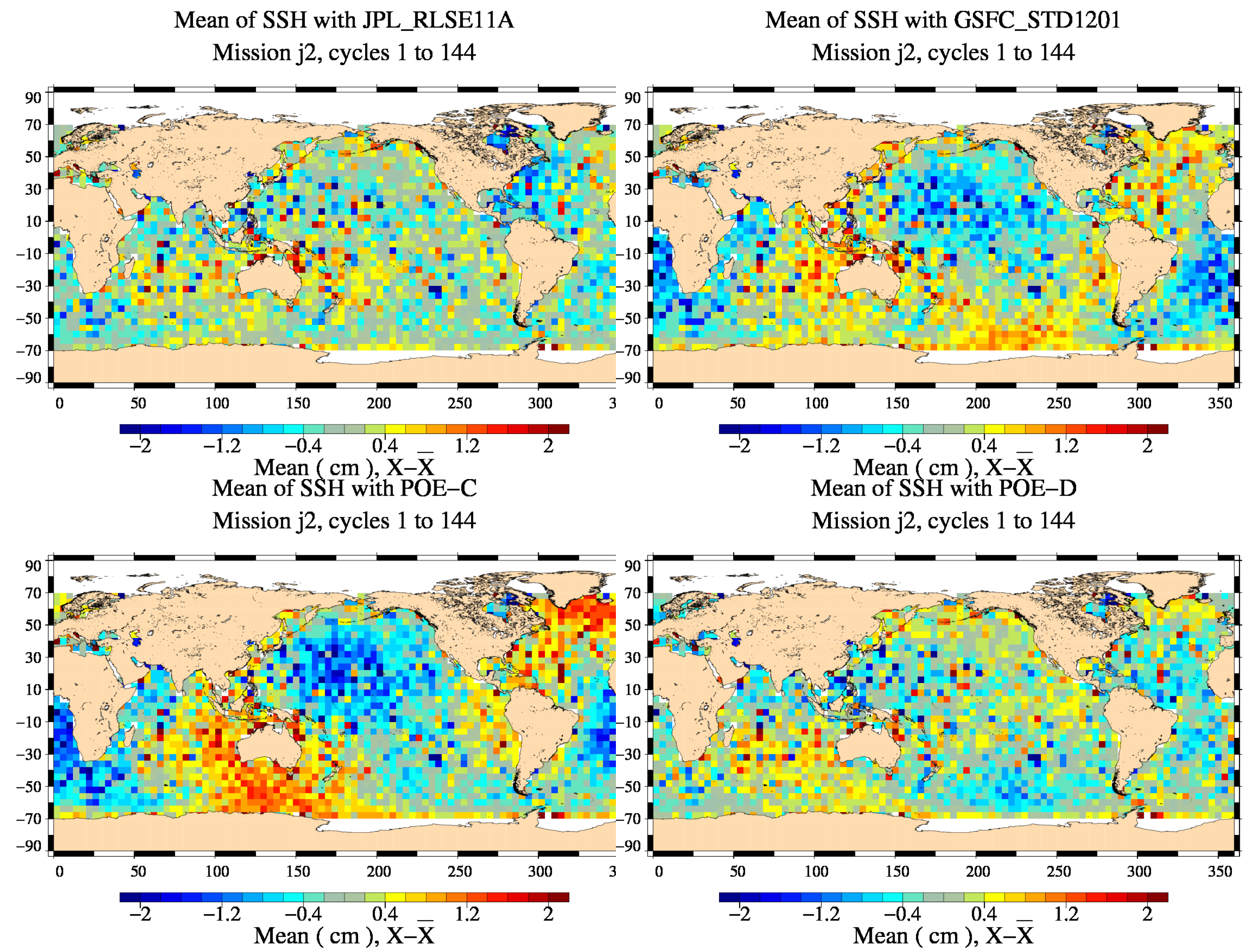

Figure 77: *Map of mean of SSH crossovers differences using JPL_RLSE11A (top left), using GSFC_STD1201 (top right), using POE-C (bottom left), and using POE-D (bottom right). Data cover Jason-2 cycles 1 to 144.*

while POE-C orbit solution shows a deterioration versus the POE-D orbit. GSFC_STD1201 orbit solution show similar performances as POE-D orbit.

Concerning global Mean Sea Level slope (see figure 80), use of all tested orbits versus use of POE-D orbit has a small impact on the slope: 0.1 mm/year. When seperating in odd and even passes, MSL slopes differences between even and odd passes are more homogeneous for JPL_RLSE11A and POE-D orbits than GSFC_STD1201 and POE-C orbits as shown values in table 10. Nevertheless, four years of data is a quite short period to compute the Mean Sea Level slope and figures have to be taken with caution.

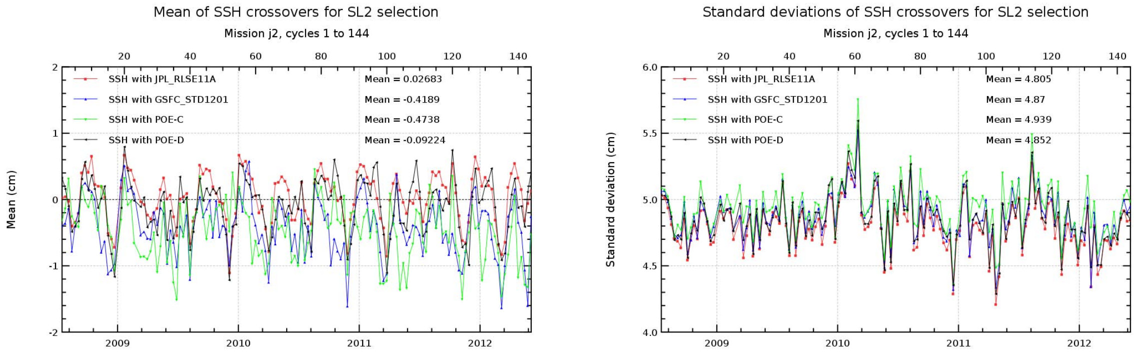

Figure 78: *Cyclic monitoring of mean (left) and standard deviation (right) SSH differences at crossovers for SL2 selection (i.e |Lat| < 50, Bathy < -1000m, low variability) using respectively JPL_RLSE11A, GSFC_STD1201, POE-C and POE-D. Data cover Jason-2 cycles 1 to 144.*

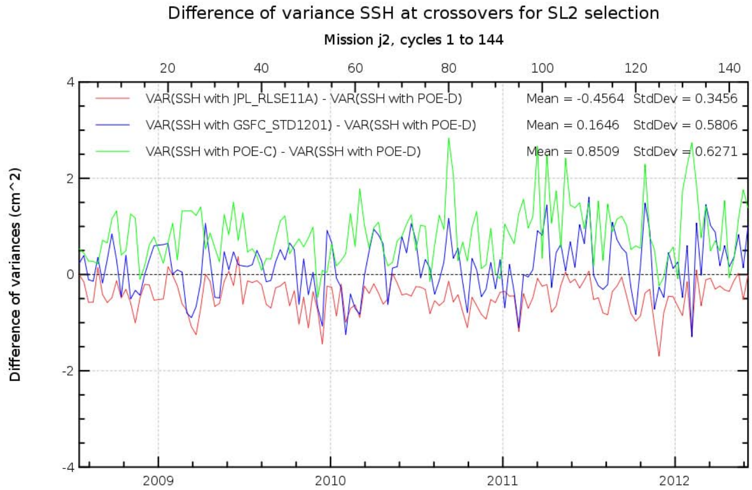

Figure 79: *Cyclic monitoring of differences of SSH variances at crossovers for SL2 selection (i.e |Lat| < 50, Bathy < -1000m, low variability) using different POEs (variance(SSH using test POE) - variance(SSH using POE-D)). Data cover Jason-2 cycles 1 to 144.*

MSL	MSL slope using JPL_RLSE11A	MSL slope using GSFC_STD1201	MSL slope using POE-C	MSL slope using POE-D
global	1.71 mm/yr	1.73 mm/yr	1.75 mm/yr	1.63 mm/yr
even passes	1.75 mm/yr	1.40 mm/yr	1.38 mm/yr	1.63 mm/yr
odd passes	1.63 mm/yr	2.01 mm/yr	2.09 mm/yr	1.59 mm/yr
.../...				

MSL	MSL slope using JPL_RLSE11A	MSL slope using GSFC_STD1201	MSL slope using POE-C	MSL slope using POE-D
difference between odd and even passes	0.12 mm/yr	-0.61 mm/yr	-0.71 mm/yr	0.04 mm/yr

Table 10: *M*ean sea level slopes

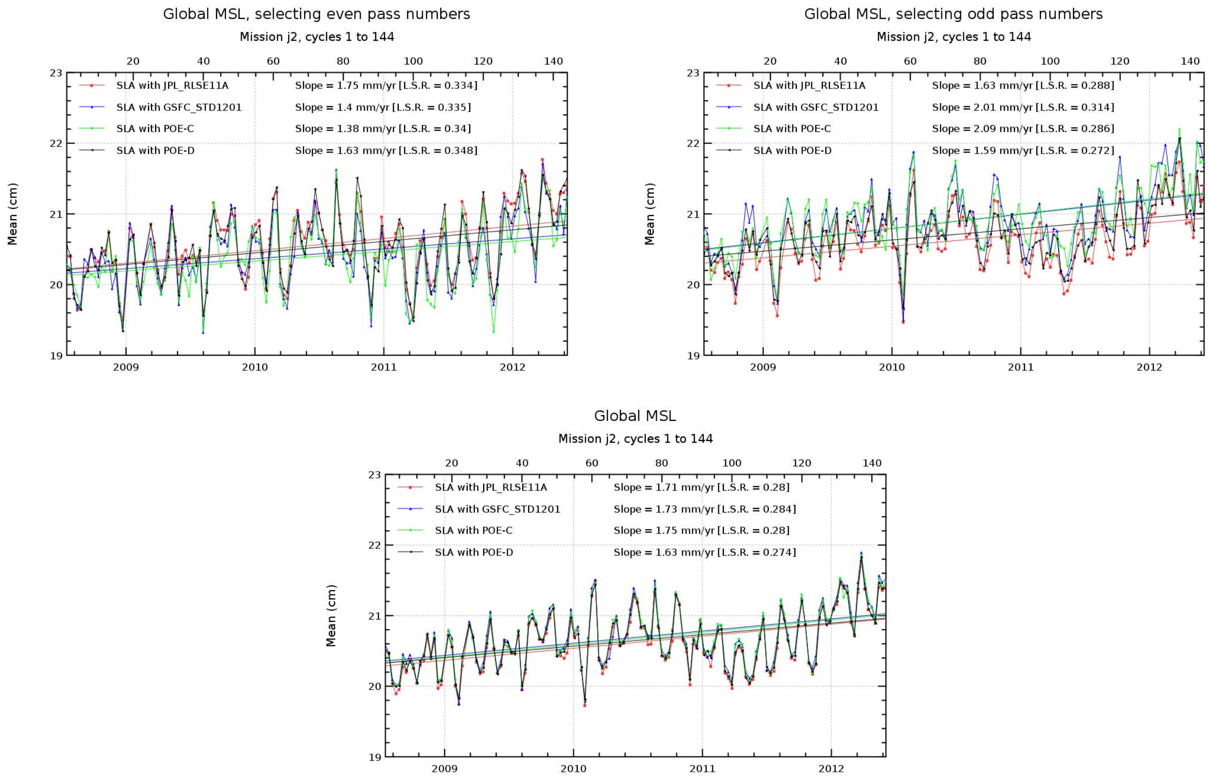

Figure 80: *Cyclic monitoring of global mean sea level separating even and odd passes (top) and all passes mixed-up (bottom) using respectively JPL_RLSE11A, GSFC_STD1201, POE-C and POE-D. Data cover Jason-2 cycles 1 to 144.*

8.5. Reduction of GMSL differences between Colorado University (CU) and AVISO from 2005 to 2011

Several institutions compute global mean sea level. Though on the global 20 years period they show similar figures, they differ when looking at shorter periods, but also concerning inter-annual signals. Till mid-2012 there were noticeable differences between AVISO and CU GMSL especially for the period from 2005 to 2011.
The objective of this part is to analyze the GMSL differences between AVISO and CU from 2005 to 2011 homogenizing on the first hand the methodologies to calculate the MSL and on the other hand the altimeter standards used in the sea level calculation.

8.5.1. GMSL differences between AVISO and CU applying the CU methodology

We have calculated the GMSL derived from AVISO and CU data applying the same CU methodology. The choice of applying CU method is arbitrary: it does not mean that CU method is better than AVISO one. After removing annual signal and filtering out frequencies lower than 2 months, differences between both GMSL have been computed and plotted (Fig. 81, blue curve) focusing only on 2005-2011 period. In order to estimate the impact of this homogeneous processing, we have also superimposed on the same figure (Fig. 81, green curve) the original GMSL differences between AVISO and CU. The trend of blue curve is reduced to 0.44 mm/yr instead of 0.87 mm/yr in green curve. We also observed a lower dispersion of GMSL differences within an interval of +/- 2 mm. For instance, the significant GMSL differences observed on the green curve in 2010 (about 3 mm) are totally removed on the blue curve. The use of the same methodology on CU and AVISO data allows us to homogenise both GMSL and to reduce the trend difference on the 2005-2011 period. However this trend difference (0.44 mm/yr) is still significant. It could be explained by the choice of altimeter standards applied in AVISO and CU processing.

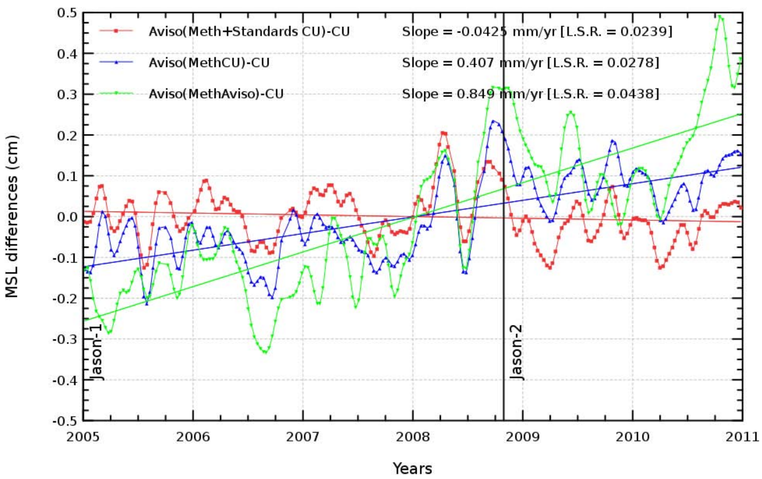

Figure 81: *Comparison between the GMSL derived from AVISO and CU data. On green curve, original methodologies and altimeter standard are used for AVISO and CU. On blue curve, the CU methodology is applied on AVISO data without changing the altimeter standards. On red curve, the AVISO MSL has been calculated with the CU methodology and the CU altimeter standards. Time series have been calculated filtering out signals lower than 2 months.*

8.5.2. Impact of altimeter standards applied on AVISO and CU for Jason-1 and Jason-2

AVISO and CU data used to compute the GMSL are derived from Geophysical Data Records (GDR) products: GDR-C for Jason-1 and **GDR-T** for Jason-2. In order to improve the MSL calculation, some standards have been replaced. Consequently, altimeter standards used by each group are not necessarily identical. They are exhaustively described on AVISO and CU websites (http://www.aviso.oceanobs.com/msl/ and http://sealevel.colorado.edu). We have analyzed these different choices made by both groups for Jason-1 and Jason-2 from 2005 to 2011. They concern the orbit solutions and the wet troposphere correction only for Jason-1 and the Sea State Bias (SSB) models for both missions:

- For the orbit, CU has applied the GSFC-STD09 orbit solutions for Jason-1 (Lemoine et al., 2010 - reference [39]). On AVISO, the CNES POE orbit solution of the GDR-C product has not been changed. For Jason-2, CNES POE orbit solution is used for both groups.

- For the SSB, CU has applied the "CLS Collinear v. 2009" SSB model (Tran et al., 2010 - reference [58]) for Jason-1 and Jason-2. On AVISO, the GDR-C and GDR-T SSB models have been used respectively for Jason-1 and Jason-2.

- For the wet troposphere correction, CU has used the JMR (Jason-1 Microwave Radiometer) replacement product for Jason-1 from cycles 228 to 259 (provided by JPL) and the GDR-C correction the other cycles. On AVISO, the GDR-C correction was used over all the period.

All the other altimeter standards are the same for both CU and AVISO groups. In order to know the impact of the CU altimeter standards on the AVISO GMSL time series, we have tested each of them separately:

- Impact of the GSFC-std09 orbit solution on AVISO GMSL:

  In order to test the impact of the GSFC orbit solution (STD09) selected by CU, we have computed the AVISO GMSL time series replacing the CNES GDR-C orbit solution by the GSFC one on the Jason-1 measurements only. In order to link Jason-1 and Jason-2 MSL time series, we have also recomputed the MSL bias between Jason-1 and Jason-2 using the Jason-2 verification phase (from July 2008 to January 2009) where Jason-1 and Jason-2 are on the same ground track spaced out by 54 seconds (AVISO website). The difference between both GMSL time series has been computed from 2005 to 2011 (fig. 82, on top left). There is a small impact on the global trend close to -0.1 mm/yr. No inter-annual or periodic signals have been detected.

- Impact of SSB "CLS Collinear v. 2009" on AVISO GMSL:

  With the same approach, we have tested the impact of SSB "CLS Collinear v. 2009" on AVISO GMSL in comparison with SSB solutions included in GDR products. The difference between both GMSL time series has been computed from 2005 to 2011 (fig. 82, on top right). Very low impact on the global trend (lower than 0.05 mm/yr), and no significant inter-annual or periodic signals have been detected. Notice that the SSB bias between new and old models is close to -2.5 mm on Jason-1 and +6 mm on Jason-2. This means that the MSL bias between Jason-1 and Jason-2 has been reduced by 8.5 mm without any impact on the global trend.

- Impact of new Jason-1 wet troposphere correction on AVISO GMSL:

For the radiometer wet troposphere correction, the JMR replacement product provided by JPL and used by CU has only been modified between Jason-1 cycles 228 to 259 (March 2008 to January 2009). With the same method, the difference between both GMSL time series has been computed from 2005 to 2011 (fig. 82, on bottom). Unlike previous studied cases (orbit and SSB), the impact on the trend is stronger since MSL AVISO trend is reduced by 0.3 mm/yr mainly due to a jump close to 1 mm between Jason-1 and Jason-2. Its interesting to clarify the reason explaining this jump. Indeed the JMR replacement wet troposphere correction has a small impact on the Jason-1 global MSL time series since averaged differences over a 10-day period are lower than 3 mm without any impact on the Jason-1 global MSL trend. But these small differences occur during the Jason-2 verification phase (from July 2008 to January 2009) which is used to calculate the MSL bias between Jason-1 and Jaon-2 as previously mentioned. Thanks to the new Jason-1 wet troposphere correction, the MSL differences between both missions are more homogenous. Therefore, the MSL bias can be calculated more accurately. In practice, the new MSL bias calculated with the new Jason-1 replacement product is 75.6 mm instead of 74.4mm. This means that Jason-2 data are fitted on Jason-1 data with a bias 1.2 mm higher whereas the Jason-1 and Jason-2 global MSL biases have not been modified. Consequently, the global MSL trend is directly impacted and reduced by about 0.3 mm/yr over the 2005-2011 period.

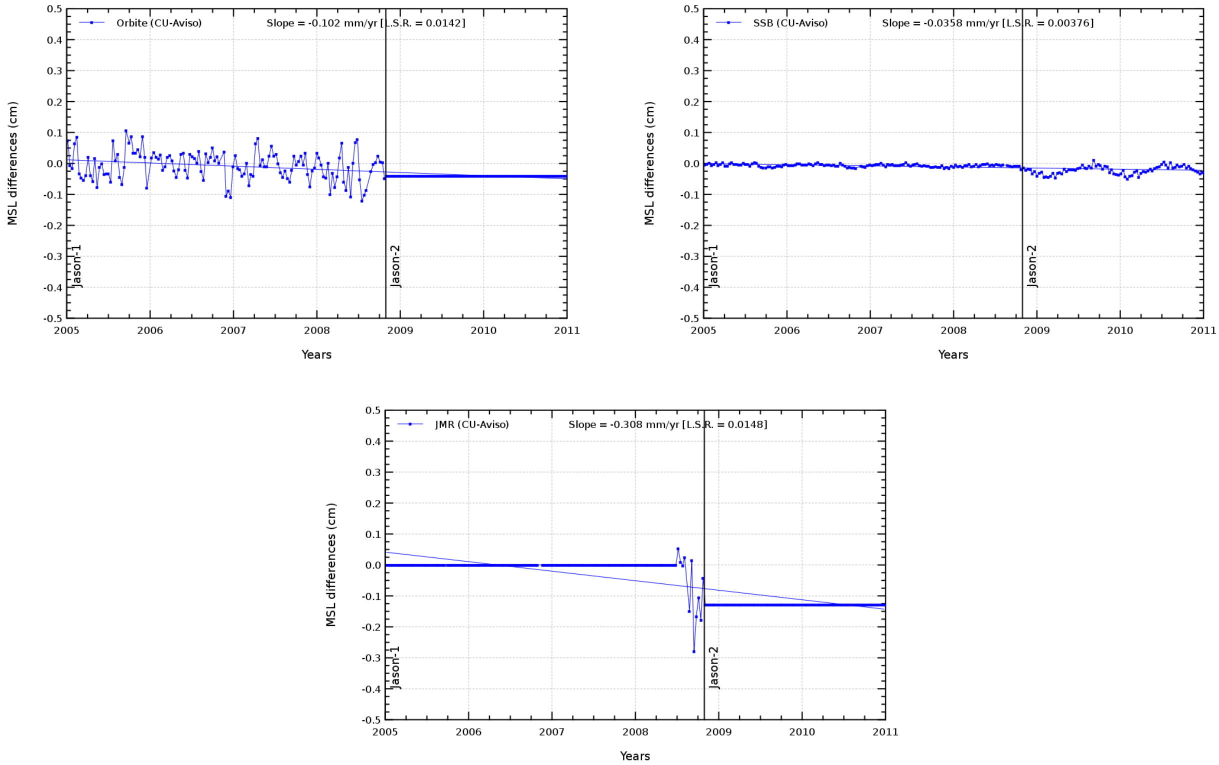

Figure 82: *Differences between global MSL time series calculated with altimeter standards applied by CU and AVISO: on bottom, Jason-1 replacement product (CU) versus GDR (AVISO) for the radiometer wet troposphere correction; on top right, impact of Jason-1 and Jason-2 SSB v2009 models (CU) versus the GDR corrections (AVISO); on top left, impact of the Jason-1 GSGC-std09 orbit solution (CU) versus the GDR one (AVISO).*

8.5.3. Total impact: methods and altimeter standards

Finally, all the altimeter standards together (orbit, SSB, and radiometer wet troposphere correction) have an impact on the trend close to -0.46 mm/yr (fig. 83). We have calculated the MSL differences between both groups applying on AVSIO side the CU altimeter standards and methodology (fig. 81, red curve). The trend difference between both global MSL is almost null (< 0.05 mm/yr) between 2005 and 2011. Method and altimeter standards explain each 50% of the trend reduction. Most of the contribution due to altimeter standard is due to the JMR replacement product for the radiometer wet troposphere correction. Notice also that the formal error provided by the least square procedure to adjust the slope is reduced to 0.024 mm/yr instead of 0.044 mm/yr, highlighting a better consistency between both time series. The reasons explaining the small remaining differences are likely due to the processing applied in order to remove the spurious altimeter measurements over ocean.

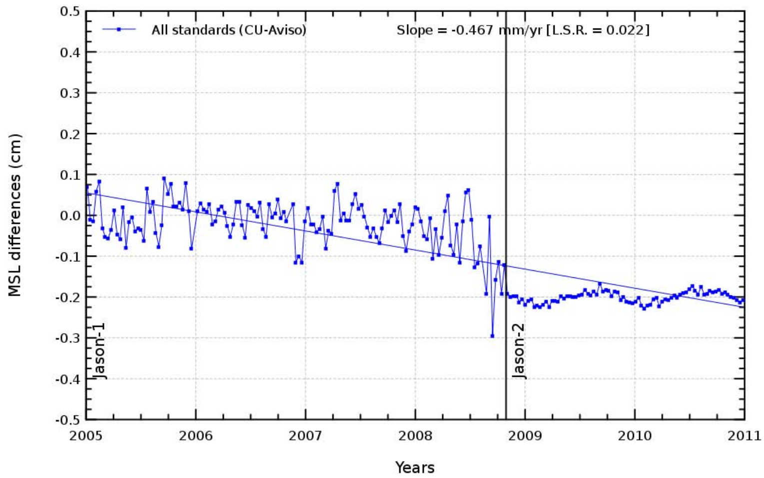

Figure 83: *Differences between global MSL time series calculated with all CU altimeter standards (Orbit, SSB and wet troposphere correction) versus AVISO ones.*

Note that since september 2012, AVISO GMSL uses for Jason-1 the JMR replacement product.

9. Conclusion

Jason-2 is in orbit since 20th of June, 2008. During the flight formation phase, which lasted 20 cycles (till 2009-01-26), Jason-2 flew with Jason-1 (55s apart) over the same historical TOPEX/Poseidon ground track. This allowed extensive verification and validation of the data, as both satellites observed the same geophysical phenomena. OGDR and IGDR data quality was already approved during OSTST 2008 meeting in Nice. OGDR products were distributed to users since mid-December 2008 and IGDR since mid-January 2009. The GDR production started end of February 2009 and was released in version T to users since August 2009. More than 4 years of GDR data are now available. In 2012, the whole mission was reprocessed in standard GDR-D.

The flight formation phase has shown that Jason-2 data quality is excellent, at least of the same order as the Jason-1 one. The raw data coverage is similar to Jason-1's over ocean and improved in coastal areas. Thanks to the new altimeter tracking modes, the availability of land measurements is significantly improved. Over ocean, the valid data coverage is similar since the additional Jason-2 raw measurements are removed by the editing procedure. The additional measurements in coastal areas and over rivers and lakes benefit to projects such as PISTACH.

The altimetric parameter analysis has shown a similar behavior compared to Jason-1. Some biases exist as between dual-frequency ionosphere correction, but they are stable. Though Jason-2 radiometer performances are improved especially near coasts, stability problems are observed in Jason-2 IGDR product (small jumps (versus JMR or ECMWF model) occurred in 34 GHz channel). During 2011, these stability problems became more frequent leading to jumps and drifts also in the 18.7 GHz channel. These stability problems are mostly corrected thanks to the ARCS system applied for GDR. For the GDR-D reprocessing, new calibration coefficients were used. According to the JPL, cycles 001 to 113 have climate data record quality calibrations, cycles 114 to 140 have intermediate quality calibrations and cycle 141 and onwards have operational (ARCS) quality calibrations. But even the new calibration coefficients are not able to correct rapid drifts which occur within a cycle (as happened around cycle 120).

The SSH performances analyzed at crossovers or along-track highlight similar performances between Jason-1 and Jason-2. The consistency between both SLA is remarkable with a small geographically correlated signal lower than 1 cm. This signal is removed using GSFC orbits proving the sensibility of the orbit calculation for the detection of geographically correlated biases. The fact that several production centers (CNES, JPL, GSFC) compute different kinds (tri-technic, GPS only, Doris+SRL) of Jason-2 precise orbit solutions, gives also a great opportunity to understand more about the impact of orbit on altimetry data and to explain some of the observed signals.

The flight formation phase between Jason-1 and Jason-2 allowed us to check accurately the Jason-2 mission. As during the Jason-1/TOPEX flight formation phase, we also learned a lot from Jason-1 measurement quality. To balance all these excellent results and especially the quasi-perfect SSH consistency between both missions, both systems can contain similar errors undetectable with the analyzes performed here. Comparisons with external and independent datasets (Tide gauges, Temperature/Salinity profiles, ...) are thus essential to detect potential errors.

The more of 4 years of Jason-2 data show excellent quality. Scientific studies and operational applications therefore benefit from the combination of Jason-2, Jason-1, and Envisat data. The 2012 reprocessing of the whole mission in GDR-D standard has improved the dataset in comparison to the GDR-T standard for meso-scales (improved coherence at crossover points), as well as on longer time scales (coherence between ascending and descending passes is improved).

The remaining open points which needs further investigation or surveillance are:

- the stability of the AMR
- the remaining signal of approximatly 120 days in the monitoring of the ascending/descending crossover differences.
- the exessive altimeter rain flag
- the sea state bias, which is quite different from the one of Jason-1 (nevertheless new sea state bias look-up tables (presented at OSTST 2012 by Tran et al.[[60]]) are available for Jason-1 and Jason-2)
- the radiometer processing is different between Jason-1 and Jason-2
- there remains a hemispherical bias linked to orbit solutions

10. References

References

[1] Ablain, M., A. Cazenave, G. Valladeau, and S. Guinehut. 2009 : A new assessment of the error budget of global mean sea level rate estimated by satellite altimetry over 1993-2008. *Ocean Sci*, **5, 193-201**. Available at http://www.ocean-sci.net/5/193/2009/os-5-193-2009.pdf

[2] Ablain, M., S. Philipps, M. Urvoy, N. Tran, and N. Picot (2012) Detection of Long-Term Instabilities on Altimeter Backscattering Coefficient Thanks to Wind Speed Data Comparisons from Altimeters and Models, *Marine Geodesy*, **35:S1, 258-275**. Available at http://www.tandfonline.com/doi/pdf/10.1080/01490419.2012.718675

[3] AVISO and PODAAC User Handbook. IGDR and GDR Jason-1 Products. Edition 4.1, October 2008. SMM-MU-M5-OP-13184-CN (AVISO), JPL D-21352 (PODAAC). Available at http://www.aviso.oceanobs.com/fileadmin/documents/data/tools/hdbk_j1_gdr.pdf.

[4] Beckley, B. D. , Zelensky, N. P. , Holmes, S. A. , Lemoine, F. G. , Ray, R. D. , Mitchum, G. T. , Desai, S. D. and Brown, S. T. (2010) Assessment of the Jason-2 Extension to the TOPEX/Poseidon, Jason-1 Sea-Surface Height Time Series for Global Mean Sea Level Monitoring, *Marine Geodesy*, **33:1, 447 - 471**. Available at http://pdfserve.informaworld.com/96442__925511460.pdf

[5] Bertiger, Willy , Desai, Shailen D. , Dorsey, Angie , Haines, Bruce J. , Harvey, Nate , Kuang, Da. , Sibthorpe, Ant and Weiss, Jan P. (2010) Sub-Centimeter Precision Orbit Determination with GPS for Ocean Altimetry. *Marine Geodesy*, **33:1, 363 - 378**. Available at http://pdfserve.informaworld.com/858128__925510150.pdf

[6] Bertiger, Willy , Desai, Shailen D. , Haines, Bruce J., R. DeCarvalho, and A. Dorsey (2010) Jason-2/OSTM Precision Orbit Determination with GPS *Oral presentation at OSTST meetting, Lisbon, Portugal*, Available at http://www.aviso.oceanobs.com/fileadmin/documents/OSTST/2010/oral/19_Tuesday/bertiger.pdf

[7] E. Bronner and G. Dibarboure, May 24th, 2012: Technical Note about the Jason-1 Geodetic Mission. *SALP-NT-MA-EA-16267-CNv1.0*. Available at: http://www.aviso.oceanobs.com/fileadmin/documents/data/duacs/Technical_Note_J1_Geodetic_Mission.pdf

[8] Philipps, S., M. Ablain, G. Valladeau, and J.-F. Legeais. Jason-2 validation and cross calibration activities (Annual report 2011). Reference: CLS.DOS/NT/12-005. Nomenclature: SALP-RP-MA-EA-22042-CLS. Available at http://www.aviso.oceanobs.com/fileadmin/documents/calval/validation_report/J2/annual_report_j2_2011.pdf.

[9] Ollivier A., M. Guibbaud. Envisat RA2/MWR ocean data validation and cross-calibration activities. Yearly report 2012. SALP-RP-MA-EA-22163-CLS, CLS.DOS/NT/12-292.

[10] Roinard, H., S. Philipps. Jason-2 reprocessing impact on ocean data (cycles 001 to 145). Comparison of Jason-2 Gdr-D with Gdr-T, as well as with Jason-1 Gdr-C and Envisat Gdr v2.1. SALP-RP-MA-EA-22140-CLS. CLS.DOS/NT/12.222.

[11] Roinard, H., S. Philipps. Jason-2 reprocessing impact on ocean data (cycles 001 to 020). Comparison of Jason-2 Gdr-D with Gdr-T, as well as with Jason-1 Gdr-C. SALP-RP-MA-EA-22118-CLS. CLS.DOS/NT/12.138. Available at ftp://avisoftp.cnes.fr/AVISO/

pub/jason-2/documentation/gdr_d_calval_report/JA2_GDR_D_validation_report_cycles1to20_V1_1.pdf

[12] Valladeau, G.. Validation of altimetric data by comparison with tide gauge measurements for TOPEX/Poseidon, Jason-1, Jason-2 and Envisat. SALP-NT-MA-EA-22157-CLS, CLS.DOS/NT/12-259.

[13] Legeais J.-F. and S. Dupuy. 2012 annual report: Validation of altimeter data by comparison with in-situ T/S Argo profiles for T/P, Jason-1, Jason-2 and Envisat missions. CLS-DOS/NT/12-261. SALP-RP-MA-EA-22176-CLS.

[14] Boening, C., J. K. Willis, F. W. Landerer, R. S. Nerem, and J. Fasullo (2012), The 2011 La Niña: So Strong, the Oceans Fell, *Geophys. Res. Lett.*, doi:10.1029/2012GL053055, in press.

[15] Boy, François and Jean-Damien Desjonqueres. 2010. Note technique datation de linstant de reflexion des échos altimètres pour POSEIDON2 et POSEIDON3 *Reference: TP3-JPOS3-NT-1616-CNES*

[16] Brown G.S., "The average impulse response of a rough surface and its application", *IEEE Transactions on Antenna and Propagation*, Vol. AP 25, N1, pp. 67-74, Jan. 1977.

[17] Brown S., S. Desai, and W. Lu "Initial on-orbit performance assessment of the advanced microwave radiometer and performance of JMR GDR-C", *Oral presentation at OSTST meeting, Nice, France, 9-12 november 2008*. Available at http://www.aviso.oceanobs.com/fileadmin/documents/OSTST/2008/oral/brown_calval.pdf

[18] Brown, S., S. Desai, W. Lu, and A. Sibthorpe. 2009. Performance Assessment of the Advanced Microwave Radiometer after 1 Year in Orbit. *Oral presentation at OSTST meeting, Seattle, USA*. Available at: http://www.aviso.oceanobs.com/fileadmin/documents/OSTST/2009/oral/Brown.pdf

[19] S. Brown. 2010. A Novel Near-Land Radiometer Wet Path-Delay Retrieval Algorithm: Application to the Jason-2/OSTM Advanced Microwave radiometer. *IEEE TGRS vol. 48 n°4*. Available at ftp://podaac.jpl.nasa.gov/allData/ostm/preview/L2/AMR/docs/Brown_TGARS_2010.pdf

[20] Cerri, L. , Berthias, J. P. , Bertiger, W. I. , Haines, B. J. , Lemoine, F. G. , Mercier, F. , Ries, J. C. , Willis, P. , Zelensky, N. P. and Ziebart, M. (2010) Precision Orbit Determination Standards for the Jason Series of Altimeter Missions, *Marine Geodesy*, **33:1, 379 - 418**. Available at http://pdfserve.informaworld.com/816985__925509111.pdf

[21] Cerri, L., A. Couhert, S. Houry, F. Mercier. 2011. Improving the long-term stability of the GDR orbit solutions. *Oral presentation at OSTST meeting, San Diego, USA*. Available at http://www.aviso.oceanobs.com/fileadmin/documents/OSTST/2011/oral/02_Thursday/Splinter3POD/05_Cerri.pdf.

[22] Chambers, D., P., J. Ries, T. Urban, and S. Hayes. 2002. Results of global intercomparison between TOPEX and Jason measurements and models. *Paper presented at the Jason-1 and TOPEX/Poseidon Science Working Team Meeting, Biarritz (France), 10-12 June.*

[23] Collard, F. (2005). Algorithmes de vent et période moyenne des vagues JASON à base de réseaux de neurons. BO-021-CLS-0407-RF. Boost Technologies.

[24] Commien, L., S. Philipps, M. Ablain and N. Picot. 2009. SSALTO CALVAL Performance assessment Jason-1 GDR "C"/GDR "B". *Poster presented at OSTST meeting, Seattle, USA*. Available at: http://www.aviso.oceanobs.com/fileadmin/documents/OSTST/2009/poster/commien.pdf

[25] Couhert, A., L. Cerri, F. Mercier, S. Houry. 2010. Status of Jason-1 and Jason-2 GDR orbits. *Talk presented at OSTST meeting, Lisbon, Portugal*. Available at: http://www.aviso.oceanobs.com/fileadmin/documents/OSTST/2010/oral/couhert.pdf

[26] DeCarvalho, R., S. Brown, B. Haines and S. Desai. 2009. Global cross calibration and validation of the Jason-1 and Jason-2/OSTM data products. *Oral presentation at OSTST meeting, Seattle, USA*. Available at: http://www.aviso.oceanobs.com/fileadmin/documents/OSTST/2009/oral/deCarvalho.pdf

[27] Desjonqueres, J.-D., G. Carayon, J.-L. Courriere, and N. Steunou "POSEIDON-2 In-Flight results", *Oral presentation at OSTST meeting, Nice, France, 9-12 november 2008*. Available at http://www.aviso.oceanobs.com/fileadmin/documents/OSTST/2008/oral/desjonqueres.pdf

[28] Desjonquères, J. D. , Carayon, G. , Steunou, N. and Lambin, J. (2010) Poseidon-3 Radar Altimeter: New Modes and In-Flight Performances, *Marine Geodesy*, **33:1, 53 - 79**. Available at http://pdfserve.informaworld.com/542982__925503482.pdf

[29] Dettmering, Denise and Bosch, Wolfgang (2010) Global Calibration of Jason-2 by Multi-Mission Crossover Analysis, *Marine Geodesy*, **33:1, 150 - 161**. Available at http://pdfserve.informaworld.com/315039__925510361.pdf

[30] Dorandeu.,J., M. Ablain, Y. Faugère, F. Mertz, 2004 : Jason-1 global statistical evaluation and performance assessment. Calibration and cross-calibration results. *Marine Geodesy* **27: 345-372.**

[31] Faugère, Y. et al. 2009. The SLOOP project: preparing the next generation of altimetry products for open ocean. *Poster presented at OSTST meeting, Seattle, USA*. Available at: http://www.aviso.oceanobs.com/fileadmin/documents/OSTST/2009/poster/Faugere2.pdf

[32] Faugère, Y. et al. 2010. CROSS-CALIBRATION between ENVISAT and JASON-1/2. *Oral presentation at OSTST meeting, Lisbon, Portugal*. Available at: http://www.aviso.oceanobs.com/fileadmin/documents/OSTST/2010/oral/19_Tuesday/Tuesday_afternoon/faugere.pdf

[33] Jason-2 Version "T" Geophysical Data Records : Public Release, August 2009. Available at : http://www.aviso.oceanobs.com/fileadmin/documents/data/products/Jason-2_GDR_T_disclaimer.pdf

[34] Gourrion, J., Vandemark, D., Bailey, S., Chapron, B., Gommenginger, G.P., Challenor, P.G. and Srokosz, M.A., 2002: A two-parameter wind speed algorithm for Ku-band altimeters, *Journal of Atmospheric and Oceanic Technology*. **19(12) 2030-2048**.

[35] Dumont, J.-P., V. Rosmorduc, N. Picot, S. Desai, H. Bonekamp, J. Figa, J. Lillibridge, R. Sharroo, 2011: OSTM/Jason-2 Products Handbook. CNES: SALP-MU-M-OP-15815-CN. EUMETSAT: EUM/OPS-JAS/MAN/08/0041. JPL: OSTM-29-1237. NOAA/NESDIS: Polar Series/OSTM J400. Available at http://www.aviso.oceanobs.com/fileadmin/documents/data/tools/hdbk_j2.pdf

[36] Hernandez, F. and P. Schaeffer, 2000: Altimetric Mean Sea Surfaces and Gravity Anomaly maps inter-comparisons. AVI-NT-011-5242-CLS, 48 pp. CLS Ramonville St Agne.

[37] Huffman, G. and D.T.Bolvin, 2009: TRMM and Other Data Precipitation Data Set Documentation. Available at ftp://precip.gsfc.nasa.gov/pub/trmmdocs/3B42_3B43_doc.pdf

[38] Imel, D.A. 1994. Evaluation of the TOPEX/POSEIDON dual-frequency ionospheric correction. *J. Geophys. Res.*, **99, 24,895-24,906**.

[39] Lemoine, F., N.P. Zelensky, S. Melachroinos, D.S. Chinn, B.D. Beckley, D.D. Rowlands, and S.B. Luthcke. 2011. GSFC OSTM (Jason-2), Jason-1 & TOPEX POD Update. *Oral presentation at OSTST meeting, San Diego, USA*. Available at http://www.aviso.oceanobs.com/fileadmin/documents/OSTST/2011/oral/02_Thursday/SplinterPOD/03Lemoine_etal_SWT2011_v01.pdf.

[40] Le Traon, P.-Y., J. Stum, J. Dorandeu, P. Gaspar, and P. Vincent, 1994: Global statistical analysis of TOPEX and POSEIDON data. *J. Geophys. Res.*,**99, 24619-24631.**

[41] MSEs (CNES, NASA, NOAA, EUMETSAT). 2011. GDR Status. *Oral presentation (by N. Picot) at OSTST meeting, San Diego, USA*. Available at http://www.aviso.oceanobs.com/fileadmin/documents/OSTST/2011/oral/03_Friday/Plenary/GDRProducts/02PicotGDR_status_2011.pdf.

[42] Obligis, E., L. Eymard, M. Ablain, B. Picard, J.F. Legeais, Y. Faugere and N. Picot, 2010. The wet tropospheric correction for altimetry missions: A mean sea level issue.*Oral presentation at OSTST meeting, Lisbon, Portugal*. Available at http://www.aviso.oceanobs.com/fileadmin/documents/OSTST/2010/oral/19_Tuesday/OBLIGIS.pdf.

[43] Ollivier A., Faugere Y., Granier N., 2008: Envisat RA-2/MWR ocean data validation and cross-calibration activities. Yearly report. Technical Note CLS.DOS/NT/09.10, Contract N° SALP-RP-MA-EA-21633-CLS http://www.aviso.oceanobs.com/fileadmin/documents/calval/validation_report/EN/annual_report_en_2008.pdf

[44] Ollivier A., Faugere Y., P. Thibaut, G. Dibarboure, and J.-C. Poisson, 2008: Investigation on the high frequency content of Jason-1 and Jason-2. CLS.DOS/NT/09-027

[45] Ollivier A., M. Guibbaud, Faugere Y. Envisat RA2/MWR ocean data validation and cross-calibration activities. Yearly report 2011. SALP-RP-MA-EA-22062-CLS, CLS.DOS/NT/12-021.

[46] Otten M., C. Flohrer, T. Springer, and W. Enderle. 2011. Generating precise and homogeneous orbits for Jason-1 and Jason-2. *Oral presentation at OSTST meeting, San Diego, USA*. Available at http://www.aviso.oceanobs.com/fileadmin/documents/OSTST/2011/oral/03_Friday/Splinter6POD/01_Otten.pdf.

[47] Peltier, 2004, Global Glacial Isostasy And The Surface of The Ice-Age Earth: The ICE-5G (VM2) Model and GRACE. *Annual Review of Earth and Planetary Sciences*, May 2004, **Vol. 32, Pages 111-149**, doi: 10.1146/annurev.earth.32.082503.144359

[48] Philipps, S., M. Ablain, J. Dorandeu, P. Thibaut, N. Picot and J. Lambin. 2006. SSALTO CALVAL Performance assessment Jason-1 GDR 'B'/GDR 'A'. *Poster presented at OSTST meeting, Hobbart, Australia*. Available at: http://www.aviso.oceanobs.com/fileadmin/documents/OSTST/2006/ablain1.pdf

[49] Picot, N., P. Thibaut, N. Tran, S. Philipps, J.C. Poisson, T. Moreau, and E. Bronner. 2010. New Jason-2 GDR-C standards. *Oral presentation at OSTST meeting, Lisbon, Portugal*. Available at http://www.aviso.oceanobs.com/fileadmin/documents/OSTST/2010/oral/PThibaut_Jason2.pdf.

[50] Picot, N., P. Thibaut, N. Tran, S. Philipps, J.C. Poisson, E. Bronner, C. Garcia and many others. 2011. Jason-2 GDR-D standards. *Oral presentation at OSTST meeting, San Diego, USA*. Available at http://www.aviso.oceanobs.com/fileadmin/documents/OSTST/2011/oral/02_Thursday/Splinter5IP/05NPicot_et_al_OSTST_2011_J2-GDRD-Standards.pdf.

[51] Schaeffer, P., A. Ollivier, Y. Faugere, E. Bronner, and N. Picot. The new CNES CLS 2010 Mean Sea Surface. *Oral presentation at OSTST meeting, Lisbon, Portugal, 18-20 october 2010*. Available at http://www.aviso.oceanobs.com/fileadmin/documents/OSTST/2010/oral/19_Tuesday/Schaeffer.pdf.

[52] Schaeffer, P., Y. Faugere, J.-F. Legeais, A. Ollivier, T. Guinle, and N. Picot (2012). The CNES_CLS11 Global Mean Sea Surface Computed from 16 Years of Satellite Altimeter Data. *Marine Geodesy* **35: sup1, 3-19**. Available at http://www.tandfonline.com/doi/abs/10.1080/01490419.2012.718231

[53] Solar Radio Flux (10.7cm) (daily solar data). Available at http://www.swpc.noaa.gov/ftpmenu/indices/old_indices.html

[54] Thibaut, P. O.Z. Zanifé, J.P. Dumont, J. Dorandeu, N. Picot, and P. Vincent, 2002. Data editing: The MQE criterion. *Paper presented at the Jason-1 and TOPEX/Poseidon Science Working Team Meeting, New-Orleans (USA), 21-23 October*.

[55] Thibaut, P., J.-C. Poisson, A. Ollivier, S. Philipps, and M. Ablain: "Jason-2 waveforms, tracking and retracking analysis", *Oral presentation at OSTST meeting, Nice, France, 9-12 november 2008*. Available at http://www.aviso.oceanobs.com/fileadmin/documents/OSTST/2008/oral/thibaut.pdf

[56] Moreau, T., P. Thibaut, 2009. Etude dépointage Poseidon-3: optimisation de l'angle d'ouverture d'antenne. CLS-DOS-NT-09-028. 15 pp, CLS Ramonville St. Agne.

[57] P. Thibaut. Bilan des activités d'expertise altimétriques menées en 2009 : Lot 2D. SALP-RP-MA-EA-21808-CLS, CLS-DOS-NT-10-029.

[58] Tran, N. , Labroue, S. , Philipps, S. , Bronner, E. and Picot, N. (2010) Overview and Update of the Sea State Bias Corrections for the Jason-2, Jason-1 and TOPEX Missions, *Marine Geodesy*,**33:1, 348 - 362**. Avialable at http://pdfserve.informaworld.com/804727__925502357.pdf

[59] Tran, N., P. Thibaut, J.-C. Poisson, S. Philipps, E. Bronner, and N. Picot. Jason-1, Jason-2 and TOPEX Sea State Bias. Overview and Updates. *Oral presentation at OSTST meeting, Lisbon, Portugal, 18-20 october 2010*. Avialable at http://www.aviso.oceanobs.com/fileadmin/documents/OSTST/2010/oral/TRAN.pdf

[60] N. Tran, S. Philipps, J.-C. Poisson, S. Urien, E. Bronner, and N. Picot. Impact of GDR_D standards on SSB corrections. *Oral presentation at OSTST meeting, Venice, Italy, 27-28 September 2012*. Available at http://www.aviso.oceanobs.com/fileadmin/documents/OSTST/2012/oral/02_friday_28/01_instr_processing_I/01_IP1_Tran.pdf.

[61] World Meteorological Organization. 2010. El Nino/ La Nina Update (30 March 2010). Available at http://www.wmo.int/pages/prog/wcp/wcasp/documents/El_Nino_Mar10_Eng.pdf.

[62] World Meteorological Organization. 2011. El Nino/ La Nina Update (17 November 2011). Available at http://www.wmo.int/pages/prog/wcp/wcasp/documents/El_Nino_Nov11_Eng.pdf.

Jason-1, Jason-2 and Envisat. SALP-NT-MA-EA-22046-CLS, CLS.DOS/NT/12-016.

[63] Valladeau, G., S. Philipps. Jason-1 validation and cross calibration activities (Annual report 2009).SALP-RP-MA-EA-21795-CLS, CLS.DOS/NT/10-005.

[64] Valladeau, G., S. Philipps. Jason-1 validation and cross calibration activities (Annual report 2010).SALP-RP-MA-EA-21903-CLS, CLS.DOS/NT/10-332.

[65] Zlotnicky, V. 1994. Correlated environnemental corrections in TOPEX/POSEIDON, with a note on ionomospheric accuracy. *J. Geophys. Res.*, **99, 24,907-24,914**

11. Annex

This annex contains posters presented at OSTST meeting in 2012.

11.1. Poster presented at OSTST meeting in 2012

The following posters, presented at OSTST meeting 2012 in Venice (Italy), are also available on Aviso web-site:
http://www.aviso.oceanobs.com/en/courses/sci-teams/ostst-2012/ostst-2012-posters.html.

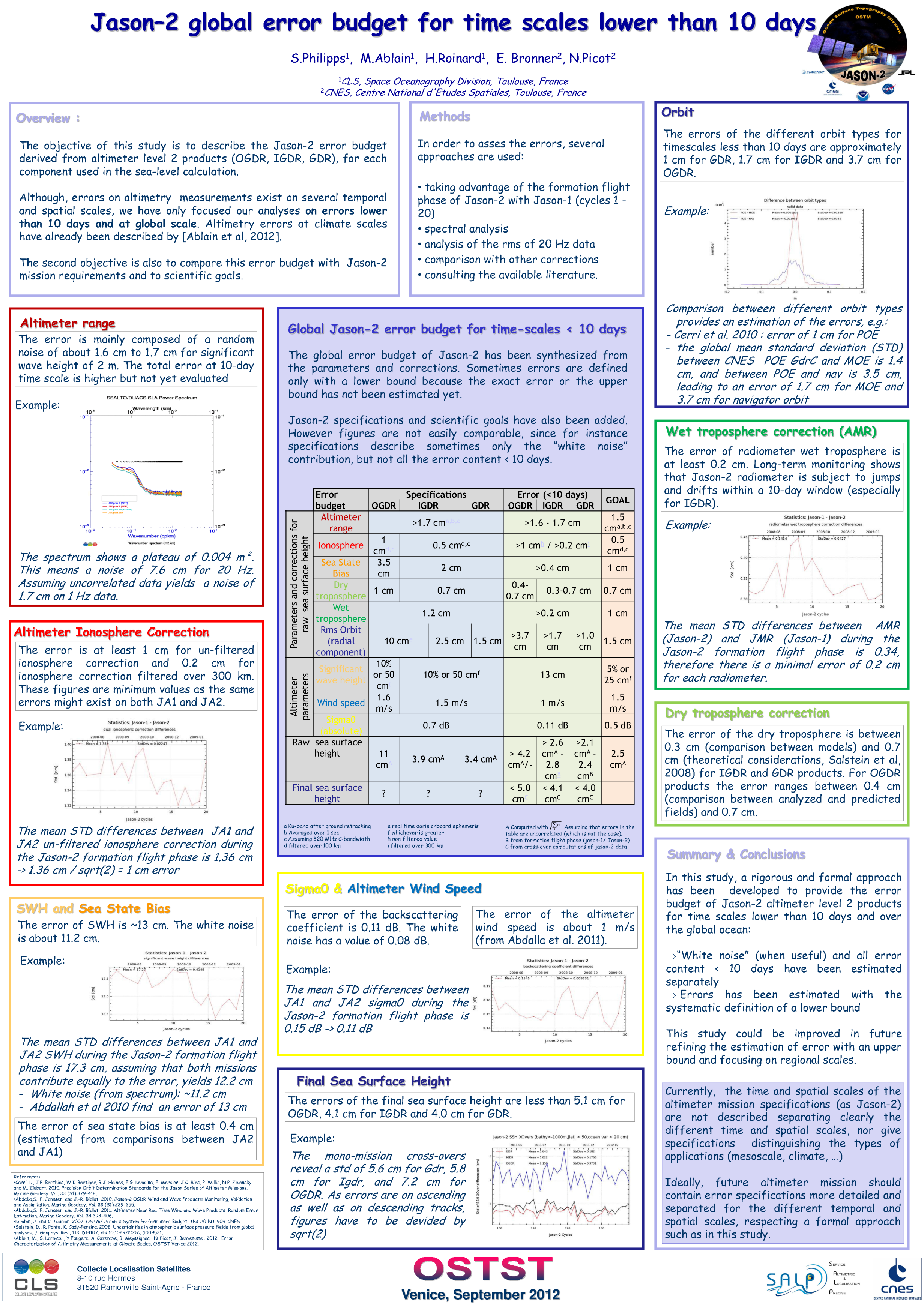

Jason-2 global error budget for time scales lower than 10 days

S.Philipps[1], M.Ablain[1], H.Roinard[1], E. Bronner[2], N.Picot[2]

[1]CLS, Space Oceanography Division, Toulouse, France
[2]CNES, Centre National d'Etudes Spatiales, Toulouse, France

Overview :

The objective of this study is to describe the Jason-2 error budget derived from altimeter level 2 products (OGDR, IGDR, GDR), for each component used in the sea-level calculation.

Although, errors on altimetry measurements exist on several temporal and spatial scales, we have only focused our analyses **on errors lower than 10 days and at global scale**. Altimetry errors at climate scales have already been described by [Ablain et al, 2012].

The second objective is also to compare this error budget with Jason-2 mission requirements and to scientific goals.

Methods

In order to asses the errors, several approaches are used:

- taking advantage of the formation flight phase of Jason-2 with Jason-1 (cycles 1 - 20)
- spectral analysis
- analysis of the rms of 20 Hz data
- comparison with other corrections
- consulting the available literature.

Orbit

The errors of the different orbit types for timescales less than 10 days are approximately 1 cm for GDR, 1.7 cm for IGDR and 3.7 cm for OGDR.

Example:

Comparison between different orbit types provides an estimation of the errors, e.g.:
- *Cerri et al. 2010 : error of 1 cm for POE*
- *the global mean standard deviation (STD) between CNES POE GdrC and MOE is 1.4 cm, and between POE and nav is 3.5 cm, leading to an error of 1.7 cm for MOE and 3.7 cm for navigator orbit*

Altimeter range

The error is mainly composed of a random noise of about 1.6 cm to 1.7 cm for significant wave height of 2 m. The total error at 10-day time scale is higher but not yet evaluated

Example:

The spectrum shows a plateau of 0.004 m². This means a noise of 7.6 cm for 20 Hz. Assuming uncorrelated data yields a noise of 1.7 cm on 1 Hz data.

Altimeter Ionosphere Correction

The error is at least 1 cm for un-filtered ionosphere correction and 0.2 cm for ionosphere correction filtered over 300 km. These figures are minimum values as the same errors might exist on both JA1 and JA2.

Example:

The mean STD differences between JA1 and JA2 un-filtered ionosphere correction during the Jason-2 formation flight phase is 1.36 cm -> 1.36 cm / sqrt(2) = 1 cm error

SWH and Sea State Bias

The error of SWH is ~13 cm. The white noise is about 11.2 cm.

Example:

The mean STD differences between JA1 and JA2 SWH during the Jason-2 formation flight phase is 17.3 cm, assuming that both missions contribute equally to the error, yields 12.2 cm
- *White noise (from spectrum): ~11.2 cm*
- *Abdallah et al 2010 find an error of 13 cm*

The error of sea state bias is at least 0.4 cm (estimated from comparisons between JA2 and JA1)

References:
- Cerri, L., J.P. Berthias, W.I. Bertiger, B.J. Haines, F.G. Lemoine, F. Mercier, J.C. Ries, P. Willis, N.P. Zelensky, and M. Ziebart. 2010. Precision Orbit Determination Standards for the Jason Series of Altimeter Missions. Marine Geodesy. Vol. 33 (S1):379-418.
- Abdalla,S., P. Janssen, and J.-R. Bidlot. 2010. Jason-2 OGDR Wind and Wave Products: Monitoring, Validation and Assimilation. Marine Geodesy. Vol. 33 (S1):239-255.
- Abdalla,S., P. Janssen, and J.-R. Bidlot. 2011. Altimeter Near Real Time Wind and Wave Products: Random Error Estimation. Marine Geodesy. Vol. 34:393-406.
- Lambin, J. and C. Tourain. 2007. OSTM/ Jason-2 System Performances Budget. TP3-J0-NT-909-CNES.
- Salstein, D., R. Ponte, K. Cady-Pereira. 2008. Uncertainties in atmospheric surface pressure fields from global analyses. J. Geophys. Res., 113, D14107, doi:10.1029/2007JD009531.
- Ablain, M., G. Larnicol , Y Faugere, A. Cazenave, B. Meyssignac , N. Picot, J. Benveniste . 2012. Error Characterization of Altimetry Measurements at Climate Scales. OSTST Venice 2012.

Global Jason-2 error budget for time-scales < 10 days

The global error budget of Jason-2 has been synthesized from the parameters and corrections. Sometimes errors are defined only with a lower bound because the exact error or the upper bound has not been estimated yet.

Jason-2 specifications and scientific goals have also been added. However figures are not easily comparable, since for instance specifications describe sometimes only the "white noise" contribution, but not all the error content < 10 days.

	Error budget	Specifications OGDR	Specifications IGDR	Specifications GDR	Error (<10 days) OGDR	Error (<10 days) IGDR	Error (<10 days) GDR	GOAL
Parameters and corrections for raw sea surface height	Altimeter range	>1.7 cm[a,b,c]			>1.6 - 1.7 cm			1.5 cm[a,b,c]
	Ionosphere	1 cm[d,c]	0.5 cm[d,c]		>1 cm[h] / >0.2 cm[i]			0.5 cm[d,c]
	Sea State Bias	3.5 cm	2 cm		>0.4 cm			1 cm
	Dry troposphere	1 cm	0.7 cm		0.4-0.7 cm	0.3-0.7 cm		0.7 cm
	Wet troposphere	1.2 cm			>0.2 cm			1 cm
	Rms Orbit (radial component)	10 cm[e]	2.5 cm	1.5 cm	>3.7 cm	>1.7 cm	>1.0 cm	1.5 cm
Altimeter parameters	Significant wave height	10% or 50 cm[f]	10% or 50 cm[f]		13 cm			5% or 25 cm[f]
	Wind speed	1.6 m/s	1.5 m/s		1 m/s			1.5 m/s
	Sigma0 (absolute)	0.7 dB			0.11 dB			0.5 dB
Raw sea surface height		11 cm[A]	3.9 cm[A]	3.4 cm[A]	> 4.2 cm[A]/ -	> 2.6 cm[A] - 2.8 cm[B]	>2.1 cm[A] - 2.4 cm[B]	2.5 cm[A]
Final sea surface height		?	?	?	< 5.0 cm[C]	< 4.1 cm[C]	< 4.0 cm[C]	

a Ku-band after ground retracking
b Averaged over 1 sec
c Assuming 320 MHz C-bandwidth
d filtered over 100 km
e real time doris onboard ephemeris
f whichever is greater
h non filtered value
i filtered over 300 km
A Computed with $\sqrt{\sum_i \sigma_i}$, Assuming that errors in the table are uncorrelated (which is not the case).
B from formation flight phase (jason-1/ Jason-2)
C from cross-over computations of jason-2 data

Sigma0 & Altimeter Wind Speed

The error of the backscattering coefficient is 0.11 dB. The white noise has a value of 0.08 dB.

The error of the altimeter wind speed is about 1 m/s (from Abdalla et al. 2011).

Example:

The mean STD differences between JA1 and JA2 sigma0 during the Jason-2 formation flight phase is 0.15 dB -> 0.11 dB

Final Sea Surface Height

The errors of the final sea surface height are less than 5.1 cm for OGDR, 4.1 cm for IGDR and 4.0 cm for GDR.

Example:

The mono-mission cross-overs reveal a std of 5.6 cm for Gdr, 5.8 cm for Igdr, and 7.2 cm for OGDR. As errors are on ascending as well as on descending tracks, figures have to be devided by sqrt(2)

Wet troposphere correction (AMR)

The error of radiometer wet troposphere is at least 0.2 cm. Long-term monitoring shows that Jason-2 radiometer is subject to jumps and drifts within a 10-day window (especially for IGDR).

Example:

The mean STD differences between AMR (Jason-2) and JMR (Jason-1) during the Jason-2 formation flight phase is 0.34, therefore there is a minimal error of 0.2 cm for each radiometer.

Dry troposphere correction

The error of the dry troposphere is between 0.3 cm (comparison between models) and 0.7 cm (theoretical considerations, Salstein et al, 2008) for IGDR and GDR products. For OGDR products the error ranges between 0.4 cm (comparison between analyzed and predicted fields) and 0.7 cm.

Summary & Conclusions

In this study, a rigorous and formal approach has been developed to provide the error budget of Jason-2 altimeter level 2 products for time scales lower than 10 days and over the global ocean:

⇒"White noise" (when useful) and all error content < 10 days have been estimated separately
⇒ Errors has been estimated with the systematic definition of a lower bound

This study could be improved in future refining the estimation of error with an upper bound and focusing on regional scales.

Currently, the time and spatial scales of the altimeter mission specifications (as Jason-2) are not described separating clearly the different time and spatial scales, nor give specifications distinguishing the types of applications (mesoscale, climate, …)

Ideally, future altimeter mission should contain error specifications more detailed and separated for the different temporal and spatial scales, respecting a formal approach such as in this study.

Collecte Localisation Satellites
8-10 rue Hermes
31520 Ramonville Saint-Agne - France

OSTST
Venice, September 2012

Figure 84: *Poster presented at OSTST meeting, Venice 2012*

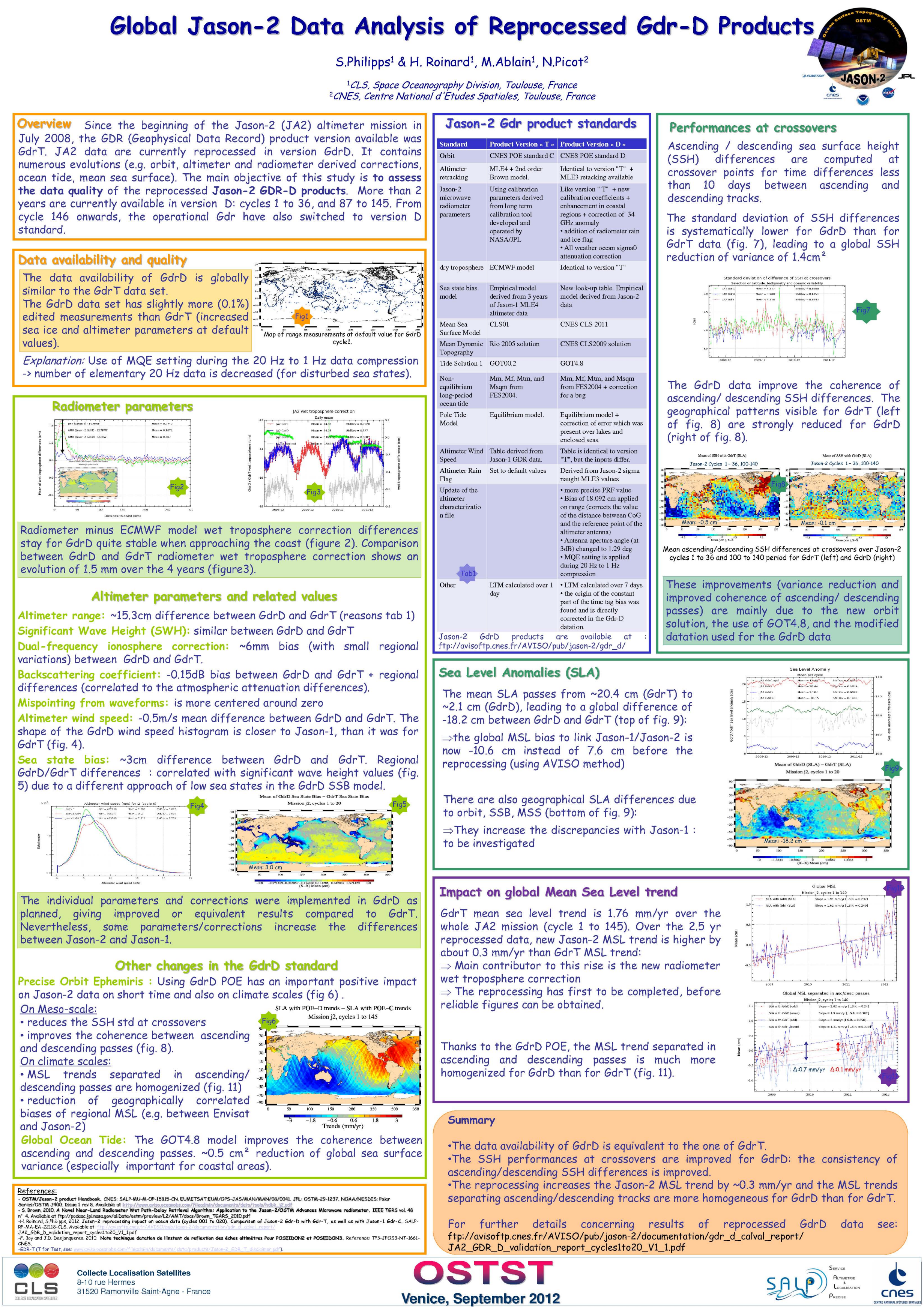

Global Jason-2 Data Analysis of Reprocessed Gdr-D Products

S.Philipps[1] & H. Roinard[1], M.Ablain[1], N.Picot[2]

[1] CLS, Space Oceanography Division, Toulouse, France
[2] CNES, Centre National d'Etudes Spatiales, Toulouse, France

Overview

Since the beginning of the Jason-2 (JA2) altimeter mission in July 2008, the GDR (Geophysical Data Record) product version available was GdrT. JA2 data are currently reprocessed in version GdrD. It contains numerous evolutions (e.g. orbit, altimeter and radiometer derived corrections, ocean tide, mean sea surface). The main objective of this study is **to assess the data quality** of the reprocessed **Jason-2 GDR-D products**. More than 2 years are currently available in version D: cycles 1 to 36, and 87 to 145. From cycle 146 onwards, the operational Gdr have also switched to version D standard.

Data availability and quality

The data availability of GdrD is globally similar to the GdrT data set.
The GdrD data set has slightly more (0.1%) edited measurements than GdrT (increased sea ice and altimeter parameters at default values).

Map of range measurements at default value for GdrD cycle1.

Explanation: Use of MQE setting during the 20 Hz to 1 Hz data compression -> number of elementary 20 Hz data is decreased (for disturbed sea states).

Radiometer parameters

Radiometer minus ECMWF model wet troposphere correction differences stay for GdrD quite stable when approaching the coast (figure 2). Comparison between GdrD and GdrT radiometer wet troposphere correction shows an evolution of 1.5 mm over the 4 years (figure3).

Altimeter parameters and related values

Altimeter range: ~15.3cm difference between GdrD and GdrT (reasons tab 1)

Significant Wave Height (SWH): similar between GdrD and GdrT

Dual-frequency ionosphere correction: ~6mm bias (with small regional variations) between GdrD and GdrT.

Backscattering coefficient: -0.15dB bias between GdrD and GdrT + regional differences (correlated to the atmospheric attenuation differences).

Mispointing from waveforms: is more centered around zero

Altimeter wind speed: -0.5m/s mean difference between GdrD and GdrT. The shape of the GdrD wind speed histogram is closer to Jason-1, than it was for GdrT (fig. 4).

Sea state bias: ~3cm difference between GdrD and GdrT. Regional GdrD/GdrT differences : correlated with significant wave height values (fig. 5) due to a different approach of low sea states in the GdrD SSB model.

Mean of GdrD Sea State Bias – GdrT Sea State Bias
Mission j2, cycles 1 to 20

The individual parameters and corrections were implemented in GdrD as planned, giving improved or equivalent results compared to GdrT. Nevertheless, some parameters/corrections increase the differences between Jason-2 and Jason-1.

Other changes in the GdrD standard

Precise Orbit Ephemiris : Using GdrD POE has an important positive impact on Jason-2 data on short time and also on climate scales (fig 6) .

On Meso-scale:
- reduces the SSH std at crossovers
- improves the coherence between ascending and descending passes (fig. 8).

On climate scales:
- MSL trends separated in ascending/ descending passes are homogenized (fig. 11)
- reduction of geographically correlated biases of regional MSL (e.g. between Envisat and Jason-2)

SLA with POE–D trends – SLA with POE–C trends
Mission j2, cycles 1 to 145
Trends (mm/yr)

Global Ocean Tide: The GOT4.8 model improves the coherence between ascending and descending passes. ~0.5 cm^2 reduction of global sea surface variance (especially important for coastal areas).

References:
- OSTM/Jason-2 product Handbook. CNES: SALP-MU-M-OP-15815-CN. EUMETSAT:EUM/OPS-JAS/MAN/MAN/08/0041. JPL: OSTM-29-1237. NOAA/NESDIS: Polar Series/OSTM J400. Issue 1 rev 8. Available at http://www.aviso.oceanobs.com/fileadmin/documents/data/tools/hdbk_j2.pdf
- S. Brown. 2010. A Novel Near-Land Radiometer Wet Path-Delay Retrieval Algorithm: Application to the Jason-2/OSTM Advances Microwave radiometer. IEEE TGRS vol. 48 n° 4. Available at ftp://podaac.jpl.nasa.gov/allData/ostm/preview/L2/AMT/docs/Brown_TGARS_2010.pdf
-H. Roinard, S.Philipps, 2012. Jason-2 reprocessing impact on ocean data (cycles 001 to 020). Comparison of Jason-2 Gdr-D with Gdr-T, as well as with Jason-1 Gdr-C. SALP-RP-MA-EA-22118-CLS. Available at: ftp://avisoftp.cnes.fr/AVISO/pub/jason-2/documentation/gdr_d_calval_report/ JA2_GDR_D_validation_report_cycles1to20_V1_1.pdf
-F. Boy and J.D. Desjonqueres. 2010. Note techinque datation de l'instant de reflextion des échos altimétres Pour POSEIDON2 et POSEIDON3. Reference: TP3-JPOS3-NT-1661-CNES.
-GDR-T (T for Test, see: www.aviso.oceanobs.com/fileadmin/documents/ data/products/Jason-2_GDR_T_disclaimer.pdf).

Jason-2 Gdr product standards

Standard	Product Version « T »	Product Version « D »
Orbit	CNES POE standard C	CNES POE standard D
Altimeter retracking	MLE4 + 2nd order Brown model.	Identical to version "T" + MLE3 retacking available
Jason-2 microwave radiometer parameters	Using calibration parameters derived from long term calibration tool developed and operated by NASA/JPL	Like version " T" + new calibration coefficients + enhancement in coastal regions + correction of 34 GHz anomaly • addition of radiometer rain and ice flag • All weather ocean sigma0 attenuation correction
dry troposphere	ECMWF model	Identical to version "T"
Sea state bias model	Empirical model derived from 3 years of Jason-1 MLE4 altimeter data	New look-up table. Empirical model derived from Jason-2 data
Mean Sea Surface Model	CLS01	CNES CLS 2011
Mean Dynamic Topography	Rio 2005 solution	CNES CLS2009 solution
Tide Solution 1	GOT00.2	GOT4.8
Non-equilibrium long-period ocean tide	Mm, Mf, Mtm, and Msqm from FES2004.	Mm, Mf, Mtm, and Msqm from FES2004 + correction for a bug
Pole Tide Model	Equilibrium model.	Equilibrium model + correction of error which was present over lakes and enclosed seas.
Altimeter Wind Speed	Table derived from Jason-1 GDR data.	Table is identical to version "T", but the inputs differ.
Altimeter Rain Flag	Set to default values	Derived from Jason-2 sigma naught MLE3 values
Update of the altimeter characterizatio n file		• more precise PRF value • Bias of 18.092 cm applied on range (corrects the value of the distance between CoG and the reference point of the altimeter antenna) • Antenna aperture angle (at 3dB) changed to 1.29 deg • MQE setting is applied during 20 Hz to 1 Hz compression
Other	LTM calculated over 1 day	• LTM calculated over 7 days • the origin of the constant part of the time tag bias was found and is directly corrected in the Gdr-D datation.

Tab1

Jason-2 GdrD products are available at : ftp://avisoftp.cnes.fr/AVISO/pub/jason-2/gdr_d/

Sea Level Anomalies (SLA)

The mean SLA passes from ~20.4 cm (GdrT) to ~2.1 cm (GdrD), leading to a global difference of -18.2 cm between GdrD and GdrT (top of fig. 9):

⇒the global MSL bias to link Jason-1/Jason-2 is now -10.6 cm instead of 7.6 cm before the reprocessing (using AVISO method)

There are also geographical SLA differences due to orbit, SSB, MSS (bottom of fig. 9):

⇒They increase the discrepancies with Jason-1 : to be investigated

Mean of GdrD (SLA) – GdrT (SLA)
Mission j2, cycles 1 to 20

Impact on global Mean Sea Level trend

GdrT mean sea level trend is 1.76 mm/yr over the whole JA2 mission (cycle 1 to 145). Over the 2.5 yr reprocessed data, new Jason-2 MSL trend is higher by about 0.3 mm/yr than GdrT MSL trend:
⇒ Main contributor to this rise is the new radiometer wet troposphere correction
⇒ The reprocessing has first to be completed, before reliable figures can be obtained.

Thanks to the GdrD POE, the MSL trend separated in ascending and descending passes is much more homogenized for GdrD than for GdrT (fig. 11).

Δ:0.7 mm/yr Δ:0.1 mm/yr

Performances at crossovers

Ascending / descending sea surface height (SSH) differences are computed at crossover points for time differences less than 10 days between ascending and descending tracks.

The standard deviation of SSH differences is systematically lower for GdrD than for GdrT data (fig. 7), leading to a global SSH reduction of variance of 1.4cm²

The GdrD data improve the coherence of ascending/ descending SSH differences. The geographical patterns visible for GdrT (left of fig. 8) are strongly reduced for GdrD (right of fig. 8).

Mean ascending/descending SSH differences at crossovers over Jason-2 cycles 1 to 36 and 100 to 140 period for GdrT (left) and GdrD (right)

These improvements (variance reduction and improved coherence of ascending/ descending passes) are mainly due to the new orbit solution, the use of GOT4.8, and the modified datation used for the GdrD data

Summary

- The data availability of GdrD is equivalent to the one of GdrT.
- The SSH performances at crossovers are improved for GdrD: the consistency of ascending/descending SSH differences is improved.
- The reprocessing increases the Jason-2 MSL trend by ~0.3 mm/yr and the MSL trends separating ascending/descending tracks are more homogeneous for GdrD than for GdrT.

For further details concerning results of reprocessed GdrD data see: ftp://avisoftp.cnes.fr/AVISO/pub/jason-2/documentation/gdr_d_calval_report/ JA2_GDR_D_validation_report_cycles1to20_V1_1.pdf

Collecte Localisation Satellites
8-10 rue Hermes
31520 Ramonville Saint-Agne - France

OSTST
Venice, September 2012

Figure 85: *Poster presented at OSTST meeting, Venice 2012*